Gonçalo Rodrigues Puidival Marques

Licenciado em Bioquímica

Development of antibodies against the Notch pathway ligand JAG1 using phage display technology

Dissertação para obtenção do Grau de Mestre em Biotecnologia

Orientador: Doutora Ana Barbas, Bayer, iBET
Co-orientador: Doutora Gabriela Silva, iBET

Júri:

Presidente: Prof. Doutor Rui Oliveira, FCT-UNL
Arguente: Doutor André Filipe da Costa Faustino, iBET
Vogal: Doutora Ana Barbas, Bayer, iBET

FACULDADE DE CIÊNCIAS E TECNOLOGIA
UNIVERSIDADE NOVA DE LISBOA

Setembro 2019

Gonçalo Rodrigues Puidival Marques

Licenciado em Bioquímica

Development of antibodies against the Notch pathway ligand JAG1 using phage display technology

Dissertação para obtenção do Grau de Mestre em Biotecnologia

Orientador: Doutora Ana Barbas, Bayer, iBET
Co-orientador: Doutora Gabriela Silva, iBET

Júri:

Presidente: Prof. Doutor Rui Oliveira, FCT-UNL
Arguente: Doutor André Filipe da Costa Faustino, iBET
Vogal: Doutora Ana Barbas, Bayer, iBET

FACULDADE DE CIÊNCIAS E TECNOLOGIA
UNIVERSIDADE NOVA DE LISBOA

Setembro 2019

Development of antibodies against the Notch pathway ligand JAG1 using phage display technology

Acknowledgements

Queria começar por agradecer à Doutora Ana Barbas por me ter recebido no seu laboratório e por me ter permitido fazer parte deste projecto desafiante, assim como toda a ajuda que me prestou durante este ano.

Queria agradecer também à Doutora Gabriela Silva que foi incansável no seu apoio a vários níveis, que sempre demonstrou disponibilidade em me ajudar quando necessitava e que sempre fez o que estava ao seu alcance para que esta tese fosse bem-sucedida.

Gostaria de agradecer à direcção do iBET por me ter permitido realizar o projecto de tese nas suas instalações.

Um obrigado especial para a futura Doutora Joana Sales-Dias que teve uma paciência de santa para me explicar todas as minhas dúvidas e por me ter ensinado grande parte do que eu aprendi este ano.

Obrigado a todos os membros que pertencem ou pertenceram ao laboratório satélite da Bayer Healthcare Pharma durante a minha presença. Um muito obrigado ao Hugo, Khrystyna e Bia pelo apoio e conhecimento que me transmitiram, e à Sofia Silva pelo contributo na correcção desta tese e pelos seus ensinamentos. Queria igualmente agradecer à Raquel e Clara pelo apoio técnico em alguns ensaios e a todos os restantes membros - Inês, Fernanda, Sofia Rebelo, Daniel, Bernardo, Marta, Susana, Lígia, Sandra, António - pelo excelente ambiente que criaram para que eu me pudesse sentir bem-vindo e parte do grupo.

Queria agradecer a todos os meus amigos que me ajudaram a completar mais esta etapa na minha vida e que me têm vindo a acompanhar desde há muitos anos.

Por fim, mas em primeiro queria agradecer à minha família em especial aos meus pais e ao meu irmão porque sem vocês eu não teria chegado aqui.

Um Muito Obrigado a Todos!

Abstract

The Notch signaling pathway is a cell-to-cell communication system that plays crucial roles during the embryonic development and in the tissue homeostasis. In mammals, this pathway is constituted by four Notch receptors (Notch1-4) and five Notch ligands (DLL1, 3 and 4, and JAG1 and 2). Binding of the ligands to the receptors in adjacent cells leads to the activation of the Notch pathway and the regulation of a multitude of genes that control many cellular processes such as stem cell self-renewal, cell differentiation, proliferation, and survival. Deregulated expression of Notch signaling components are observed in many cancers, including breast, and shown to be implicated in tumor growth, recurrence and drug resistance. JAG1 is one of the five Notch ligands that is overexpressed in aggressive cancers and mediates many of the Notch signaling tumorigenic functions. JAG1 overexpression promotes cancer cell survival, proliferation, migration, metastasis, cancer stem cell population maintenance, tumor-associated angiogenesis, and allows tumor cells to escape the immune surveillance.

The goal of this work was to develop specific anti-JAG1 antibodies using phage display technology. To achieve that we used the Human Single Fold scFv Tomlinson library I+J and recombinant JAG1-EGF3-Fc protein as antigen. After several rounds of selections, 84 scFv clones capable to recognize and bind to recombinant JAG1 proteins were isolated. The binding of the 84 scFvs towards the JAG1 was tested by ELISA assays using recombinant JAG1 proteins. Additionally, the binding of anti-JAG1 scFvs to endogenous cellular JAG1 was tested by flow cytometry. Sequencing analysis of the selected clones allowed the identification of 19 unique anti-JAG1 scFvs. One was reformatted into two anti-JAG1 IgGs: one with a glycosite in HCDR2 and the other without. These IgG molecules were characterized by ELISA and SDS-PAGE, and our data showed that after reformatting they were no longer able to recognize JAG1.

Keywords: Notch signaling pathway, JAG1, cancer, Phage Display, scFv, antibodies.

Resumo

A via de sinalização do Notch é um sistema de comunicação celular que desempenha um papel crucial no desenvolvimento embrionário e na homeostasia dos tecidos. Nos mamíferos, esta via é constituída por quatro receptores e cinco ligandos. A ligação dos ligandos aos receptores de células adjacentes ativa a via Notch e conduz à modulação da expressão de múltiplos genes que controlam vários processos celulares, tais como renovação das células estaminais, diferenciação, proliferação e sobrevivência celular. Vários componentes desta via encontram-se sobre-expressos em diferentes tipos de cancro e estão associados ao crescimento e recorrência tumoral, e à resistência contra medicamentos. O JAG1 é um dos cinco ligandos da via Notch que se encontra sobre-expresso em cancros agressivos e que medeia muitas das funções tumorais da via Notch. A sobre-expressão do JAG1 promove a sobrevivência, proliferação, migração, e invasão das células cancerosas, a manutenção das células estaminais cancerígenas, a angiogénese tumoral, e permite que as células tumorais escapem à vigilância imunológica.

O objetivo deste trabalho consistiu em obter anticorpos específicos contra JAG1 usando a tecnologia de phage display. Para isso, utilizamos a biblioteca I + J scFv Tomlinson Human Single Fold e a proteína recombinante JAG1-EGF3-Fc como antigénio. Após várias rondas de seleção, foram isolados 84 clones contendo fragmentos de anticorpo (scFvs) capazes de ligarem a proteínas JAG1 recombinantes. A especificidade destes 84 scFvs foi testada em ensaios de ELISA utilizando proteínas recombinantes JAG1. A ligação dos scFvs anti-JAG1 ao JAG1 celular também foi analisada por citometria de fluxo. A análise da sequenciação destes clones permitiu a identificação de 19 scFv anti-JAG1 únicos. Um deles foi reformatado em dois anti-JAG1 IgGs: um com um local de glicosilação no HCDR2 e o outro sem esse local. Estas moléculas foram caracterizadas por ELISA e SDS-PAGE, e os nossos resultados mostraram que estes anticorpos perderam a capacidade de reconhecer a proteína JAG1 ao serem reformatados.

Palavras-chave: Sinalização da via Notch, JAG1, Cancro, Phage Display, scFv, anticorpos.

Contents

List of Figures

List of Tables

List of Formulas

Abbreviations

°C – Celsius
µg – Microgram
µL – Microliters
µM – Micromolar
2YT - 2X yeast extract + tryptone medium
Ab – Antibody
ADAM - A Disintegrin and A Metalloproteinase
ANK - Ankyrin
Asn – Asparagine
BC - Breast cancer
BCSC – Breast cancer stem cell
bp – Base pair
CBF-1 - C-promoter binding factor 1
CD46 - Complement regulatory protein
CDR - Complementary-determining region
CFU - Colony forming unit
CH – Constant gene segments of heavy chain
C_H – Constant heavy chain
CK - Cytokeratin
CL – Constant gene segments of light chain
C_L – Constant light chain
CRD - Cysteine-rich region
CSCs - Cancer stem cells
CTR – Control
DH – Diversity gene segments of heavy chain
DLL - Delta like ligands
DMEM - Dulbecco's modified eagle medium
DMSO - Dimethyl sulfoxide
DNA - Deoxyribonucleic acid
dNTP's - Deoxyribonucleotide triphosphate
DOS - Delta and OSM-11 Motif
DPBS - Dulbecco's Phosphate Buffer Saline
DSL - Delta/Serrate/Lag-2
DTT – Dithiothreitol
E.coli - Escherichia coli
ECD - Extracellular domain
EDTA - Ethylenediaminetetraacetic acid
EGF3 - Epidermal growth factor-3
EGFR - Epidermal growth factor receptor
EGFs - Epidermal growth factor like repeats
ELISA - Enzyme-linked immunosorbent assay
EMT - Epithelial-mesenchymal transition
ER - Estrogen receptor
ErbB2+ - Receptor tyrosine kinase
Fab – Fragment antigen binding
FACS - Fluorescence-activated cell sorting
FBS – Fetal bovine serum
Fc – Fragment crystallizable
FR – Framework region
Fv – Fragment variable
g - Gravitational force equivalent
GSI - γ-secretase inhibitors
HAT p300 - Histone acetyltransferase p300
HC – Heavy chain
HCAb – Heavy chain antibody
HD - Heterodimerization domain
HER2 - Human epidermal growth factor receptor-2
Hes - Hairy and enhancer-of-split
Hey - Hes-related repressor Herp
HMW – High molecular weight
HRP - Horseradish peroxidase
ICD - Intracellular domain
Ig - Immunoglobulin
IL-6 – Interleukine 6
inc – Incubator
JAG - Jagged ligands
JH – Joining gene segments of heavy chain
JL – Joining gene segments of light chain
kDa – Kilodalton
LC – Light chain
LNR - Lin12-Notch repeats
mAb - Monoclonal antibodies
MAML - Mastermind-like protein
MAPK - Mitogen-activated protein kinase
mL – Milliliter
mM – Millimolar
mRNA - Messenger RNA
Nc – Non-coated
NECD - Notch extracellular domain
NF-κB - Nuclear factor kappa-light-chain-enhancer of activated B cells
NICD - Notch intracellular domain
NLS - Nuclear localization sequence
Nm – Nanometers
NRR - Negative Control Region
Ns PEP – Non-specific peptide
O/N - Overnight
OD - Optical density
PBS - Phospahte Buffer Saline
PBST - PBS-Tween 0.05%
PCR - Polymerase chain reaction
PEG - Polyethylene Glycol
PEST - Proline (P), glutamic acid (E), serine (S), and threonine (T)
PR - Progesterone receptor
RAM - Rbp-associated Molecule
Rbp - Retinol-binding protein
rpm - Rotation per minute
RT - Room temperature
S - Site
scFv – Single chain fragment variable
SDS-PAGE - Sodium dodecyl sulfate–polyacrylamide gel electrophoresis

TAD - Transactivation domain
TAE - Tris-acetate-EDTA
T-ALL - T-cell acute lymphoblastic leukemia
TEA - Trimethylamine
TGF-β - Transforming growth factor beta
TMD - Transmembrane domain
TNBC - Triple negative breast cancer
V – Variable
VH – Variable gene segments of heavy chain
V_H – Variable heavy chain
VL – Variable gene segments of light chain
V_L – Variable light chain
γ-secretase - Gamma-secretase
κ – Kappa light chain
λ – Lambda light chain

1. Introduction

1.1 Cancer

Cancer is a complex disease caused by deregulation of various biologic functions (Hassanpour et al., 2017). It is believed that cancer results from the accumulation of mutations and epigenetic alterations (e.g. abnormal DNA methylation, histone modifications, and nucleosome positioning) that alter the expression of particular genes leading to an increase or decrease of their functional effects. Many factors can promote mutations, like the lifestyle (drinking alcohol, smoking, bad diets), chemical compounds, environmental chemical substances, viruses, bacteria, and radiation (Coyle et al., 2017; Hassanpour et al., 2017).

Cancer has become one of the major health problems in the world in recent years (Ke et al., 2017; Siegel et al., 2018)(Figure 1.1). It is expected to be one of the major causes of death and the principal barrier to increasing life expectancy in the near future. There were approximately 18 million new cancer cases and 10 million cancer deaths worldwide in 2018, according to the Global Cancer Observatory (Siegel et al., 2018). In men, the most common types of cancer are prostate, lung, and colorectal cancer. Women, on the other hand, are most affected by breast, lung, uterine corpus, and colorectal cancer (Siegel et al., 2019).

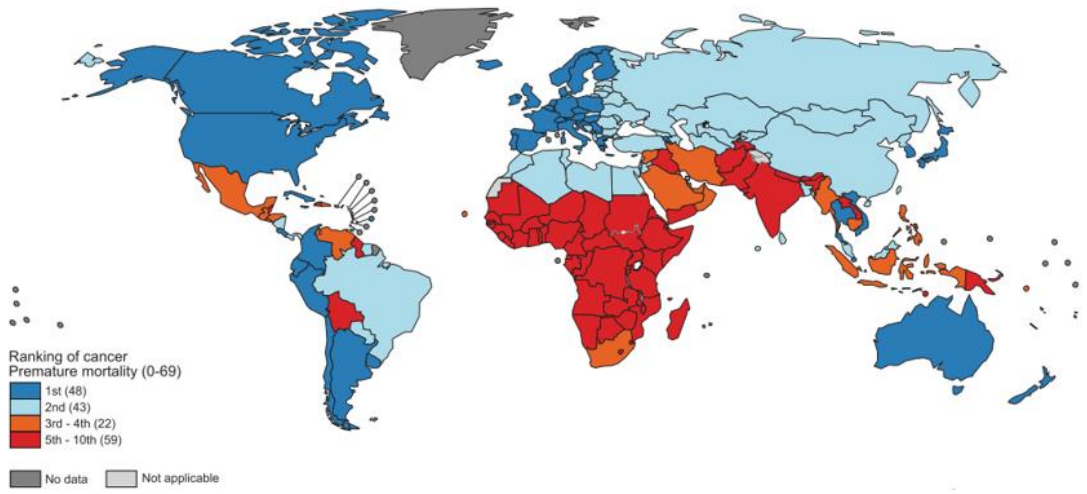

Figure 1.1. Global map presenting the national ranking of cancer as a cause of death in ages below 70 years in 2015 (Siegel et al., 2019).

In the United States prostate, lung and bronchus, and colorectal cancers account for 42% of all cases in men, with prostate cancer alone being responsible for nearly 1 in 5 new diagnoses. For women, the 3 most common cancers are breast, lung, and colorectal, which collectively represent one-half of all new diagnoses; breast cancer (BC) alone accounts for 30% of all new cancer diagnoses in women (Figure 1.2). It is expected that in 2019 in the United States 1,762,450 new cases will be diagnosed, being breast, prostate, lung and colorectal cancers the main responsible (Siegel et al., 2019).

Estimated New Cases

Males			Females		
Prostate	174,650	20%	Breast	268,600	30%
Lung & bronchus	116,440	13%	Lung & bronchus	111,710	13%
Colon & rectum	78,500	9%	Colon & rectum	67,100	8%
Urinary bladder	61,700	7%	Uterine corpus	61,880	7%
Melanoma of the skin	57,220	7%	Melanoma of the skin	39,260	4%
Kidney & renal pelvis	44,120	5%	Thyroid	37,810	4%
Non-Hodgkin lymphoma	41,090	5%	Non-Hodgkin lymphoma	33,110	4%
Oral cavity & pharynx	38,140	4%	Kidney & renal pelvis	29,700	3%
Leukemia	35,920	4%	Pancreas	26,830	3%
Pancreas	29,940	3%	Leukemia	25,860	3%
All Sites	**870,970**	**100%**	**All Sites**	**891,480**	**100%**

Estimated Deaths

Males			Females		
Lung & bronchus	76,650	24%	Lung & bronchus	66,020	23%
Prostate	31,620	10%	Breast	41,760	15%
Colon & rectum	27,640	9%	Colon & rectum	23,380	8%
Pancreas	23,800	7%	Pancreas	21,950	8%
Liver & intrahepatic bile duct	21,600	7%	Ovary	13,980	5%
Leukemia	13,150	4%	Uterine corpus	12,160	4%
Esophagus	13,020	4%	Liver & intrahepatic bile duct	10,180	4%
Urinary bladder	12,870	4%	Leukemia	9,690	3%
Non-Hodgkin lymphoma	11,510	4%	Non-Hodgkin lymphoma	8,460	3%
Brain & other nervous system	9,910	3%	Brain & other nervous system	7,850	3%
All Sites	**321,670**	**100%**	**All Sites**	**285,210**	**100%**

Figure 1.2. The ten leading cancer types for the estimated new cancer cases and deaths by Sex, United States, 2019. Estimates exclude basal cell and squamous cell skin cancers and in situ carcinoma except urinary bladder (Siegel et al., Cancer Statistics, 2019).

In Portugal**,** according to the Global Cancer Observatory, there were 58199 new cancer cases and 28960 cancer deaths in 2018. Colorectal, breast, prostate, and lung cancers are the most common cancers diagnosed, with gastric cancer also showing a high incidence in both sexes (Figure 1.3).

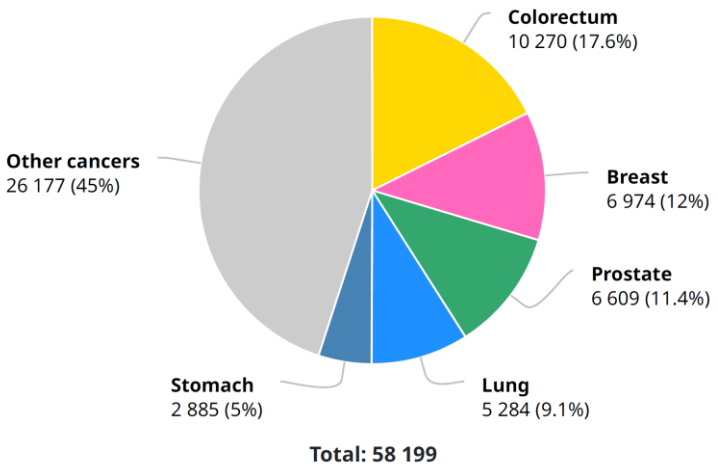

Figure 1.3. Number of new cancer cases in the portuguese population in 2018 for both sexes and all ages (International Agency for Research on Cancer - World Health Organization, 2018).

Nowadays there are many effective methods to treat the cancer disease, such as surgery, radiation, and chemotherapy, and also new methods are being developed to increase the likelihood of survival with minor side effects like immunotherapy (Ke et al., 2017). However, some types of cancer still have a high mortality rate, like lung cancer, that is responsible for the death of nearly 25% of all cancer cases, and prostate cancer with a mortality rate of 10% (Siegel et al, 2019). Also, BC has a high mortality rate with 1 in 7 women dying from this disease.

1.1.1 Breast Cancer

Breast cancer is the major type of cancer diagnosed among women worldwide, and the second leading cause of cancer death (Siegel et al., 2018; Siegel et al., 2019)(Figure 1.4). In women, approximately 1 in 4 cancer cases are BC, which is correlated with hereditary and genetic factors, but mainly with non-hereditary factors like the nutrition, anthropometry and physical activity (Siegel et al., 2018). Breast cancer is a highly heterogeneous group of genetical and epigenetical diseases, exhibiting a variety of clinical features (Riaz et al., 2013; Dai et al., 2017).

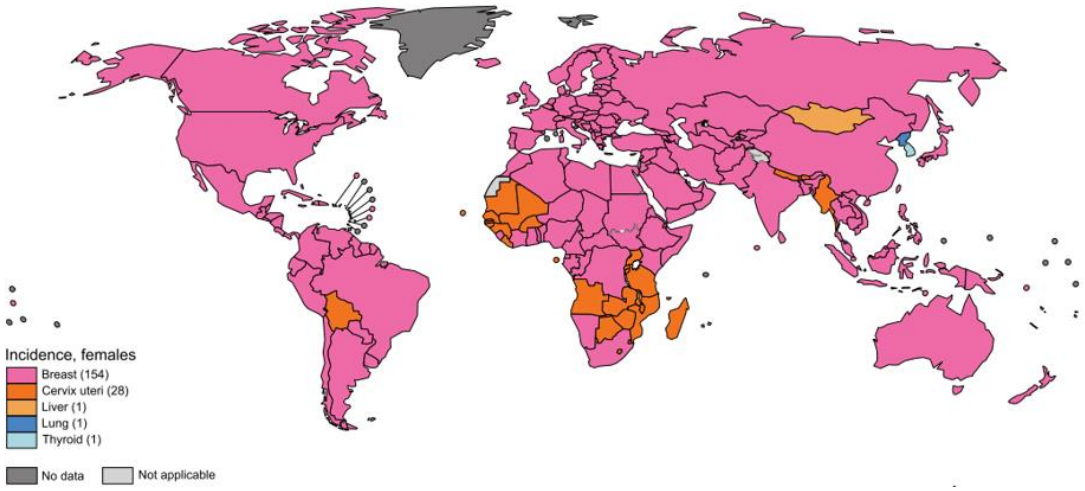

Figure 1.4. Global maps presenting the most common type of cancer incidence in 2018 in each country among women (Siegel et al., 2018).

Breast cancer can be classified into different subtypes based on the gene expression profile: basal-like, ErbB2^{+}/human epidermal growth factor 2 (HER2)$^{+}$, normal breast-like, luminal subtype A and luminal subtype B (Malhotra et al., 2010)(Figure 1.5).

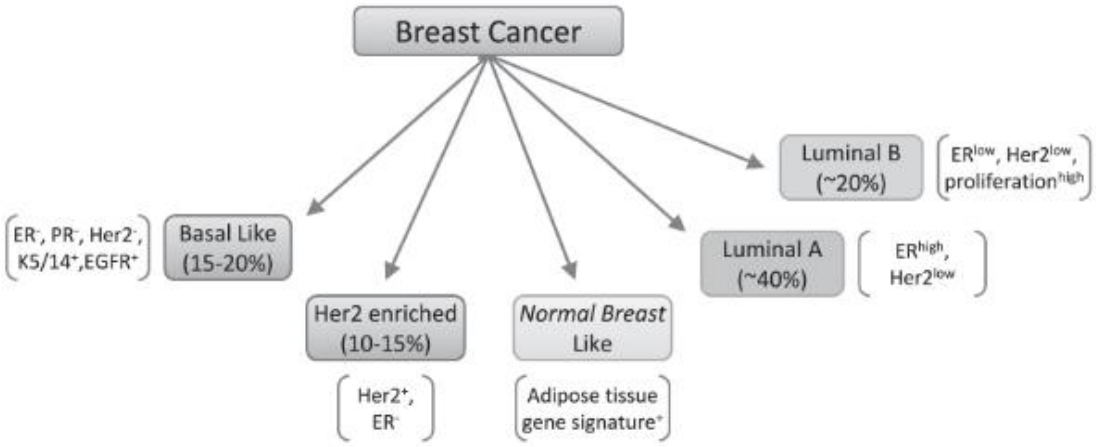

Figure 1.5. Molecular classification of BC. Breast cancer can be divided into five different subtypes: basal-like; HER2$^+$; normal breast like; luminal A and luminal B based on the gene expression profile (adapted from Malhotra et al., 2010).

The luminal tumors are positive for the estrogen (ER) and/or progesterone (PR) hormone receptors, and the majority responds well to therapy. Luminal A tumors (ER$^+$, PR$^+$, HER$^-$) which represent the most common BC subtype, are characterized by high expression levels of ER and/or PR receptors and low proliferation (Ozlem Yersal et al., 2014). Patients with luminal A BC have a good prognosis and a small relapse rate (Ozlem Yersal et al., 2014). The luminal B tumors (ER$^+$, PR$^+$, HER2$^+$) have a more aggressive phenotype and higher proliferation rate than the luminal A tumors, which leads to a worse prognosis (Ozlem Yersal et al., 2014)(Figure 1.6). HER2$^+$ tumors are characterized by the expression of the HER2 receptor that promotes uncontrolled growth, proliferation, invasion, and metastasis of cancer cells. Though HER2$^+$ have a more aggressive biological and clinical behavior (Figure 1.6), treatments that specifically target HER2, e.g. monoclonal antibodies Trastuzumab (Herceptin) and Pertuzumab (Perjeta), are very effective against this type of cancer. These treatments are so effective that the prognosis for HER2$^+$ BC is actually quite good (Ozlem Yersal et al., 2014; Dai et al., 2015). Basal-like cancers, which are often found in women with BRCA1 mutations, are infiltrating ductal tumors with solid growth pattern, especially aggressive clinical behavior (Figure 1.6) and high rate of metastasis (Ozlem Yersal et al., 2014). These tumors are generally triple-negative breast cancers (TNBC) since they do not express the ER and PR hormones nor the HER2 protein. However, they typically overexpress the epidermal growth factor receptor (EGFR) and different combinations of basal cytokeratins CK5, CK14, CK17 (Ozlem Yersal et al., 2014; Reis et al., 2006). Normal breast-like cancers are poorly characterized and have been grouped into the classification of intrinsic subtypes with fibroadenomas and normal breast samples, and usually do not respond to chemotherapy (Ozlem Yersal et al., 2014; Dai et al., 2015). This type of BC lacks the expression of ER, PR, and HER2 proteins, and can also be classified as TNBC but not basal-like since it is negative for CK5 and EGFR. The metastasis of BC usually occurs to the bones, lungs, liver, and brain (Ozlem Yersal et al., 2014).

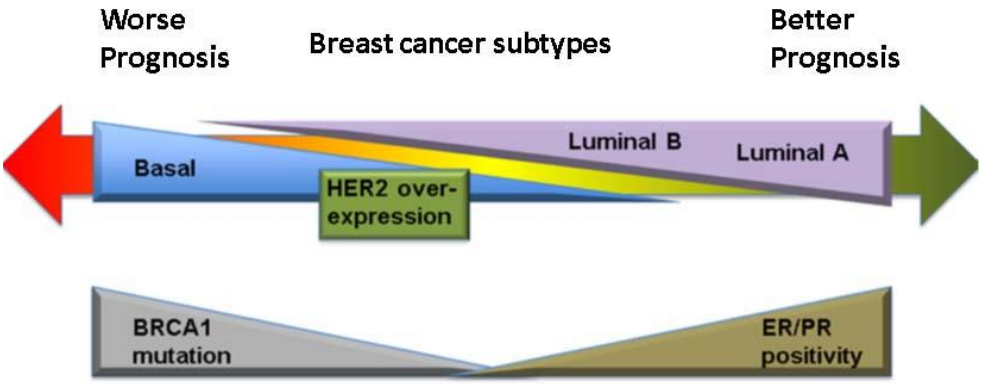

Figure 1.6. Patient outcome based on BC subtypes. The luminal A and luminal B BCs are positive for ER and PR and usually have a Better prognosis. $HER2^{+}$ BC carry a poor prognosis but respond well to target therapy. Basal-like BCs are often associated with the BRCA1 mutation and have the worse prognosis (adapted from Dai et al., 2015).

1.2 Notch Signaling Pathway

1.2.1 History of the Notch

In March 1913, Thomas Hunt Morgan's group identified a mutation in *Drosophila*, that they called "*Notch".* This mutation was responsible for a loss of a wing margin tissue from the distal tip of the wing as described by John Dexter in 1914 (Kopan, 2012). Notch mutant flies also exhibited additional wing veins and bristle abnormalities (Kopan, 2012). In the 1930s Donald Poulson was the first one to connect Notch to development through his ground-breaking work on hemizygous Notch mutant embryos (Kopan, 2012). Notch functions as a receptor of a novel intracellular signaling pathway were established in the 1980s and 1990s (Kopan, 2012).

1.2.2 Notch Signaling Pathway

The Notch signaling is an evolutionarily conserved pathway present in most multicellular organisms that is crucial for a multitude of cellular processes, including proliferation, apoptosis, migration, growth, and differentiation, during embryonic and post-natal development by facilitating short-range signaling between cells in contact (Sethi et al., 2011). In mammals, this pathway is constituted by four Notch receptors (Notch1-4) and five Notch ligands (three Delta-Like ligands, DLL1,3 and 4, and two Jagged ligands, JAG1 and 2)(Sethi et al., 2011; Bray., 2016; Aster et al., 2017; Nowell et al., 2017; Meurette et al., 2018).

The Notch signaling pathway is a cell-to-cell communication system that transduces extracellular signals to the nucleus (Figure 1.7). After its synthesis in the endoplasmic reticulum, during the exocytosis process, the Notch receptor is cleaved by convertases proteins at site 1 (S1 cleavage), which regulates their trafficking and signaling activity (Logeat et al., 1998; Gordon et al., 2009; Kopan, 2012). In the Golgi complex, the receptors can be glycosylated by glycosyl-transferases. This glycosylation will determine how the receptors respond to different ligands (Kopan, 2012).

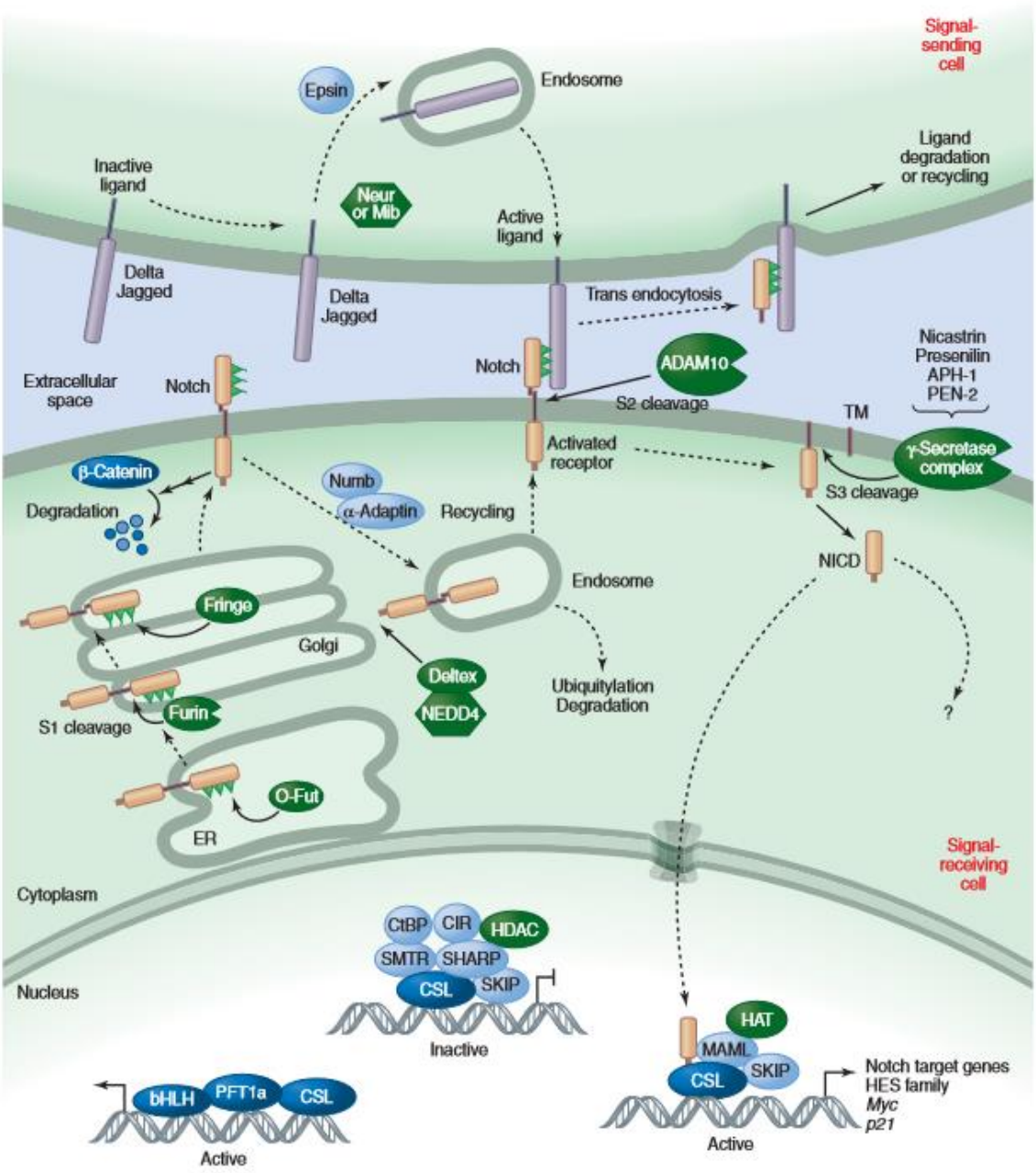

Figure 1.7. The Notch signaling pathway. When Notch ligands bind to Notch receptors on the adjacent cell surface, it elicits sequential cleavages of the receptors that realese the Notch intracellular domain leading to its migration to the nucleus to interact with DNA binding proteins, and driving the expression of target genes (Kopan, 2012).

The activation of the Notch pathway is initiated when the transmembrane region of a ligand expressed in one cell physically interacts with the extracellular region of the receptor on an adjacent cell (Gray et al., 1999; Sethi et al., 2011). Upon ligand binding to the receptor, an unfolding of the juxtamembrane negative control region (NRR) of the receptor occurs, which allows access to the extracellular metalloprotease ADAM10 to remove the extracellular domain region of the receptor by cleaving at site 2 (S2 cleavage)(Brou et al., 2000; Sethi et al., 2011; Kopan, 2012).

A third cleavage occurs in the receptor when the γ-secretase complex cuts the transmembrane domain at site 3 (S3 cleavage)(Kopan, 2012), releasing the Notch intracellular domain (NICD) (Figure 1.7)(Schroeter et al., 1998; Mumm et al., 2000; Six et al., 2003; Sethi et al., 2011). The released NICD then migrates to the nucleus, due to its nuclear localization sequence, where it interacts with the DNA-binding protein CSL (CBF-1), recruiting the adaptor protein Mastermind-like (MAML). This complex then recruits the transcriptional co-activator HATp300 and basal components of the transcription machinery to modulate the expression of Notch target genes, such as the Hes and Hey family genes, p21, c-Myc (Figure 1.7)(Logeat et al., 1998; Wu et al., 2000; Iso et al., 2003; Kopan et al., 2009; Sethi et al., 2011; Kopan., 2012)

The Notch pathway is extremely dosage-sensitive because there is no signal amplification step or secondary messengers to transmit the signal from the cell surface to the nucleus. Accordingly, every cleaved Notch molecule generates one signaling unit, and tuning the effectiveness of receptor-ligand interaction directly determines the amount of NICD in the nucleus and consequently the expression levels of the target genes (Kopan., 2012; Yamamoto et al, 2014).

To achieve a productive activation of the Notch signaling pathway the binding of the Notch receptor with the ligand needs to be in Trans and never in Cis. This means that if one cell is expressing Notch receptors, the neighboring cells need to be expressing the ligand for activation of the Notch pathway to occur (Kopan, 2012). If cells express the receptor and the ligand simultaneously, which is often the case, the ratio between the number of receptors and ligands will determine if a cell is a signal sending or a signal receiving. If the receptors are more abundant than the ligands the cell is a signal receiving cell. In case the ligands are more abundant, then the cell is a signal sending cell (Kopan, 2012).

1.2.3 Structure of the Notch Receptors and their Canonical Ligands

As described above, in mammals the Notch signaling pathway is composed by four receptors (Notch receptors 1-4) and five canonical ligands, divided in two families: the Delta-Like family which includes the DLL1, DLL3 and DLL4, and the Serrate (Jagged) family with the JAG1 and JAG2 ligands (Kopan et al, 2009). Each ligand can bind to each receptor and generates various distinct cellular responses (Andersson et al., 2011).

The Notch receptors are single-pass type-1 transmembrane proteins divided into three domains: the extracellular domain (NECD), a transmembrane domain (TMD) and NICD (Yavropoulou et al., 2015)(Figure 1.8). The NECD contains 29 to 36 tandem epidermal growth factor-like repeats (EGFs) that can be calcium-binding domains that influence signaling productivity (Timmerman et al., 2008). Moreover, these EGFs have great importance for the receptor structure and in the ligand-binding affinity (Cordle et al., 2008). A negative regulatory region (NRR) follows the EGFs region. It is composed of three cysteine-rich Lin12-Notch repeats (LNR) and a heterodimerization domain (HD)(Kopan et al., 2009).

The NRR inhibits Notch activation in the absence of ligands (Sethi et al., 2011). Next to the NRR region is the TMD that is followed by NICD. The NICD comprises a Rbp-associated Molecule (RAM) domain that is linked to seven intercellular ankyrin (ANK) repeats by a long and unstructured linker containing a nuclear localization sequence (NLS), which allows the nuclear translocation of the NICD. Right after the ANK domain is an extra NLS and a transactivation domain (TAD). In the C-terminal, a PEST sequence is present, that is responsible for the regulation of NCID stability and protein turnover (Kopan et al , 2009; Sethi et al., 2011). Notch receptor EGFs 11 and 12 are crucial in the binding between the receptor and the ligand (Rana et al., 2012) but additional EGFs may also contribute to ligand binding (Sharma et al., 2013). The receptors are translated in the endoplasmic reticulum (ER) and travel to the plasma membrane through the exocytic pathway while many posttranslational modification events occur. In the ER, the signal sequence at the N-terminal is cleaved off and the NECD undergoes sugar modifications mediated by protein glycosyltransferases (Rana and Haltiwanger, 2012; Yamamoto et al , 2014).

Ligands are also type-1 transmembrane proteins. All ligands share a common ECD organization that comprises an N-terminal domain followed by a Delta/Serrate, and Lag2 (DSL) domain and tandem EGF repeats (Kopan et al., 2009; Yamamoto et al., 2014; Yamamoto et al., 2010) (Figure 1.8). The DSL domain is highly conserved in the ligand family (Glittenberg et al., 2006; Yamamoto et al., 2010). Different studies reported that alterations in the sequence of the amino acids of the DSL domain lead to a loss of function in Notch signaling, demonstrating that this domain is essential for ligand-receptor binding (Henderson et al., 1997; Henderson et al., 1994; Tax et al., 1994). The EGF domains EGF1 and EGF2 were shown to contain regions (named DOS) important for efficient binding of the ligands to the receptors (Lafkas et al., 2015). The N-terminal region has also been reported to be important for the ligand function (Cordle et al., 2008). Based on these observations, as well as on studies on the Notch ligand interactions with the Notch receptors, a ligand minimal binding region required for the activation of the receptor that includes the N-terminal and the DSL domains and the EGF1-3 repeats was established (Henderson et al., 1994, 1997; Tax et al., 1994; Cordle et al., 2008). A single TMD and an intracellular domain (ICD), which presents very low sequence homology amongst the various ligands, follow the EGFs from the ligands (Pintar et al., 2007).

The synthesis of the ligands occurs in the ER, these then pass through the Golgi complex, and are exocytosed. Vesicular trafficking to the membrane, endocytosis, and recycling of proteins play important roles in fine-tuning the signaling strength (Yamamoto et al., 2010; Charng et al., 2014; Yamamoto et al., 2014).

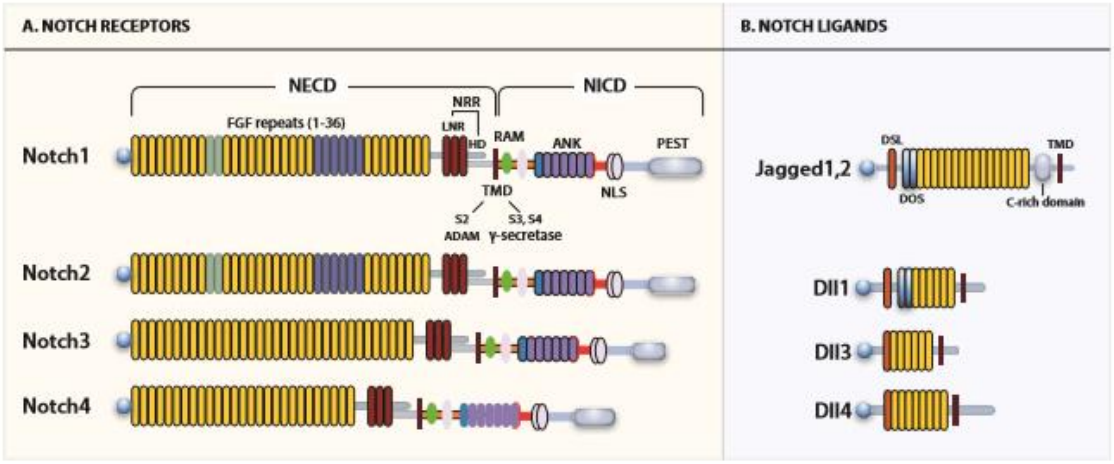

Figure 1.8. Schematic representation of Notch Receptors and Ligands. A- Representation of the four Notch receptors. B- Representation of the five Notch ligands. Notch receptors contain multiple extracellular EGF repeats. There are four mammalian Notch variations (Notch1-4) that differ in the number of repeats (29-36). EGF repeats 11-12 (yellow) and 24-29 (purple) mediate ligand interactions. Mammalian Notch proteins are cleaved by furin-type convertases, which convert the Notch polypeptide into an NECD-NICD (Notch extracellular domain-Notch transmembrane and intracellular domain) heterodimer that is connected by noncovalent interactions between the halves of the heterodimerization domain (Yavropoulou et al., 2015).

1.2.4 Notch Signaling and Diseases

The Notch signaling pathway plays crucial roles in a multitude of cellular processes. This includes the correct formation of the vascular system, development of T and B cells - either in central and peripheral lymphoid organs (Shang et al., 2016; Lamy et al., 2017), self-renewal and differentiation of the stem cells, commitment of lymphoid cell lineages (Clements et al., 2011; Lamy et al., 2017), regulation of bone physiology and breast biology (Dufraine et al., 2008; Yashiro-Ohtani et al., 2010; Clements et al., 2011; Shang et al., 2016; Lamy et al., 2017). Moreover, it participates in the innate immune responses and inflammation processes (Shang et al., 2016). In the intestine, due to the very high turnover rate of the intestinal epithelium cells, processes like proliferation, differentiation, and cell death must be tightly regulated in order to ensure homeostasis. The regulation of these processes is controlled by a relatively small number of signaling pathways, including the Notch pathway (Wilson et al., 2006). Importantly, the multiple roles of Notch signaling vary according to the tissue and cellular context (Wilson et al., 2006; Liu et al., 2010).

Abnormal activation of this pathway is associated to various diseases. Haploinsufficiency of the Notch2 and JAG1 proteins are implicated in Alagille syndrome (Andersson et al., 2011), and mutations in the Notch2 and Notch3 genes have been linked with the Hajdu-Cheney and Cadasil syndromes, respectively (Regan et al., 2013; Lamy et al., 2017). JAG2 contributes to rheumatoid arthritis (Lamy et al., 2017), and deregulation of both JAG1 and JAG2 has been shown to be implicated in airway diseases (Lafkas et al., 2015). Moreover, diverse types of cancer have been associated with the malfunction of this pathway (Lamy et al., 2017).

1.2.5 Notch as an Oncogene

T-cell acute lymphoblastic leukemia (T-ALL) was the first type of cancer associated with the Notch oncogenic role, through a chromosomal translocation that promoted the constitutive expression of a truncated form of the Notch1 protein (Ellisen et al., 1991; Yamamoto et al,2014; Brzozowa-Zasada et al., 2017; Koch et al., 2018). Many studies have shown that the deregulation of the expression of the Notch receptors and/or ligands contribute to the development of solid cancers, such as brain, breast, liver, pancreatic, ovarian, cervical, prostate, kidney, melanoma, renal and lung (Dang et al., 2000; Fiona et al, 2000; Espinoza et al., 2013; Lamy et al., 2017; Sales-Dias et al., 2019).

Notch signaling can promote tumor growth by increasing cancer cell proliferation and survival, cancer cell escape from immune surveillance, and inducing angiogenesis (Meurette and Mehlen, 2018). Notch signaling also provides epithelial tumor cells with migratory properties, facilitating metastasis (Sethi et al., 2011; Meurette and Mehlen., 2018). In addition, Notch signaling has been associated with cancer progression through the regulation of the epithelial-to-mesenchymal transition (a process needed for the metastasis of epithelial cancer cells) in cooperation with the TGFβ signaling (Zavadil et al., 2004; Timmerman et al., 2008) and β-catenin activity (Balint et al., 2005; Sethi et al., 2011). Moreover, Notch can also contribute to tumor growth and resistance by causing an immunosuppressive microenvironment by affecting the numbers and specific populations of immune cells (such as by increasing the number of regulatory T cells), cytokines, growth factors, among other factors (Meurette and Mehlen, 2018). As mentioned above, and as demonstrated in many studies, the Notch pathway tightly interacts with other signaling pathways, such as the NF-κB, PI3K/AKT/mTOR, MAPK, Wnt, BPM, in various types of cancers to potentiate the oncogenic process. Importantly, the crosstalk between Notch and the various other signaling pathways is dictated by the cellular context (Liu et al., 2006; Espinoza et al., 2013; Fitzgerald et al, 2000; Espinoza et al., 2013).

1.2.6 Notch as Tumor Suppressor

Despite having an oncogenic role, some studies have shown that Notch can also have a tumor suppressor effect (Koch et al., 2018), as a consequence of its cell-intrinsic role in promoting cell cycle exit and differentiation, thus eliminating potential cancer stem cells (CSCs) and tumour-initiating cells (Wilson et al., 2006; Koch et al., 2007; Nowell et al., 2017). For example, the development and progression of squamous cell carcinomas in epithelial tissues is associated with loss of Notch1 and Notch2 receptors (South et al., 2014; Pickering et al, 2015; Nowell et al., 2017). Studies in small-cell lung cancer, identified recurrent loss-of-function mutations in Notch family genes, particularly Notch1, in human and mouse (George et al., 2016; Nowell et al., 2017).

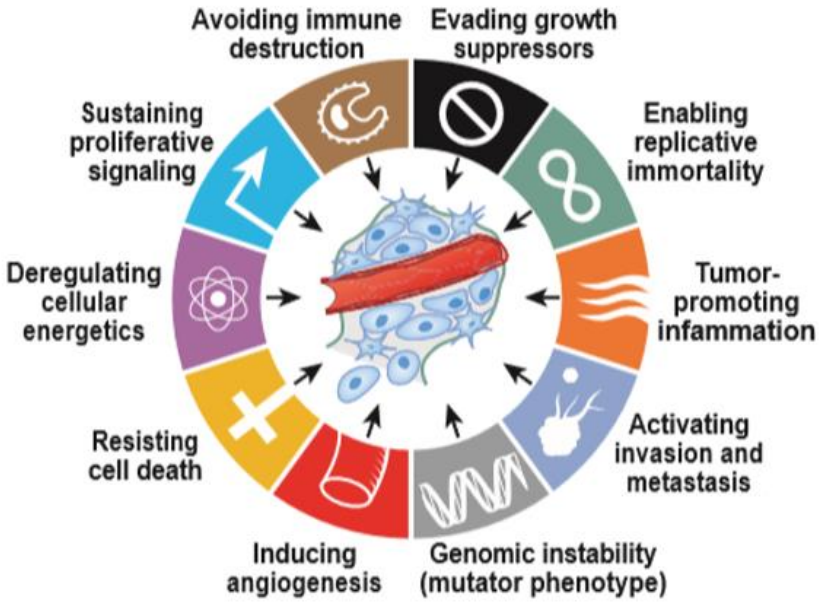

Figure 1.9. Notch signaling oncogenic and tumor supressor effects. Notch signaling has many oncogenic effects, however, it can also have a tumor suppressive effect in the tumor such as the tumor-promoting infammation (adapted from Aster et al., 2017).

1.2.7 Notch in Breast Cancer

Deregulated Notch signaling, through high expression and/or activation or its receptors or ligands, contributes to BC development (Politi et al., 2004; Mittal et al., 2009; Acar et al., 2016; Brzozowa-Zasada et al., 2017; Lamy et al., 2017). The first evidence of Notch influence in BC was a study developed in mouse models where a virus insertion in Notch1 and Notch4 gene loci, causing its constitutive expression, lead to BC development (Gallahan et al., 1987; Anne Diévart, 1999; Lamy et al., 2017).

Changes in the Notch pathway occur early in the disease progression, as demonstrated in several studies, showing that Notch signaling components are upregulated in early non-invasive stages of BC (Mittal et al., 2009; Lamy et al., 2017).

Notch1 overexpression has been documented to promote cell survival, proliferation, cell adhesion, migration, and invasion, and EMT in BC cell models (Xing et al., 2011; Bolós et al., 2013; Shao et al., 2015) as well as in a wide variety of human breast carcinomas, namely in TNBC (Lamy et al., 2017). The carcinogenic effect of the Notch2 receptor is still unclear, however, high levels of this receptor have been detected in ER^+ and luminal BCs (Fu et al., 2010; Lamy et al., 2017). High levels of Notch3 have been identified in $HER2^-$ BC (Hirose et al , 1994). Some studies indicate that Notch4 is involved in BC recurrence through its ability to regulated BC stem cell (BCSC) activity (Harrison et al., 2010; Lamy et al., 2017). JAG1 and DLL4 are the two ligands shown to have the major interference in BC biology (Lamy et al., 2017).

JAG1 has been associated with increased BC relapse, drug resistance, and metastasis

(Reedijk et al., 2005; Rizzo et al., 2008; Lamy et al., 2017), and Notch activation via JAG1 is directly implicated in tumor growth by maintaining cancer stem cell (CSC) populations, promoting cell survival, proliferation, adhesion, metastasis, tumor angiogenesis and inhibiting apoptosis (Li, 2014; Andrieu et al., 2016; Lamy et al., 2017). DLL4 is associated with tumor angiogenesis (Dufraine et al., 2008), nodal and distant metastasis (Kontomanolis et al., 2014), and may confer drug resistance to BC cells (Lamy et al., 2017; Wang et al., 2017). JAG2 has also been implicated in the promotion of BC metastasis and self-renewal of BCSC (Xing et al., 2011; Lamy et al., 2017). Simultaneous high expression of Notch1 and JAG1 correlate with poor prognostics in various BC subtypes (Reedijk et al., 2005; Mittal et al., 2009). Notch signaling can also cooperate with other oncogenes, such as Myc, in the promotion of BC (Efstratiadis et al., 2007; Mittal et al., 2009).

1.2.8 Notch Inhibition as a Promising Approach for Cancer Treatment

Since the Notch pathway has an important role in development, progression, recurrence and drug resistance of many different cancers, it is considered an important therapeutic target. The first approach to Notch inhibition was based on the use of γ-secretase inhibitors (GSI). These small molecules were responsible for reducing the levels of intracellular activated Notch by inhibiting the γ-secretase enzyme, responsible for the cleavage 3 of the Notch receptors during its activation (reviewed in Lamy et al., 2017). Various GSI molecules were developed and entered clinical trials. However, many clinical studies proved that these treatments caused serious side effects, especially gastrointestinal toxicity (Tolcher et al., 2012; Andersson et al, 2014, Lamy et al., 2017). Besides participating in cancer development and progression when dysregulated, biologic levels of Notch activity are necessary for normal cellular processes like intestine cell renewal. Accordingly, the sustained inhibition of Notch receptors by GSIs significantly affect the intestines normal biology (Fre et al., 2005; Lamy et al., 2017). The combination of chemotherapy with GSIs presented promising results in various clinical studies supporting the hypothesis that Notch inhibition and chemotherapy may have a synergistic effect (Gilbert et al., 2010; Lamy et al., 2017). Recently, to prevent the binding between the overexpressed receptors and ligands, and subsequent hyperactivation of the Notch signaling, antibodies have been developed and entered into clinical trials in patients with advanced and/or metastatic cancers. Specific antibodies against Notch receptors (Sharma et al., 2012), and ligands have been developed during the last years with promising therapeutic effects (Davis et al., 2013; Li, 2014; Zheng et al, 2017; Lamy et al., 2017).

1.3 JAG1

JAG1 is one of the five canonical ligands of the Notch signaling pathway (Li., 2014; Grochowski et al., 2016). In 1995 the rat homolog ligand was cloned for the first time and named JAG1 due to the similarity to the Drosophila gene serrate, and the first discovered

function of JAG1 was the prevention of muscle cell differentiation (Lindsell et al., 1995; Grochowski et al., 2016). In humans, the JAG1 gene was mapped on the short arm of chromosome 20 in 1997 (Grochowski et al., 2016). Later on, mutations in JAG1 were demonstrated to cause the Alagille syndrome, an autosomal dominant multisystem disorder (Li et al., 1997; Grochowski et al., 2016).

The JAG1 gene consists of 26 exons, encoding a protein with 1218 amino acid residues of approximately 124 kDa (Oda et al., 1997; Grochowski et al., 2016). It is a type-1 transmembrane protein with a small intracellular domain (ICD), a transmembrane domain (TMD) and a large extracellular domain (ECD)(Figure 1.10). The ECD is divided into four motifs. A 21-amino acid signal peptide to ensure that after synthesis the protein migrates to the cell membrane surface. An N-terminal region comprising a C2 domain that binds to phospholipid bilayers (Chillakuri et al., 2013). A DSL domain essential for the binding to the Notch receptors (as well as to the CD46 complement regulatory protein essential for the function of helper T cells (Friec et al., 2012)), followed by 16 EGF repeats, important for increasing the affinity to the Notch receptors (mostly EGF1 and EGF2). A cysteine-rich region (CRD) that is necessary to create the disulfide bonds responsible for protein stabilization. A C-terminus with a PDZ-ligand motif linked with the induction of intrinsic reverse signaling within the ligand expressing cells (Li, 2014; Guarnaccia et al., 2004; Kopan et al, 2009; Chillakuri et al., 2012; Grochowski et al , 2016). The TMD is a 26 amino acid sequence in a helical form that is responsible for anchorage of the ligand to the cellular membrane. The ICD is composed by 126 amino acid residues (Li, 2014; Grochowski et al , 2016).

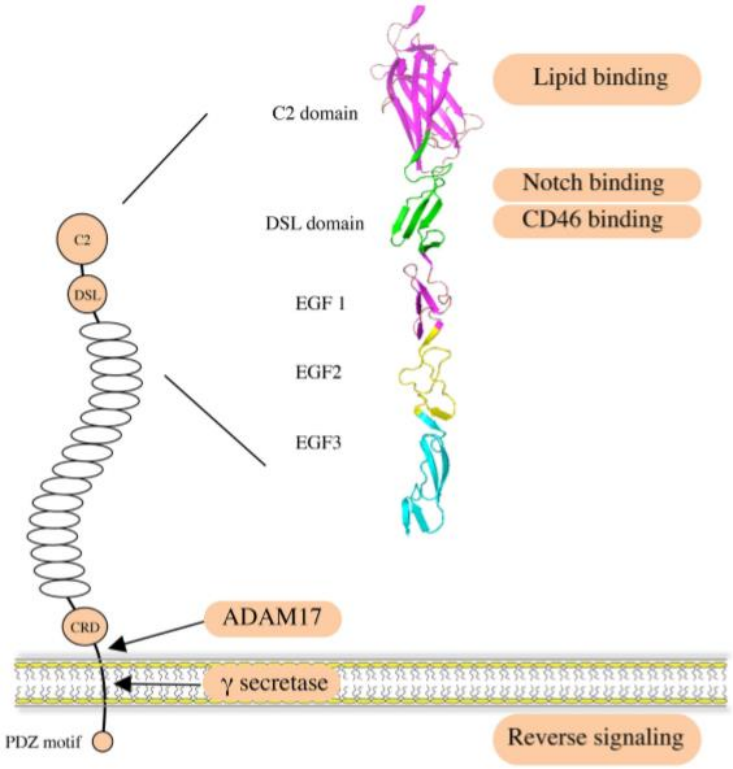

Figure 1.10. Human JAG1 Stuctrure. JAG1 is a type I transmembrane protein with an extracellular region containing 16 EGF repeats. The DSL domain that is located in the N-terminal region is reponsible for the binding to Notch receptors and the CD46 protein. A C2 domain at the very N-terminus reduces Notch activation upon binding to phospholipid bilayers. JAG1 can be cleaved by ADAM17 metalloprotease to release soluble protein that mediates paracrine Notch signaling on neighboring cells. It can also be processed intramembranously by γ-secretase to release the intracellular domain that contains a PDZ motifi responsible for the intrinsic reverse signaling induced by JAG1 (Li, 2014).

JAG1 is expressed throughout the human body at different levels, depending on the developmental phase and tissue. Heart, placenta, pancreas, and prostate have high JAG1 expressing levels, whereas lung, liver, kidney, thymus, testis, and leukocytes present low expressing levels (Jones et al, 2000; Gasperowicz et al., 2008; Grochowski, et al, 2016). Glycosylation of the Notch receptors highly influences the binding and activating capacity of JAG1 (Benedito et al., 2009; Rana et al., 2012; Li, 2014). Importantly, soluble JAG1 ECD has been shown to promote Notch signaling activity between endothelial cells and tumor cells, allowing the activation of the pathway in more distant cells. This means that JAG1 mediates the paracrine activation of the Notch pathway (Li, 2014).

1.3.1 JAG1 and Cancer

The involvement of JAG1 in cancer was initially discovered in 2005 with a study that correlated BC survival with JAG1 expression levels (Reedijk et al., 2005; Grochowski et al , 2016). Since then, JAG1 has been shown to be overexpressed in many types of cancers, such as TNBC, pancreatic, gastric, colorectal, cervical, ovarian, brain, and lung, and associated with tumor aggressiveness and decreased overall survival. JAG1 overexpression contributes to tumor growth, metastasis, recurrence and drug resistance, by acting directly on cancer cells and

modulating the tumor microenvironment. JAG1 promotes cancer cell survival, proliferation, migration, invasion, and metastasis. In the tumor microenvironment, JAG1 promotes tumor-associated angiogenesis and inhibits the immune responses against cancer cells by inducing regulatory T cells through modulation of various cytokines, and growth factors (Choi et al., 2008; Lu et al., 2013; Xing et al., 2013; Li, 2014; Grochowski et al., 2016).

Importantly, JAG1 has been shown to contribute to patient relapse, cancer metastasis and increased invasive potential, and resistance to several cancer drugs through its ability to promote the maintenance and expansion of CSCs (Creighton et al., 2009; Singh et al., 2010; Li, 2014). For instance, an *in vitro* study in BC demonstrated that the promotion of CSC-renewal is due to high expressing levels of JAG1 (Sansone et al., 2007; Li, 2014). Other studies showed that JAG1 is the main ligand driving Notch signaling-mediated CSCs maintenance.

Epithelial-mesenchymal transition (EMT) confers to the tumor cells the invasion and metastasis properties to invade the surrounding tissues and to colonize distant organs (Li, 2014). Several studies demonstrated the involvement of JAG1 in the EMT process in various cancers (Leong et al., 2007; Li, 2014). Studies in BC have shown that JAG1 is responsible for the dissemination of cancer cells to the bones and brain (Sethi et al., 2011; Xing et al., 2013).

Notably, other cancer related pathways such as TGF-β, WNT/β-catenin, IL-6, and NF-κB can induce the expression of JAG1 to potentiate their oncogenic effects (Zavadil et al., 2004; Sansone et al., 2007; Rodilla et al., 2009; Chen, et al , 2010; Li, 2014).

Considering the major effects of JAG1 in various aspects of tumor biology, JAG1 has emerged as a particularly attractive therapeutic target in various types of aggressive and/or metastatic cancer, Including TNBC (Li, 2014).

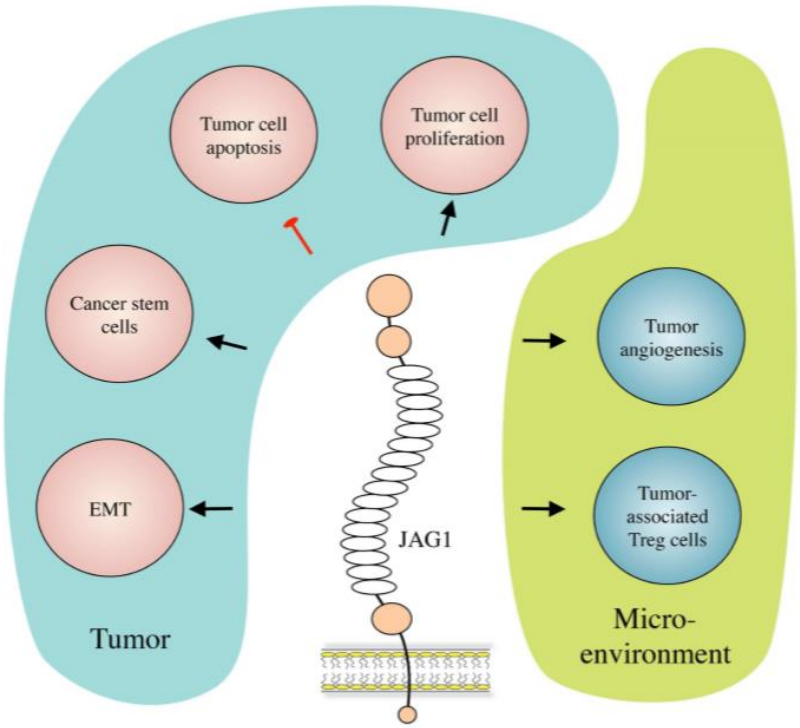

Figure 1.11. JAG1 effects in cancer. JAG1 induces tumor cell growth and inhibits their apoptosis, contributes to cancer stem cell population maintenance, and enhances cancer metastasis by inducing EMT. In the tumor microenvironment, JAG1 promotes tumor-associated angiogenesis, and inhibits tumor-specific immunity by inducing regulatory T cells (Li, 2014).

1.4 Antibodies

Antibodies (Ab) are soluble glycoproteins belonging to the immunoglobulin (Ig) family (Lòpez-Ribot et al., 2007; Schroeder et al , 2013). They are produced by plasma cells and they are found in the peripheral blood and external body fluids (Lòpez-Ribot et al., 2007). Antibodies have several functions: to neutralize viruses and identify and mark microbes and foreign/abnormal antigens for destruction (Lòpez-Ribot et al., 2007). Antibody-based therapy is now one of the most successful and important strategies for treating patients with many immune-mediated diseases and hematologic and solid tumors (Scott et al., 2012; Ecker et al., 2015).

1.4.1 Antibodies Structure

The antibodies structure consists of two identical copies of a heavy chain (HC) and two identical copies of a light chain (LC) in a Y-shaped structure. Each HC has approximately 50 kDa (450 amino acid residues) and each LC 25 kDa (212 amino acid residues) (Lòpez-Ribot et al., 2007; Schroeder et al, 2013). The heavy and light chains are linked by disulfide bonds (Williams et al, 1988; Schroeder et al, 2013). The N-terminal region of the Ab is characterized by sequence variability regions in both heavy (V_H) and light (V_L) chains (Lòpez-Ribot et al., 2007).

The Ab also contains a hinge region between the C_H1 and the C_H2 that confers flexibility to the two antigen-binding sites to operate independently, which is important due to the space between the protein molecules or the microbes (Lòpez-Ribot et al., 2007). The remaining Ab sequence is relatively constant either in the LC (C_L) or in the HC (C_H1, C_H2, and C_H3 regions).
Antibodies can also be divided into three fragments: two fragment antigen-binding (Fab) and a fraction crystallized (Fc). The Fab fragment is constituted by the V_L, C_L, V_H, and C_H1 regions, and is responsible for the binding to the antigen. The Fc fragment contains the CH2 and CH3 regions and provides a binding site to immunocompetent cells receptors (Lòpez-Ribot et al., 2007).

There are five different Ig classes (isotypes) of Ab molecules based on the number of Y units and the structure of its carboxy (C)-terminal part on the HC. The five classes of Igs are: IgG, IgM, IgA, IgE and IgD. They differ in their biological properties, functional locations and ability to react with different antigens (Goldsby et al., 2003; Murphy, 2012).
There are two types of LC, the lambda (λ) and kappa (κ), based on small differences in the polypetide sequence. However, each class can have either a λ or κ LC and no functional differences have been found between them (Schroeder et al, 2013).

The Ab binding capacity is influenced by its affinity and avidity to the antigen. Affinity is the strength of the interaction between the Ab and the antigen. Therefore, high affinity means stronger connections to the antigen at a lower Ab concentration. Avidity is the combined strength of multiple interactions between the Ab and the antigen epitopes. It is dependent on the number of epitopes and number of antibody-combining sites (Lòpez-Ribot et al., 2007).

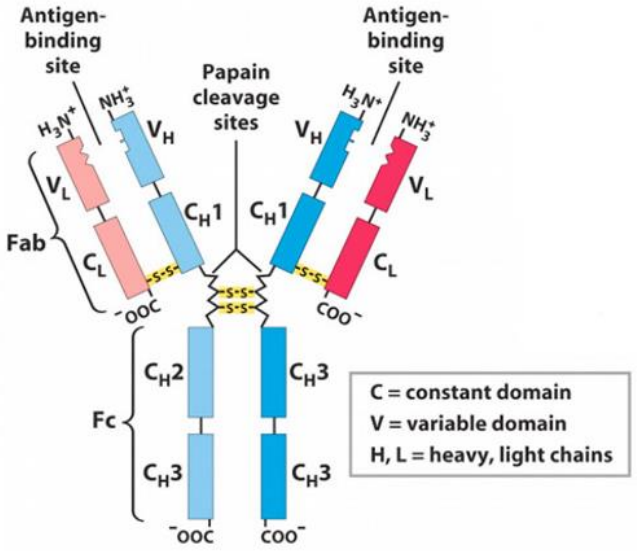

Figure 1.12. Schematic diagram of Ig structure. The Ab is constituted by two light chains and two heavy chains each organized in variable regions (VH, VL) and constant regions (CH1, CH2, CH3, CL) linked together by disulfide bonds. In the centre of the molecule there is the hinge region, represented here as "papain cleavage site". Papain is an enzyme that digests the molecule and divides it into three - two Fab fragments and one Fc fragment. Rose and red – light chains and Blue – heavy chains (Legninger, 5th edition).

The Ab specificity is determined by the variable regions (V_L and V_H). These regions contain amino acid sequences that create a three-dimensional structure specific for each antigen. These sequences are called complementary-determining regions (CDRs), and each chain contains three CDRs (CDR1, CDR2, CDR3) (Lòpez-Ribot et al., 2007). The CDRs in the HC correspond to the amino acid residues 30 to 36, 49 to 65 and 95 to 103, while in the LC correspond to the amino acids 28 to 35, 49 to 59 and 92 to 103 (Murphy, 2011). The rest of the variable domain has a more constant sequence termed the framework regions (FR). There are four frameworks, FR1, FR2, FR3, and FR4, responsible for the CDRs positioning on the surface of the chain creating a hypervariable region at the end of each Ab (Murphy, 2011). CDRs amino acid sequences determine the shape and ionic properties of the antigen-binding site, determining the specificity of the Ab (Murphy, 2011).

The Ab diversity is generated by somatic recombination in B lymphocytes, where the variable gene segments are linked to other gene segments. LC contains VL, JL, and CL gene segments and the HC contains VH, DH, JH, and CH gene segments (Figure 1.13). CL gene segments encode the constant regions (Goldsby et al, 2003). In the assembled LC variable domain, the VL gene segment encodes FR1 to 3, CDR1 and 2, and two thirds of CDR3, while JL encodes the rest of CDR3 and FR4. In the HC variable domain, VH gene segment encodes FR1 to 3, CDR1 and 2 and JH encode FR4. The CDR3 is generated in developing B cells by the joining process, containing the entire DH as well as portions of VH and JH gene segments (Paul, 2013).

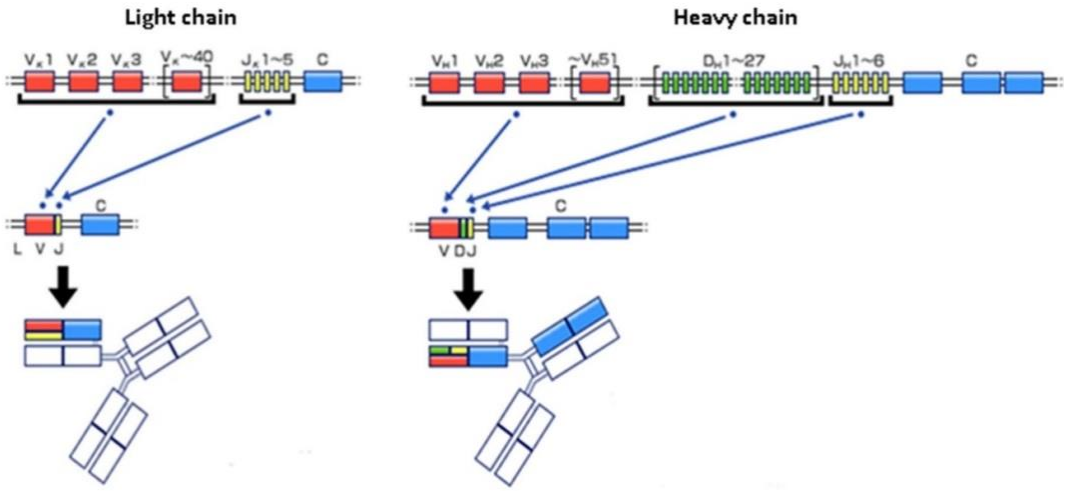

Figure 1.13. Representation of the chromosomal organization of the Ig heavy and light gene clusters. Genes of the heavy chain variable region are divided into the VH, DH and JH gene regions. The genes in the light chain variable region are divided into the VL and the JL gene regions (adapted from https://www.kyowakirin.com/antibody/basics/diversity.html).

Being the Ab glycoproteins, they suffer glycosylation as modifications. Glycosylation alters the charge profile of the Ab and can affect its stability and potency (Mo et al., 2018). Usually, an Ab is glycosylated in the Fc domain with an N-linked glycosylation on Asn297 on each of the two CH2 domains that have been shown to have little impact on Fc functions.

However, the CDRs are unique to each Ab and glycosylation in the CDRs may affect antigen binding (Mo et al., 2018). Variation in glycosylation is observed between Ab molecules as well as within the two chains on the same molecule due to differences in terminal sialic acid, galactose, N-acetyl glucosamine, and fucosylation of the core. The glycans on the CH2 interact with a hydrophobic pocket on the Fc domain that stabilizes the Ab structure (Liu et al., 2006; Sibéril et al., 2006; Schroeder et al, 2013).

1.4.2 Monoclonal Antibodies

Monoclonal antibodies (mAb) are monospecific Ab produced from identical immune cells that derive from a single clone, and are specific for a unique epitope (Xin et al, 2013). mAbs are now being used to treat many diseases, such as cancer, infectious diseases, allergy, asthma, and some autoimmune diseases, where they can neutralize substances, block receptors, bind to cells and modulate the host immune system (Schirrmann et al, 2011). Trastuzumab and pertuzumab are two examples of therapeutic mAbs used for the treatment of patients with HER2-overexpressing metastatic BC (Gianni et al., 2012; Lamy et al., 2017). The use of mAbs as therapeutic agents against Notch in recent years resulted in anti-tumor activity in different types of cancer, with the advantage of overcoming the gastrointestinal toxicities associated with GSIs (Wu et al., 2010; Sharma et al., 2012, 2013; Lamy et al., 2017). Different therapeutic approaches have been followed to develop mAbs towards various Notch signaling proteins. Some consists in targeting the receptor-ligand binding domain while others in blocking the intracellular Notch cleavage by γ-secretase enzyme through specific binding to the NRR (Wu et al., 2010; Sharma et al., 2012, 2013; Lamy et al., 2017). OncoMed Pharmaceuticals developed two therapeutic mAbs: bronticuzumab, targeting Notch1 receptor (Davis et al., 2013) and tarextumab, targeting both Notch2 and 3 receptors (Yen et al., 2015), to increase the efficacy of conventional BC therapies (Lamy et al., 2017). Bronticuzumab showed clinical benefits in phase I studies in patients with advanced solid tumors, in a patient with refractory HER2-negative BC and reduced the number of circulating tumor cells in a patient with colorectal cancer (Davis et al., 2013; Lamy et al., 2017). Tarextumab showed in a phase I study in patients with advanced solid tumors, to prolong stable disease in TNBC, sarcomas, and rectal cancer (Davis et al., 2013; Lamy et al., 2017). In both studies, small toxicity levels were obtained.

1.4.2.1 Antibody Formats

The antigen-binding fragments can be produced by biochemical digestion and include Fab, (Fab')2, and F_V. The Fab fragment is composed of the LC and the variable domain and CH1 from the HC, thus containing one antigen-binding site (Frenzel et al., 2013). Divalent (Fab')2 fragments have two antigen-binding regions, linked by disulfide bonds, and are produced by pepsin digestion of IgG or IgM Abs, which retains a portion of the hinge region. The Fv fragment is the smallest antigen-binding fragment and consists of one variable domain of the HC. The Fv fragments have low stability so single-chain Fv fragments (scFv) were developed, in which one variable region of each light and heavy chain are tethered together by a soluble linker, for stabilization of the molecule. scFvs are produced using genetic engineering

methods. scFv fragments have a complete binding site of an Ab and they are presently the most popular format, as the Fab, of recombinant Abs with wide application in healthcare and biotechnology (Frenzel et al., 2013). Evolution of this platform has also resulted in bi-scFvs, using a linker with 3-11 residues long, and in bispecific antibodies that can cross-link different antigens and thus hold promise as anti-cancer drugs. In addition to conventional Abs, camelid species contain a subset of HC Abs (hcAb) exclusively composed by HC homodimers lacking light chains. The Fab portions of these antibodies, called V_HH, are the smallest antigen-binding regions naturally found. They are stable and can be easily produced in huge quantity by using common simple protein expression systems (Muyldermans, 2013).

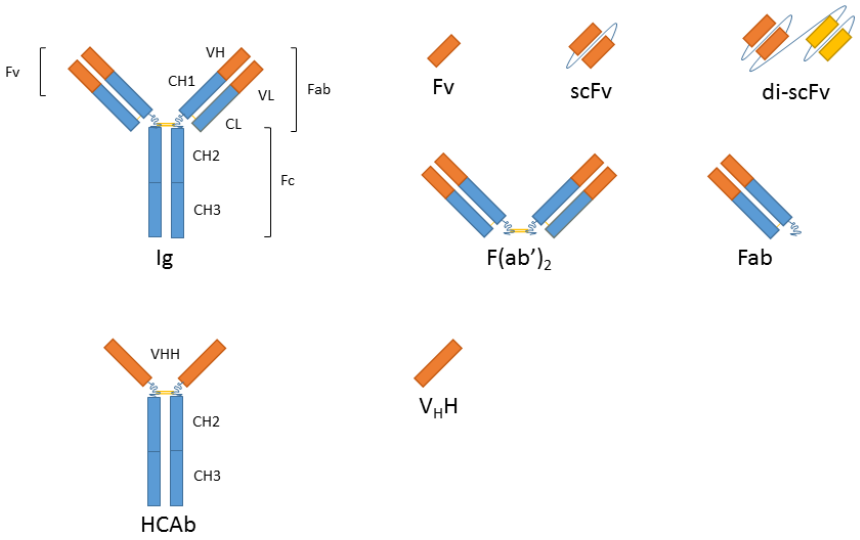

Figure 1.14. Different Ab formats. Representation of several Ab formats, including the intact IgG Ab alongside various representations of Ab fragments. Image from https://www.antibodies-online.com/resources/18/1502/antibody-and-immunoglobulin-alternatives-part-1/).

1.5 Phage Display

The phage display technology was presented by George Smith in 1985. In his work he demonstrated that foreign DNA fragments could be fused to a coat protein-coding gene of filamentous phages and expressed as a fusion proteins on the surface of phages, leaving these intact and operational (Ahmad et al., 2012; Smith and Petrenko, 1997). McCafferty proved that cloned Ab fragments could be similarly displayed on phage particles as functional proteins, and after that, the first libraries of phages were generated (Ahmad et al., 2012;).

The main purpose of this technique is the selection of peptides or proteins capable of binding with high affinity to a specific target, using the phage libraries, for drug and vaccine discovery and development (Dantas-Barbosa et al, 2012; Ahmad et al., 2012;). The phage libraries are usually constructed by mass cloning of a pool of genes encoding millions of variants of ligands into a vector, allowing the effortless construction of highly diverse collections (Hoogenboom et al., 1998). Upon expression, the protein fusion will be incorporated into new

phage particles that are assembled in the bacterium and the fusion product is then displayed on the phage surface (Hoogenboom et al., 1998)(Figure 1.15).

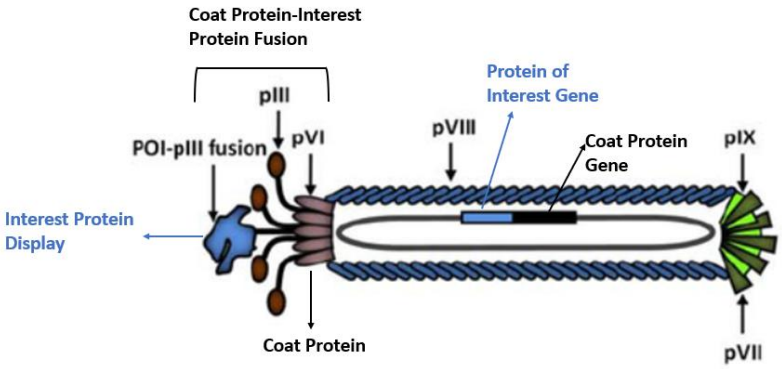

Figure 1.15. Phage Structure. Generic schematic representation of a protein-displaying phage particle. In the phage genome represented in blue is the coat protein gene and in black is the protein of interest gene.

The Phage Display technology is based on the fact that phage phenotype and genotype are physically linked. This allows the enrichment of the selected phage and also further manipulation and development of genetic and biochemical studies of the correspondent displayed proteins (Cabral, 2014; Hammers et al., 2014).

E.coli is the bacteria host normally used in phage display to display scFv and Fabs fragments (Hoet et al., 2005; Schirrmann et al., 2011).

Two different genetic systems have been developed for the expression of the proteins. One inserts directly the Ab genes into the phage genome fused to the wild-type M13 phage protein III gene (McCafferty et al., 1990; Schirrmann et al., 2011). The second and more used uncouples the Ab expression from phage propagation by providing the genes encoding the Ab: pIII fusion proteins on a phagemid in a separate plasmid. This phagemid contains a phage morphogenetic signal for packaging the vector into the assembled phage particles. This makes the Ab gene replication and expression uncoupled from the phage replication cycle, leading to higher genetic stability and a simplification of the Ab gene library amplification. For the production of Ab phage particles, a helper phage is necessary for supplying all structural proteins (Breitling et al., 1991; Hoogenboom et al., 1998; Schirrmann et al., 2011).

Phage display is a robust and versatile technique that can be easily implemented and operated (Dantas-Barbosa et al; 2012; Hoogenboom et al., 1998). It can be used for a variety of objectives, such as the identification of cell/tissue or disease-specific biomarkers, protein-protein interactions, receptor-ligand characterization, epitope mapping, gene delivery, and proteomic, functional genomic approaches and in the development of mAbs that can bind to a target of interest with high affinity (Frenzel et al., 2017).

1.5.1 Types of Phage Display Libraries

Phage Display antibody libraries are composed by the genomic information coding for

Ab variable domains, which can be derived from B cells of immune or naïve donors. These libraries usually display Ab fragments - Fab or scFv, since complete IgG molecules cannot be displayed on the phage surface due to steric hindrance. However, those Ab fragments selected by phage display can be then reformatted into complete IgG molecules and further be used in diagnosis, research and/or therapeutics (Silverman;, 2001; Hammers et al., 2014; Groff et al., 2015).

Based on the source of Ab genes used for their construction, the libraries can be divided into four categories: immune, naïve, semi-synthetic, and synthetic libraries (Rami et al., 2017). Immune libraries are constructed from B cells isolated from the spleen of immunized animals, previously infected with a specific antigen (Schirrmann et al., 2011; Rami et al., 2017). These libraries not only have the advantage that the V-genes contain hypermutations but also have the added feature that they are affinity matured inside the animals. As such, immune libraries are useful for analyzing natural humoral responses or to study *in vitro* immunization procedures. However, they present some disadvantages: i.e. each library is specific towards a unique antigen, there can be ethical issues due to the use of animals, and there is a high cost in their generation (Hoogenboom et al., 1998; Schirrmann et al., 2011; Rami et al., 2017).

The naive, semi-synthetic and synthetic libraries can be grouped as “single-pot” libraries, because they are designed to create a variety of Ab fragments capable of binding to every existing antigen, which makes them very useful for the selection of human Abs (Hoogenboom et al., 1998; Schirrmann et al., 2011) .

Naive libraries are made from a primary Ab repertoire that contains a large amount of IgM Abs capable of recognizing many different antigens. These IgMs are cloned as a naive repertoire of rearranged genes, by harvesting the V-genes from the IgM mRNA of B-cells of non-immunized human donors. The V-genes are consequently amplified from B-cell cDNA using family-based oligonucleotides, and the heavy and light chains are randomly combined and cloned to encode a library of scFv or Fab Ab fragments. These libraries can generate Ab to a large panel of antigens, including self, non-immunogenic and relatively toxic antigens (Hoogenboom et al., 1998). The affinity of the selected Abs from a naïve library is proportional to the size of the library, which contains a great number of phage particles, from which each one encodes and displays different molecules, usually 10^6–10^{11} different ligands in a population of at least 10^{12} phage molecules (Hoogenboom et al., 1998; Bazan et al., 2012).

Semi-synthetic libraries are constructed from unrearranged V genes from germline B cells or from one Ab framework in which one or several CDRs are randomized by PCR or oligonucleotide direct mutagenesis, usually within the CDR3 regions. This combination of natural and synthetic diversity increases natural diversity (Schirrmann et al., 2011; Cabral, 2014).

Synthetic libraries are generated *in vitro* by the assembly of V-gene segments from human frameworks with randomized CDR cassettes (Hoogenboom et al., 1998; Schirrmann et al., 2011). The CDR3 from the heavy chain has the most structural and sequence diversity, while the remaining CDRs have limited variation (Hoogenboom et al., 1998). These libraries

allow control over the genetic characteristics of V genes and the introduction of diversity (Silverman;, 2001).

1.5.1.1 Tomlinson Human Single Fold scFv libraries I + J

The phage display antibody libraries used for this work were the Tomlinson Human Single Fold scFv libraries I + J (reIn_0017). These synthetic libraries are composed of over 100 million distinct scFv fragments cloned in the ampicillin resistant phagemid vector pIT2 in fusion with the C-terminal region of the phage coat protein pIII (Figure 1.16). The scFv fragments are composed by a single human polypeptide comprising the V_H and Vκ (HC and LC, respectively) domains attached to one another by a flexible Glycine-Serine linker. In addition, the scFv carries two peptide tags: a His-tag that facilitates purification, and a myc-tag that allows evaluation of the scFv expression/display using an anti-c-Myc Ab. The pIT2 plasmid contains two replication origins: colE1 ori for plasmid amplification in the bacterial cells, and the M13 ori for the amplification of the plasmid in the phages. The plasmid also contains a lacZ promoter and a pelB leader sequence to drive and direct the expression of the scFv, respectively (Figure 1.16). Both libraries are based on a single human framework for V_H (V3-23/DP-47 and J_H4b) and Vκ (O12/O2/DPK9 and Jκ1) with diversified (DVT) side chains incorporated in the antigen binding sites. The Tomlinson J library also incorporates NNK side chains in the antigen binding sites. These libraries are highly diverse in the antigen binding site region thus allowing the generation of mAbs that can subsequently be reformatted into various Ab formats (Xia et al., 2013; Brinkmann et al., 2017). The Tomlinson Human Single Fold scFv libraries I + J have been previously successfully used in our laboratory for the selection of specific antibodies against the DLL1 Notch ligand (manuscript in preparation for publication).

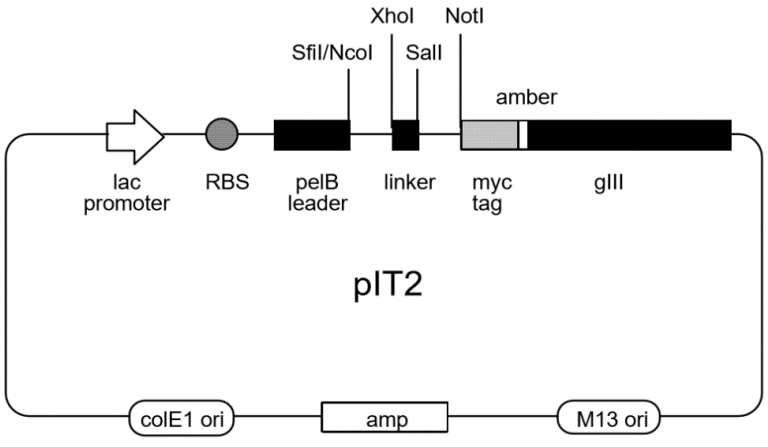

Figure 1.16. Vector map of pIT2 vector from the Tomlinson Human Single Fold scFv libraries I + J

1.5.2 Phage Display Panning

"Panning" is the name given to the *in vitro* selection process of Abs specific to an identified target,, based on their binding affinity that allows the rapid identification and

enrichment of target-specific binders from a large excess of non-binding clones (Parmley et al., 1988; Hoogenboom et al., 1998; Schirrmann et al., 2011). This is a cyclic procedure that basically consists on multiple rounds of several steps: first the phage libraries displaying the Ab repertoire are incubated with a specific target, usually protein, and washing is performed to remove non-specific or low affinity phage binders. Then, elution is performed to recover the specifically bound phages. Finally, eluted phages are amplified for the next panning round or for screening (Figure 1.17)(Hoogenboom et al., 1998). A single round of selection and amplification can lead to an enrichment of 20 to 1000-fold of a specific phage (Wang et al., 2011). Performing multiple selection rounds with selected phages increases the enrichment of specific binders (Watkins and Ouwehand, 2000), allowing the isolation of very specific antigen-binding clones (Hammers and Stanley, 2014). Three panning rounds are the most usual approach, however, there is no round limit, and this is very much dependent on the target and on the library, but usually the higher the number of rounds leads to an increase in the specificity but comes with the disadvantage of decrease in diversity. It is also common to include in each panning round a depletion step, using a non-target molecule, before the selection step in order to remove non-specific phage binders (Ferreira, 2015).

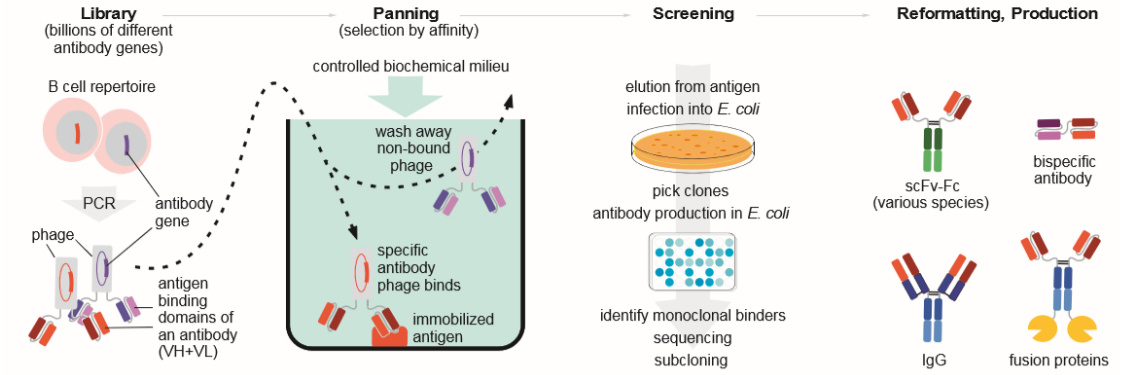

Figure 1.17.Representation of the Phage Panning strategy for the selection of Abs. Phage pool Abs are selected against a target antigen, coated on a surface. The specific phages bind to the antigen and the non-specific are removed by washing. The selected specific phages are eluted and if need amplified for a subsquent round of panning (adaped from Frenzel et al., 2017).

The success of ligand phage display relays on the combination of the display and the enrichment method (Hoogenboom et al., 1998).

If the antigen is presented in a more complex environment, for example panning on cells, the selection procedure becomes more difficult as other antigens are also present and the expression levels of our target may be low, requiring more rounds of panning and more sophisticated protocols (Dantas-Barbosa et al., 2012; Hammers et al., 2014).

After panning, the specific antigen-binding phages, or the corresponding soluble Ab fragments, are analyzed by ELISA assays towards the target antigen. The individual binders that specifically recognize the antigen by ELISA are selected and their DNA isolated and sequenced to identify the unique clones. Those unique clones can be then reformatted into IgG

(or other Ab formats, depending on their purpose) and further biochemically characterized (Winter et al, 1991; Schirrmann et al., 2011).

1.6 Aim

The main objective of this thesis was to develop specific anti-JAG1 Abs for BC therapies using phage display technology. The main tasks of this thesis are:

1. Selection of JAG1 specific Abs by phage display technology using the commercial Tomlinson Human scFv libraries I+J and recombinant JAG1 proteins as antigens;
2. Evaluation of the binding properties of selected unique scFv JAG1 Ab fragments to recombinant JAG1 proteins by ELISA;
3. Assessment of the epitope of the best anti-JAG1 scFv binders using different peptides of conserved JAG1 regions.

2. Materials and Methods

2.1 Mammalian cell Culture

Human breast cancer cell lines MCF-7 (ATCC HTB-22) and MDA-MB-231 (ATCC HTB-26) were cultured in high glucose, pyruvate DMEM medium (#41966) supplemented with 10% heat-inactivated fetal bovine serum (FBS), 100µg/mL penicillin and streptomycin (#15140-122), and 0.1mM non-essential amino acids (#11140-035), in the case of MCF-7 cells. Media and reagents were purchased from Gibco. Cells were incubated at 37˚C in a humidified atmosphere and 5% CO_2. Culture media was replaced every 2–3 days.

2.2 Bacterial cell culture and glycerol stock preparation

The *Escherichia coli* (*E. coli*) strain used was: TG1 (Lucigen) - F' [traD36 proAB+ lacIq lacZΔM15] supE thi-1Δ(lac-proAB) Δ(mcrB-hsdSM)5 (rK-mK). The helper phage used for phage display was M13KO7 (InvitrogenTM).

Initially the *E. coli* was grown in plates containing minimal media, composed by 1% glucose; 2mM of $MgSO_4$; 0.1mM of $CaCl_2$; 0.005 % thionine; 15g/L of agar and 1x M9 minimal salts (Sigma-Aldrich, M6030), during 48 hours at 37°C. For the panning assays, and the amplification of selected clones (described below), a sample of the bacteria grown in minimal media was scraped from the plates, and cultured in 5mL of 2x Yeast Extract Tryptone (2YT) medium (16g/L of Tryptone, 10g/L of Yeast Extract and 5g/L of NaCl) with 1% glucose, in 50mL falcon tubes overnight (O/N) at 37°C and 250 rpm.

Bacteria infected with the phage output pools from each round of selection were plated in 2YT agar plates (2YT medium with 15g/L of agar) with 1% of glucose and 10 µg/mL ampicillin, and incubated O/N at 37°C. For the bacterial glycerol stocks, the bacteria on the plates were scraped using 5-10mL of 2YT medium containing 15% of glycerol (VWR Chemicals, #24385.295), centrifuged (Eppendorf, centrifuge 5810R) at 3220 xg for 20 minutes at RT. The supernatant was discarded, and the resulting bacterial cells were resuspended in 3mL of 2YT with 15% of glycerol, aliquoted in cryovials, and frozen at -80ºC.

2.3 Bacteria Growth Curve

TG1 cells were grown O/N in 2YT medium supplemented with 1% of glucose and incubated at 37ºC and 250 rpm. After this, two pre-inoculums were prepared, where 5µL of the O/N culture was added into 96-well suspension culture plates, previously filled with 100µL/well of fresh 2YT medium with 1% of glucose. In parallel the necessary amount of the O/N culture was diluted in 5mL of fresh 2YT medium with 1% of glucose in order to obtain an OD_{600nm} of

0.05.

In the next day, two inoculums were prepared, one in 96-well suspension culture plates and the other in 50mL falcon tubes, prepared with fresh 2YT medium with 1% of glucose (100µl/well of 96-well plate and 10 mL/50 mL falcon tubes), in order to obtain an OD_{600nm} between 0.05 and 0.1. Monitoring of the OD_{600} at several time points was performed through the experiment. The growth curves were determined by plotting the optical densities (OD_{600nm}) of bacterial suspensions at the different times for each tested condition.

2.4 Phage Display

2.4.1 Panning

The panning strategy consisted in three rounds of selection, using the Tomlinson Human Single Fold scFv Libraries I + J or the Tomlinson I alone and the JAG1-EGF3-Fc recombinant protein as antigen, preceded by a depletion step with an Fc control protein (corresponding to the Fc portion of the antigen).

The recombinant JAG1-Fc fused proteins and the Fc control protein were previously generated in the laboratory using the JAG1 cDNA (Sino Biological, HG11648-M) and the pFUSE-IgG1-Fc vector (InvivoGen, pfuse-hg1fc1) basically as described in (Sales-Dias et al, 2019).

Pannings were performed using immunotubes (Maxisorp Startube, Thermo Scientific, 75X12 NUNC-IMMUNO) pre-coated O/N at 4ºC with 25µg/mL (for the first and second rounds) or 12.5µg/mL (for the third round) of an anti-human IgG (Fc specific) antibody (Sigma, I2136) in a final volume of 4mL of PBS. On the next day, the immunotubes were washed three times with PBS and coated with 25µg/mL of JAG1-EGF3-Fc protein (target) or the Fc control protein (depletion) in a final volume of 4mL of PBS for one hour at RT with gentle shaking (Stuart rotator, SB3). After this incubation step, the immunotubes were washed three times with PBS 0.05% Tween (Sigma-Aldrich, P7949)(PBST/0.05%) and blocked with 1mL of 2% skim milk (Nestlé Molico, #5601001135309) in PBS for two hours at RT with gentle shaking. After two hours, the immunotubes were washed three times with PBST/0.05%.

For the 1st round of the panning, the Human Single Fold scFv libraries I and J were mixed in a final volume of 1mL at a concentration of $1.4x10^{13}$ and $1.7x10^{13}$ cfu's/mL, respectively, to a final concentration of $3.1x10^{13}$ cfu's/mL. When using the library I individually, the final concentration of the library was $1.84x10^{13}$ cfu's/mL. The phages were precipitated using 250µL of PEG-NaCl (Sigma-Aldrich, #81260) for one hour on ice. After the precipitation step, the phage libraries were centrifuged (Eppendorf, centrifuge 5417R) at 14000 xg for 10 minutes at 4°C. The supernatant was discarded and the resulting pellet containing the phages was resuspended and blocked in 1mL of 2% skim milk in PBS for 30 minutes at RT with gentle shaking.

Precipitated and blocked phages were then added to the depletion immunotube (coated with the control Fc control protein) and incubated for 30 minutes at RT with gentle shaking – depletion step. After incubation, the depleted phages were transferred to the target immunotube

(coated with the JAG1-EGF3-Fc protein) and incubated 1 hour at RT with gentle shaking, for the selection of specific JAG1-EGF3 binders. After incubation, the supernatant was discarded and the immunotube was washed five times with 4mL of 2% milk with PBST/0.05%, followed by five times with 4 mL of PBST/0.05%, and once with 4mL PBS. Thereafter, the phages were eluted from the immunotubes by incubating for 8 minutes at RT with gentle shaking with a solution containing 67mM TEA (Fluka Analytical, #990279) in 300µL of PBS. The supernatant with the eluted phages was neutralized with 625mM Tris-HCl (Invitrogen, #15567-817) and mixed by inversion and kept on ice. The solution was then transferred to an Eppendorf tube.

2.4.2 Phage Amplification in *E. coli* TG-1 cells

To proceed between rounds, previously grown TG1 *E. coli* cells pre-inoculated into 5mL of 2YT medium as described above were diluted in 30mL of 2YT medium with 1% of glucose in a 250mL Erlenmeyer flask in order to obtain an OD_{600nm} of 0.05 and incubated at 37°C and 250 rpm. When the inoculum reached an OD_{600nm} of 0.4-0.5, 3.75mL of the inoculum was mixed with 3mL of 2YT medium and 750µL of the eluted phages from each selection round. This mix was incubated for 30 minutes at 37°C. After incubation the mix was centrifuged for 10 minutes at 3220 xg at RT, and the supernatant was discarded. Cells were resuspended in 1mL of 2YT medium with 1% glucose. Then 300µL from mix were used for the glycerol stocks (prepared as described above) and the other 700µL of the cell's solution were added to 10mL of 2YT medium with 1% of glucose and 100µg/mL ampicillin (Sodium Salt, BioChemica, A0839). The cells were then infected with helper phage M13K07 ($5x10^{10}$ cfu's/mL). The culture was incubated for 30 minutes at 37°C. The incubation was followed by a centrifugation for 10 minutes at 4°C and 3000g. After, the pellet was resuspended in 50mL of 2YT with 0.1% of glucose, ampicillin (100µg/mL) and kanamycin (Disulfate Salt, Sigma Aldrich, K1876, 50µg/mL), and incubated O/N at 30°C and 250 rpm.

In the next day, the bacteria culture was centrifuged at 3220 xg for 30 minutes at 4°C. 10mL of PEG/NaCl was added to 40mL of the supernatant and incubated on ice for 1 hour. After that, the culture was centrifuged at 3220 xg for 30 minutes at 4°C. The supernatant was discarded, and the pellet was re-centrifuged at 3220 xg for 2 minutes at 4°C for the removal of the remaining supernatant. The pellet containing the phages was resuspended in 1mL of PBS, transferred to Eppendorf tubes, and centrifuged at 11600 xg for 10 minutes at RT. The supernatant was then transferred to a new tube for the next panning rounds.

2.4.3 Titration of phage inputs and phage outputs from the panning strategy

Inputs and outputs from the panning were evaluated by titration of the phages. For that, 10µL from the pool phages, before depletion (Input 1), after depletion (Input 2), and after selection (Output) were collected into different Eppendorf tubes. Serial dilutions of the inputs and outputs were prepared until dilution 10^{-12} and 10^{-7}, respectively, using 90µL of 2YT medium with 1% of glucose and ampicillin (100µg/mL). 10µL of each phage dilution was mixed with 50µL of *E. coli* (TG1) at OD_{600nm} of 0.4-0.5 along with 40µL of 2YT with 1% of glucose. After

incubation at 37°C for 30 minutes, dilutions 10^{-8} to 10^{-12} of the inputs and 10^{-4} to 10^{-7} of the outputs were plated in 2YT with 1% of glucose and ampicillin (100µg/mL) agar plates. Non-infected *E. coli* TG1 cells at OD_{600nm} of 0.4-0.5 were also plated in 2YT with 1% of glucose and ampicillin (100µg/mL) agar plates as well as in in 2YT with 1% of glucose and kanamycin (50µg/mL) agar plates as controls to check phage contamination. Plates were incubated O/N at 37°C. The number of colonies for each dilution was counted, and the number of colony forming units (cfu)/mL calculated according to the Formula 2.1. The percentage of phage recovery was also calculated following Formula 2.2 and the enrichment between rounds following Formula 2.3.

$$\frac{\#colonies \times dilution\ factor}{plated\ volume\ (\mu L)} \times 1000 = cfu/mL$$

Formula 2.1. Colony forming units (cfu) per mL calculation from colonies counted on plates.

$$\frac{output\ phages\ in\ round\ n}{input\ phages\ in\ round\ n} \times 100 = Phage\ recovery\ in\ round\ n\ (\%)$$

Formula 2.2. Percentage of phage recovery in a determined round of selection.

$$\frac{Specific\ phages\ recovery\ in\ round\ n}{Specific\ phages\ recovery\ in\ round\ n-1} = Enrichment\ in\ round\ n$$

Formula 2.3. Enrichment increase in recovered phages in a determined round of selection relatively to the previous round.

2.5 ELISA

2.5.1 scFv-on-phage ELISA

E. coli TG1 bacteria colonies that were infected with phage pools from the output of panning rounds 2 and 3, were randomly picked with a toothpick and incubated in 150µL/well of 2YT media supplemented with 1% of glucose and ampicillin (100µg/mL) in a 96 well culture plate (greiner bio-one, #655185). The plates were incubated O/N at 37°C at 180 rpm. Then, 5µL of the O/N culture were diluted in 100µL of 2YT medium with 1% of glucose and ampicillin (100µg/mL) and incubated at 37°C and 180 rpm. After 2 hours and 30 minutes, when the culture reached an OD_{600nm} between 0.4 and 0.5, each well was infected with 10^9 cfu's of M13K07 helper phage and incubated for 1 hour at 37°C at 30 rpm. Then, the plate was centrifuged for 10 minutes at 1800 xg and 4°C, the pellets were resuspended with 200µL/well of 2YT media supplemented with 0.1% of glucose, ampicillin (100µg/mL) and kanamycin (50µg/mL), and incubated O/N at 30°C and 180 rpm.

96 wells Maxisorp plates (Thermo Scientific, #44-2404-21) were coated with 5µg/mL of JAG1-EGF3-Fc or control Fc proteins or anti-c-Myc antibody (Roche, #11667203001) and incubated O/N at 4°C. A non-coated Maxisorp plate was used as a negative control for ELISA.

After coating, the plates were washed 3X with 200µL/well of PBS and blocked for 1 hour at RT with 200µL/well of 2% milk in PBS. The plates were washed 3X with PBS, 50µL/well of phages were added to each well and the plates were incubated for 1 hour at RT.

After incubation with the phages, the plates were washed 3X with PBST/0.05% and 100µL of the secondary anti-M13-HRP antibody (Sino Biological, #11973-MM05T-H) diluted 1:5000 in PBS was added to each well. The plates were incubated for 1 hour at RT. After incubation the plates were washed 3X with PBST/0.05% and 50µL of the colorimetric substrate for horseradish peroxidase, 3,3',5,5'-tetramethylbenzidine (Life Technologies, #002023) were added to each well, in the dark, until negative controls began to react, between 5 to 10 minutes. 50µL of sulfuric acid (H_2SO_4) (VWR chemicals, #30149.291, 1M) were added to each well to stop the reaction. Absorbance was measured at 450nm in a Multiskan™ FC (Thermo Scientific).

2.5.2 Epitope mapping

In order to evaluate the specificity of the selected scFv to the different epitopes from the JAG1 protein, an ELISA assay similar to the one described in the section 2.5.1 was conducted. The differences in this protocol were on the ELISA plates used, because the peptides tested were biotinylated so were coated on Streptavidin Plates (Greiner Bio-One, #655990) at 1µg/mL in PBS.

Proteins tested were: recombinant Fc, JAG1-EGF3-Fc, JAG1-ECD-Fc, DLL1-EGF3-Fc, DLL1-ECD-Fc, anti-c-Myc Ab. Peptides tested were: JAG1-DSL, JAG1-EGF1, JAG2-DSL, JAG2-EGF1, DLL1-DSL, DLL1-EGF1, non-specific peptide.

Peptides were diluted in two different solutions. In one solution, the peptides were used in their native conformation, and in the other they were linearized with 5mM 1,4-Dithiothreitol (DTT)(Sigma Aldrich, D9779) for 30 minutes at 37°C.

2.5.3 ELISA with full IgG's

In order to evaluate the binding properties of the reformatted anti-JAG1 IgGs to the JAG1 proteins an ELISA assay was conducted.

96-well Maxisorp plates were coated with JAG1-EGF3-Fc, JAG1-ECD-Fc, recombinant Fc and a positive control protein for the secondary Ab at 5µg/mL in PBS and incubated O/N at 4°C. After incubation, the plates were washed 3X with 200µL/well of PBS and blocked with 200µL/well of 2% milk in PBS for 1 hour at RT. After blocking, the plates were washed 3X with 200µL/well of PBS. 2-fold serial dilutions of anti-JAG1 IgG's (starting from 100µg/mL) were prepared and incubated for 1 hour at RT on the blocked 96-well maxisorp plates. After the incubation with the IgG's, the plates were washed 3X with PBST/0.05%. Then, the plates were incubated for 1 hour at RT with 100µL/well of anti-human IgG (Fab Specific)-HRP conjugated antibody (Sigma Aldrich, 2.5µg/mL, A0293) in PBS for the detection of anti-JAG1 IgG´s binding. The rest of the procedure was performed as described in section 2.5.1 ELISA.

2.6 DNA Extraction

The plasmid DNA was extracted using the NZYMiniprep kit (NZYTech, MB01001) according to the manufacturer protocol.

Briefly, a single colony of each of the selected anti-JAG1 scFv clones was grown in 5mL of 2YT media supplemented with 1% glucose and ampicillin (100µg/mL) and incubated O/N at 37°C and 250 rpm. After incubation, each culture was centrifuged for 5 minutes at 12000 xg. The supernatant was discarded, and the pellet resuspended in 250µL of the A1 buffer by vigorous vortex. Then, 250µL of A2 buffer was added and mixed by inverting the tube 6-8 times. The tube was incubated at RT for a maximum of 4 minutes before the addition 300µL of the A3 buffer. Then, the tube was inverted 6-8 times, to mix the buffers, and centrifuged for 15 minutes at 12000 xg. The supernatant was loaded into a spin column inserted into a 2mL collecting tube and centrifuged for 1 minute at 11000 xg. The flow-through was discarded, and 500µL of the AY buffer was loaded into the column. The column was centrifuged for 1 minute at 12000 xg and the flow-through was discarded. 600µL of the A4 buffer was added to the column and another centrifugation step was performed for 1 minute at 12000 xg.

The spin column was re-inserted into a new collecting tube and centrifuged for 2 minutes at 12000 xg to remove residual washing buffers. Plasmid DNA was then eluted with 30µL of molecular biology grade H2O, its concentration determined using a nanodrop ND-2000C spectrophotometer and stored at -20ºC. All centrifugations were performed at RT.

2.7 PCR

In order to evaluate the integrity of the scFv DNA, a PCR was conducted. The primers used in this reaction were the LMB3 (forward), pHEN sequence (reverse), and the Link Sequence (reverse) (all obtained from Integrated DNA Technologies) - Table 2.1. Two reaction solutions were prepared, one with the LMB3 and pHEN primers, and the second with the LMB3 and Link sequence primers, to ensure that the entire scFv sequence was present. The first reaction tube aims at the amplification of the entire DNA sequence while the second one amplifies a fraction of the DNA ranging from the 5´end until half of the scFv DNA fragment. PCR reactions containing 3% DMSO (New England BioLabs, B0515A), 15 mM dNTP's NZY Mix (nzytech, MB086), 1X Phusion Buffer (Thermo Scientific, F-518), 1U Phusion Polymerase (Thermo Scientific, F-530S), 25 mM of each primer set, and molecular biology grade H2O were transferred to PCR tubes containing 2ml of DNA template (50µg/µL) or H2O (used as negative control). The PCR reactions were performed in a thermocycler (Bio-Rad, MyCycler) under the following conditions: pre-incubation at 98°C for 30 seconds, followed by 30 cycles of a 10 seconds denaturing at 98°C, a 20 seconds annealing step at 58-65°C and an extension step of 1 minute at 72°C, ending with a 10 minutes final extension step at 72°C. When PCR reaction terminated samples were kept at 4°C. The samples were analyzed by DNA electrophoresis

using an agarose gel (section 2.11).

Table 2.1- Primers used to amplify scFv selected against the JAG1-EGF3-Fc protein. (F)-forward primer, (R)-reverse primer.

Primer	Sequence
LMB3	5'-CAG GAA ACA GCT ATG AC-3' (F)
Link Sequence	5'-CGA CCC GCC ACC GCC GCT G-3' (R)
pHEN Sequence	5'-CTA TGC GGC CCC ATT CA-3' (R)

2.8 DNA Sequencing

The DNA sequencing reactions were performed at GATC Biotech. The scFv DNA samples were extracted according to section 2.4. DNA solutions at 100ng/µL of each scFv were prepared in molecular biology grade water. Subsequently, 5µL of each DNA were added to 1.5 mL Eppendorf tubes containing 5µL of LMB3, pHEN sequence, or Link sequence primers, each at 5µM. Reactions were sent to the GATC Biotech for sequencing. Once the results were available, the data was analyzed using the Chromas and Clone Manager softwares.

2.9 Binding of selected anti-JAG1 scFv clones to endogenous JAG1 protein in MDA-MB-231 and MCF-7 cells by flow cytometry

The ability of selected anti-JAG1 scFv to bind to cellular endogenous JAG1 protein were evaluated by flow cytometry assays (Phage FACS) using MDA-MB-231 and MCF-7 breast cancer cells, which express high and low levels of JAG1, respectively (laboratory data, figure 3.14). In these assays, the binding of the phage particles displaying the specific scFv fragments to cells were determined using an anti-M13 antibody. For this, in the day previously to the Phage FACS experiment, scFv phages were prepared as described in section 2.6.

MCF-7 and MDA-MB-231 cells were harvested at 80-90% confluence with Trypsin-EDTA (0.05%)(Gibco, #25300062) using the standard protocol. After harvesting, cells were centrifuged for 5 minutes at 300 xg and 4°C and the supernatant was discarded. The resulting cell pellets were resuspended in FACS buffer (composed of PBS with 3% FBS (Gibco by life technologies, #10500-064) 0.05% Sodium Azide (Sigma Aldrich, S2002)). Next, the cell number was determined with a hematocytometer and cell solutions at $1X10^6$ cells/mL were prepared in FACS buffer for each cell line. Then, 100µL/well of each cell suspension were added to the respective 96-U-bottom plate, previously coated with 200µL/well of FACS buffer, according to the experimental setup (one plate for each cell type). Cells were then incubated for 30 minutes at RT for antigen blocking. Meanwhile, the plates with the scFv clones, that grew O/N at 37°C as described above, were centrifuged for 20 minutes at 2000 xg at 4°C to discard bacteria slurry and the resulting supernatant was collected to a 96-well polypropylene deep well plate natural RNase/DNase-free (1mL)(Thermo Scientific-Nunc, #260252). After the incubation period, cells

were centrifuged for 5 minutes at 300 xg and 4°C, the supernatant was discarded by swinging out the plate by hand, and the cell pellets were resuspended in 50µL of the scFv supernatant, according to the experimental setup. In the non-stained and secondary antibody control conditions, cells were resuspended in 50µL of FACS buffer. Next, cells were incubated for 45 minutes at 4°C with soft agitation in an orbital shaker. After incubation, cells were centrifuged as above and the supernatant was discarded. Cells were then washed 3X by resuspending the pellets with 200µL of FACS buffer, followed by centrifugation for 5 minutes at 300 xg and 4°C, with the supernatant being discarded by swinging out the plate by hand after each wash.

After the last washing step, cells were resuspended in 100µL/well of the primary antibody anti-M13 Biotin at 1µg/mL (Abcam, #17269), which is specific to the gp13 phage coat protein. After 45 minutes of incubation at 4ºC, cells were centrifuged for 5 minutes at 300 x g and 4°C and the supernatants were discarded. Cells were washed 3X as previously described. Thereafter, cells incubated with primary antibody were resuspended in 100µL/well of the secondary antibody Streptavidin-Alexa-488 at 1.5µg/mL (Life Technologies, S11223) to detect the primary antibody. Secondary control samples (i.e. cells to which scFv clones were not added) were also incubated with secondary antibody alone to evaluate the unspecific binding of this antibody. Unstained control cells were resuspended in FACS buffer only.

Cells were incubated for 20-30 minutes at 4°C with soft agitation and then washed 3X as described above. Lastly, cells were resuspended in 150µL of FACS buffer, samples were analyzed on a FACS Canto II Flow Cytometer and the results were evaluated with the FlowJo software.

2.10 Evaluation of glycosylation level of anti-JAG1 IgGs by PNGase F assay

To assess the glycosylation level of the IgG's, a PNGase F assay (New England Biolabs, P0705S) was performed to remove the N-glycans groups under denaturing and non-denaturing conditions according to the manufacturer's instructions. The results were then evaluated by SDS-PAGE.

2.10.1 Denaturing Conditions

In brief, 5µg of each JAG1 IgG or a control glycoprotein (New England BioLabs, ref: #P7817S) was mixed with 1µL of Glycoprotein Denaturing Buffer (10X) (New England BioLabs, #B1704S) and PBS to make up a final volume of 10µL in a 1.5 mL Eppendorf tube. The proteins were denatured by incubating the reaction at 99°C for 10 minutes, followed by a chilling down on ice. After that, a spin-down was performed on the tubes. Next 2µl of GlycoBuffer 2 (10X) (New England BioLabs, #B3704S), 2µl of 10% NP-40 (New England BioLabs, #B2704S) and 6µl of PBS to make up a final volume of 20µL were added to each denatured IgG or control glycoprotein. Finally, 1µL of the PNGase F (New England BioLabs, 500.000U/mL, #P0704S) was added to each tube and mixed gently. The tubes were incubated at 37°C for 1 hour.

2.10.2 Non-denaturing Conditions

20µg of each IgG was mixed with 2µl of GlycoBuffer 2 (10X), 5µL of PNGase F and the PBS necessary to make a total reaction volume of 20µl in a 1.5mL Eppendorf tube. The tubes were incubated for 24 hours at 37°C.

2.11 Agarose Gel Electrophoresis

Analysis of the PCR products was performed using agarose gel electrophoresis. 1.5% agarose gels were prepared by premixing 150µL of 1XTAE buffer (5-Prime, 50X, #2500060) with agarose (Seakem LE Agarose, Lonza, # 5000). After dissolving the agarose in a microwave, 7.5µL of Red Safe (iNtRON Biotechnology, #21141) was added to the solution when it was at 37°C, mixed and poured into a previously assembled gel tray containing a well-forming comb. After the polymerization, the tray with agarose gel was placed in a DNA electrophoresis chamber containing 1xTAE buffer and the combs were removed. DNA samples were prepared by mixing18µL of each DNA sample with 2µL of 10XOrange G loading buffer (Life Technologies). Once prepared, the DNA samples were loaded in the correspondent wells along with 8µL the molecular weight DNA Marker Ladder III (Nzytech, MB044), for the identification of the DNA sizes. The gel was run at 180 Volts for about 45 minutes and the DNA bands were visualized under UV light using a BioRad ChemiDoc MP imaging system.

2.12 SDS-PAGE electrophoresis

For an SDS-PAGE electrophoresis, the Invitrogen pre-cast 4-12% Bis-Tris Gels were used (Invitrogen, NuPAGE, NP0321BOX) following the suppliers instructions. Protein samples were prepared for running in reducing and non-reducing conditions. Samples were prepared by adding 2µg of each IgG, 4µL of 4XLDS (Invitrogen, NuPAGE, NP0007), 1.5µL of 10XReduce Agent (Invitrogen, NuPAGE, NP0004), added only for the reducing samples, and PBS to a final volume of 16µL. The protein solutions with the reducing agent were heated at 99°C for 5-10 minutes in a thermostat (Eppendorf thermostat plus). Samples were centrifuged (12000 xg, 1 minute, RT) and loaded onto the gels along with the 8µL of the molecular weight marker Precision Plus Protein Standards All Blue (BioRad, #161-0373). The gel was run at 80 Volts for 15 minutes and 150 Volts for an hour afterword's using 1XMOPS buffer (Novex by life technologies-NuPAGE, 20X, NP0001). After the run, the gels were stained with Instant Blue (expedeon, ISB1L) following the manufacturers protocol. After destaining, images of the gels with the protein bands were acquired in the BioRad ChemiDoc MP imaging system.

3. Results and Discussion

The presentation of the results is going to be based on the pannings made to select the antibodies, where the results of each strategy will be presented chronologically, followed by the binding tests performed with the selected scFv and obtained IgGs against the JAG1 recombinant protein to evaluate their binding ability and specificity.

3.1 Selection of JAG1 scFv antibodies by Phage Display

3.1.1 1st Library Panning

The main objective of this thesis was the development of antibodies against the Notch ligand JAG1. For that, the phage display technology using the commercially available human scFv phage display Tomlinson I+J libraries was used.

To generate specific antibodies with potential to block JAG1 binding to Notch receptor, a truncated version of JAG1 protein designated JAG1-EGF3-Fc, containing the minimal binding region of the ligand to the receptor, was used as the antigen in our panning strategies. The panning was conducted in immunotubes and the amount of phages used in the first round was 10^{13} pfu's. In order to have the correct conformation of the JAG1-EGF3 protein exposed during the scFv selection procedure, it was immobilized via its Fc region to the immunotubes using an anti-human IgG-Fc specific Ab. The panning strategy consisted in three rounds of selection with the JAG1-EGF3-Fc protein. Each round was preceded by two depletion steps, one using a non-coated immunotube and another with an immunotube coated with the off-target (anti-human IgG-Fc specific Ab + Fc control protein), in order to remove unspecific binders (Figure 3.1). The selected phages were amplified between each round. In order to increase the selection specificity the amount of the JAG-EGF3-Fc protein was decreased by half in the third round of selection.

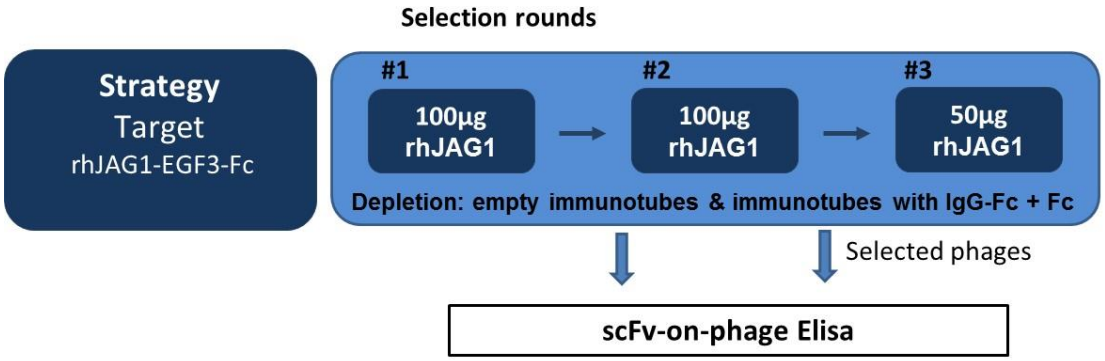

Figure 3.1- Strategy used for the selection of scFv specific for recombinant JAG1-EGF3 protein.

For each round of selection, the total amount of phages added (phage input) and recovered (phage output) was calculated to determine the percentage of input phage recovery

and the enrichment values between rounds.

Table 3.1. Phage concentration, recovery and enrichment for each round of 1st panning

Panning Round	Phage Input (cfu's/mL)	Phage Output (cfu's/mL)	% of input phage recovery	Enrichment
1st Round	1.3×10^{13}	1.4×10^{10}	0.1	---
2nd Round	7×10^{13}	6.8×10^{8}	9.7×10^{-4}	9.7×10^{-3}
3rd Round	2.8×10^{13}	2.1×10^{8}	7.5×10^{-4}	0.77

After the first round of selection, it is expected to have a reduction in the number of phages due to the fact that a considerable amount of non-binding phages is washed away. On the contrary, in the following rounds a gradual increase in the phage concentration should occur resultant of the enrichment of the selected phage (Xiaokun Li, 2018). In our panning, the output result for the first round was 1.4×10^{10} cfu's/mL, which is extremely high in comparison to the reported values of 10^{8} to 10^{4} (Lai, 2016). Analysis of the results obtained for the second and third rounds showed these values were also in the higher range but in acceptable levels with 6.8×10^{8} cfu's/mL after the second round and to 2.1×10^{8} cfu's/mL after the third round (table 3.1). These results indicated that something occurred in the first round. That either the depletion step was ineffective or the washing of the immunotube containing the JAG1-EGF3-Fc was not well performed, resulting in a high phage output number.

3.1.2 Characterization of selected clones by scFv-on-Phage ELISA

To evaluate the binding properties of the scFv clones selected from the panning, a scFv-on-phage ELISA assay was conducted in 96-wells plates, where the phages from 88 bacteria colonies from the second and third rounds, picked randomly, were tested for their ability to bind the JAG1-EGF3-Fc recombinant protein (non-immobilized, i.e. directly coated, and immobilized via its Fc portion). As presented in Figure 1.16, in this library, the scFv are expressed as c-Myc tag proteins, and c-Myc is only expressed in phages that are displaying their scFv correctly on their cell surfaces. Therefore, in order to evaluate the expression and correct display of the scFvs, the presence of c-Myc tag was also assessed by evaluating the binding of the selected clones to an anti-c-Myc Ab. Through the detection of the c-Myc tag, we were able to identify the clones with good scFv display, and, thus evaluate if the signal observed with the recombinant JAG1 and Fc control proteins was in fact related to a specific binding between scFvs and the antigen.

Results from these assays showed that none of the picked clones from the second round were expressing the scFv, as evidenced by their absence of binding to the anti-c-Myc Ab (i.e. by the absence of c-Myc tag being expressed by the phage)(data not shown). This result suggested that probably the TG1 bacteria were not expressing the phages and this could be

due to the fact that they were not infected at the correct cell density. This hypothesis was supported by the observation that the 96-well plates, in which the bacteria were grown, presented some evaporation in the outermost wells that likely affected their growth. Probably the correct bacterial density was not achieved impairing the formation of the F-pilus necessary for the infection process to occur efficiently.

From the 88 clones tested from the third round, only 11 were expressing the scFv based on the detection of binding to the anti-c-Myc Ab (blue bars in Figure 3.2). This value corresponds only to 12.5% of the total amount of clones, which is much lower than what would be expected for this library (50-75% scFv display). A positive result was considered when the absorbance value measured was 5 times higher than the absorbance value of the negative control, which in this experiment corresponded to the uncoated wells. Accordingly, in this experiment, signals above or equal 0.3 were considered positive. As shown in Figure 3.2 (green and yellow bars) four clones were capable of recognizing specifically the JAG1-EGF3-Fc proteins: A3, B3, C3, and C6, presenting high absorbance values. In comparison to clones A3, B3, and C6, the clone C3 showed a lower signal, however, we decided to continue to evaluate their binding properties since these bound to both JAG1-EGF3-Fc non-immobilized and immobilized proteins, and because only few number of positive clones had been obtained in this 1st panning. The remaining seven clones were discarded because either they did not recognize the JAG1-EGF3-Fc protein or also recognized the Fc negative control protein (red bars in Figure 3.2).

Evaluation of the binding ability of the selected JAG1 scFvs to non-immobilized (green bars) and immobilized (yellow bars) JAG1-EGF3-Fc proteins showed similar absorbance values, indicating that the Fc region does not have an influence on the capacity of the scFv to recognize the JAG1-EGF3-Fc protein. The high values obtained with the Fc-oriented protein with clones F9 and G5 (yellow bars) are likely mostly due to the recognition of the Fc protein fraction and not to the JAG1-EGF3 itself, since they did not recognize the non-immobilized JAG1-EGF3-Fc protein but recognized the Fc control protein. The same hypothesis applies to the clone F5 (Figure 3.2).

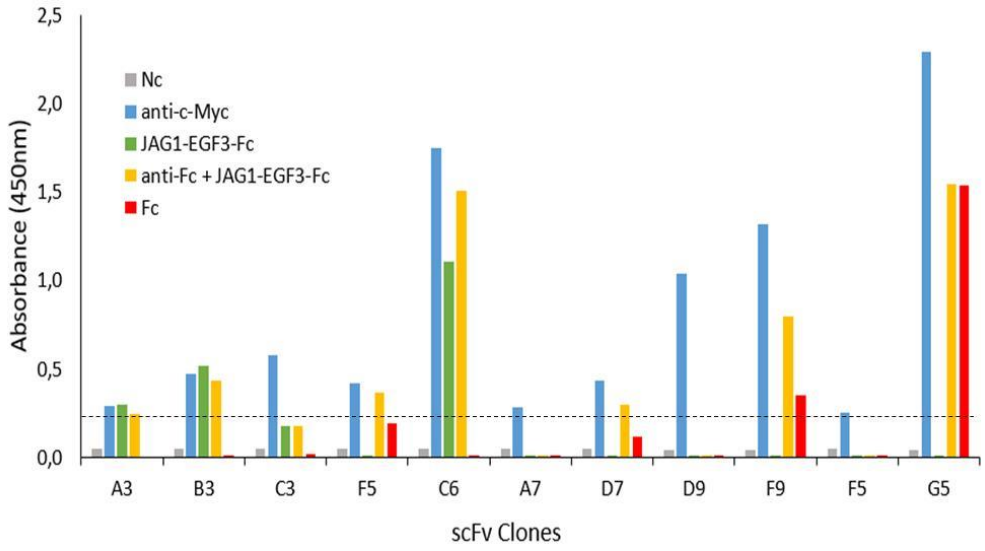

Figure 3.2. scFv-on-Phage ELISA of selected clones from round 3 of 1st panning. The graphic shows the binding of the indicates clones to non-coated (Nc) wells and wells coated with anti-c-Myc Ab, JAG1-EGF3-Fc, Fc-oriented-JAG1-EGF3-Fc, and control Fc proteins. Clones A3, B3, C3 and C6 demonstrate phage expression, binding towards the JAG1-EGF3-Fc protein and no binding to the Fc protein.

The JAG1 and DLL1 proteins present a significant degree of homology between their EGF regions (Kopan, 2009). Therefore, to ensure that the selected scFv were specific towards the JAG1 ligand, their specificity was also tested through an ELISA assay by evaluating their ability to bind to truncated DLL1-Fc recombinant proteins. Two different constructs were assayed - a DLL1-EGF3-Fc, containing the minimal binding region of the ligand to the Notch receptor, and a DLL1-ECD-Fc with the full-length extracellular domain. The binding ability of the clones towards the recombinant JAG1 protein with the full ECD – JAG1-ECD-Fc, was also evaluated to find out if the presence of the complete ECD would change the protein conformation in a way that would impair scFv recognition. A negative control using a non-coated plate was also tested. An anti-DLL1 specific scFv, previously selected with the DLL1-EGF3-Fc protein by phage display, and capable of recognizing both recombinant DLL1 proteins was used as a positive control for the DLL1 proteins. To control the scFv expression and validate the results, coating with the anti-c-Myc Ab was also performed.

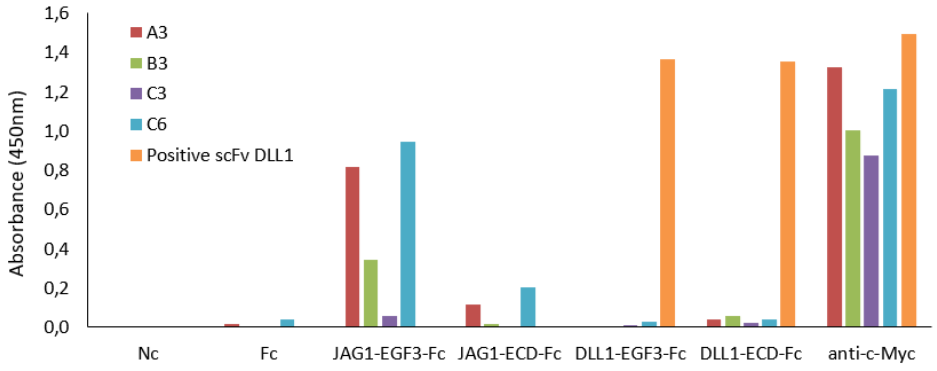

Figure 3.3. scFv-on-phage ELISA specificity assay using JAG1, DLL1 and Fc proteins and anti-c-Myc Ab. The graphic shows the binding of the indicates clones to non-coated (Nc) wells and wells coated with anti-c-Myc Ab, and recombinant Fc, JAG1-EGF3-Fc, JAG1-ECD-Fc, DLL1-EGF3-Fc and DLL1-ECD-Fc proteins. Clones A3, B3 and C6 demonstrate specificity towards the recombinant JAG1 proteins, indicated by the high absorbance value in the JAG1 proteins and residual absorbance values in the DLL1 ones.

As illustrated in Figure 3.3, the negative control behaved as expected, validating the experiment, by showing no signal in the non-coated wells. Due to the same reason explained before, signals with absorbance intensity values 5 times higher the background were considered positive. By looking at the results obtained with the anti-c-Myc Ab, corresponding to the c-Myc expression and scFv display, we can see that all the evaluated scFv clones are being expressed.

From the Figure 3.3 we can also see that the clone C3, which previously presented a reduced signal, again showed a weak signal indicating it may be a very weak binder or a false positive clone. However, we decided to continue to study this clone due to the few positive hits we had at that time. The remaining A3, B3 and C6 clones confirmed their specificity towards the JAG1-EGF3-Fc protein as demonstrated by the ELISA values obtained. However, the signals obtained with the JAG1-ECD-Fc protein were significantly lower, suggesting that the presence of the full ECD in the protein changes its structure leading to an alteration in the binding capacity of the antibody fragments. We can also see that the tested scFv are specific for the JAG1 proteins, since they do not bind to the DLL1 recombinant proteins, as evidenced by the absence of signal in the wells coated with these proteins. These results suggest that the binding site that the scFv recognizes in the JAG1-EGF3-Fc protein is specific for the JAG1 ligand. The integrity of the DLL1 proteins was established by the use of the positive scFv control that was able to recognize both recombinant DLL1 proteins but none of the JAG1 constructs.

3.1.3 Epitopes ELISA assay

After selecting the scFv capable of binding to the JAG1-EGF3-Fc protein and evaluating their binding properties and specificity, we tried to identify regions within the JAG1-EGF3 protein to which they bind by scFv-on-phage ELISA using peptides specific to the DSL and EGF1 regions, shown to be important in the ligand binding to the receptor (Friec et al., 2012). Binding of the anti-JAG1 scFv to specific peptides corresponding to DLS and EGF1 regions of the DLL1 and JAG2 ligands was also tested, because they present significant homology. In addition, a nonspecific peptide was used as a negative control. Since the conformation of the peptides may influence the binding of the scFv fragments, two ELISA assays were conducted – one with linearized peptides with DTT and another with non-treated/native peptides.

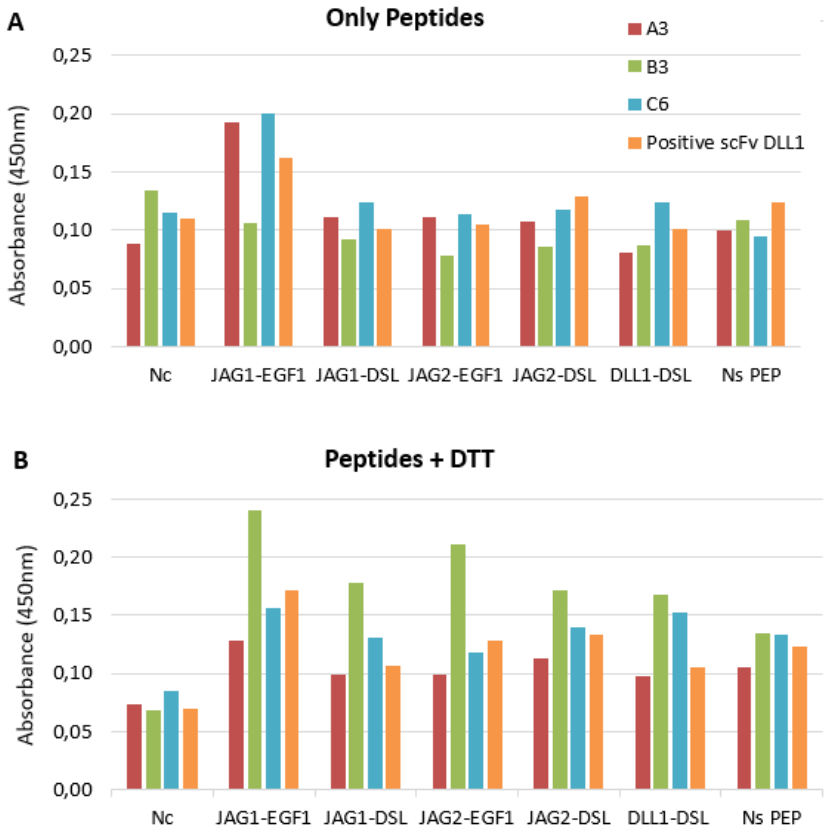

Figure 3.4. scFv-on-phage ELISA assay using specific peptides corresponding to the to the DSL and EGF1 domais of the JAG1, JAG2 and DLL1 proteins. The graphics in **(A)** and **(B)** show the binding of anti-JAG1 scFv clones A3, B3, C6 and anti-DLL1 scFv to non-coated (Nc) wells and wells coated with native (A) and linearized (B) JAG1-EGF1, JAG1-DSL, JAG2-EGF1, JAG2-DSL, DLL1-EGF1, DLL1-DSL and non-specific (Ns PEP) peptides.

In these experiments, we were not able to identify the specific region to which the scFv bind. As shown in Figure 3.4, panel A, using peptides in their native conformation, the difference between the signal values of the binding of the various clones to the peptides and the negative control peptide are very low in comparison to those obtained in non-coated control wells not allowing to conclude if there is any positive result. Besides that, the absorbance values obtained with the control non-specific peptide are not significantly different from those obtained with the different peptides for JAG1, JAG2 and DLL1 proteins (less than 2-3 times its value), indicating that there was no binding between the scFv and the peptides. The results presented in Figure 3.4, panel B, using the peptides treated with DTT, show the scFv were not capable of recognizing the linearized peptides sequences either. These results could suggest that a bigger sequence of the JAG1 ligand is necessary for the binding to occur.

3.1.4 Bacterial Growth Kinetics

As mentioned above, for the infection to occur, bacteria need to develop the F-pilus structure (Jacobson, 1972). In the case of the TG1 *E. coli* strain, the F-pilus is developed between a bacterial cell density of 0.4 to 0.5. To assess if the problems we faced during the evaluation of the scFv clones selected from the second round were due to a defective infection

because bacteria were not at the correct cell density, a bacterial growth curve assay was performed. Several different growth conditions were tested during this experiment.

We wanted to address if bacterial growth in 96-well plates or falcon tubes would affect their development in a significant way.

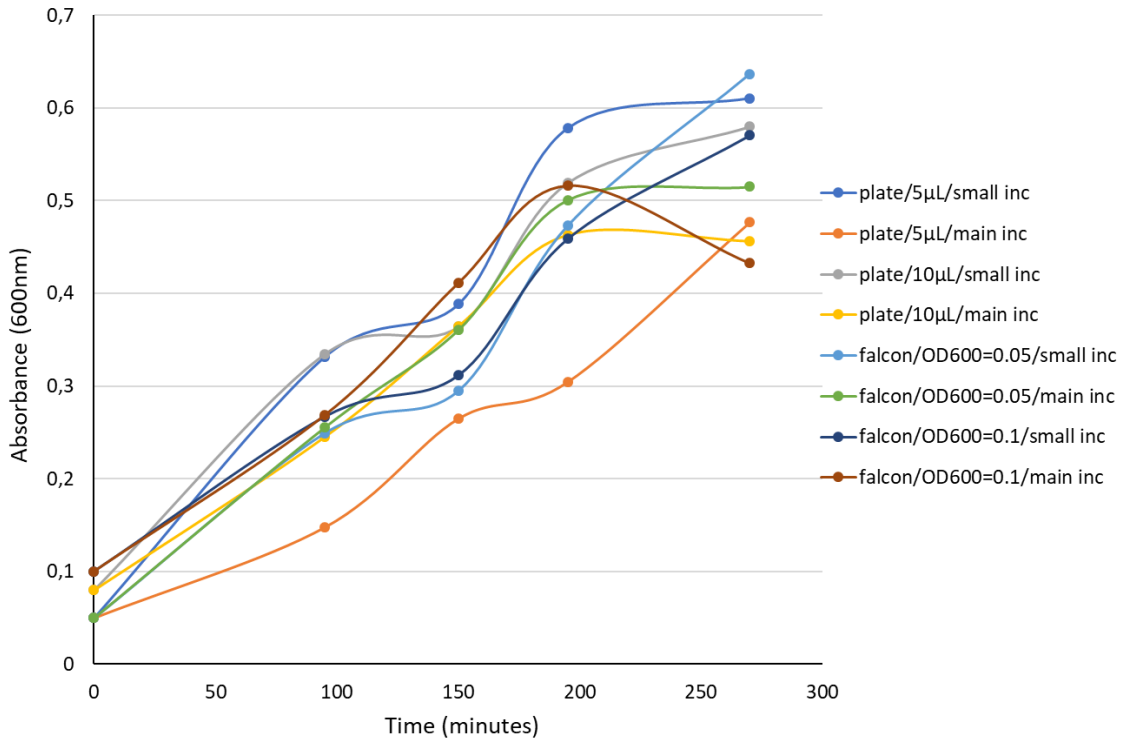

Figure 3.5. TG1 *E. coli* strain growth curves. TG1 bacteria growth was tested under different conditions. In 96-well plates vs. 50 mL falcon tubes; in a small incubator vs. the laboratory main room incubator; 96-well plates with 100 µL media inoculated with 10µL vs. 5µL of bacteria; and in a 50 mL falcon tubes with an initial OD_{600nm} of 0.05 vs. 0.1. inc, incubator.

The results from this experiment showed that there was not a significant difference in the bacterial growth between the bacteria incubated in 96-well plates and the ones in the falcon tubes, with the exception of the 96-well plate inoculated with 5µL of bacteria (orange line in Figure 3.5, plate/5µL/main inc) that presented a slower growth. These results demonstrate that the volume/vessel format used for bacterial cell growth does not have much influence in their growth rate.

Two different incubators in our laboratory were tested, a small one in the “phage-room” (Zhicheng) and the other in the main room of the laboratory (Innova44). We wanted to see whether the use of different incubators influenced the bacterial growth rate. In Figure 3.5, we can observe that in falcon tubes’ experiment, where the only difference is the incubator, there are no significant differences in the bacterial growth. However, in the plates we see a different situation. When the plates were incubated in the main laboratory (plate/10µL/main inc (yellow) and plate/5µL/main inc (orange)), the cultures grew much more slowly when compared to the ones that grew in the other incubator (blue and grey lines). This could influence the bacteria

infection, since the incubation time needed to achieve the correct OD_{600nm} for infection in this last case would need to be higher. Usually, the incubation time before infection varied between 120 and 150 minutes, and this could mean that while the plate incubated in the main laboratory (yellow and orange lines) would have an OD_{600nm} ranging from 0.2 to 0.3, the other plate (blue and grey lines) might already have reached the ideal OD_{600nm} of 0.4, and thus be ready for infection.

Another parameter evaluated during this assay was the initial OD_{600nm} of the inoculum. Keeping the remaining parameters, we saw that the bacteria inoculated with higher OD_{600nm} reached the intended optical density of 0.4 earlier, as expected (Figure 3.5).

Given this, we decided that all incubations for the panning and ELISA assays would be performed in the main laboratory incubator using a starting $OD_{600\ nm}$ of 0.05.

3.1.5 PCR and sequencing analysis of the selected anti-JAG1 clones

3.1.5.1 DNA Extraction

To further characterize the 4 scFv selected for binding to the JAG1-EGF3-Fc protein by scFv-on-phage ELISA, it was necessary to check their DNA sequences for integrity and to determine their nucleotide sequences to see if they shared the same sequence or were unique clones. DNA from all 4 scFv was extracted using a DNA mini-kit (NZYMiniprep), following the protocol provided.

After the phagemid DNA extraction, the DNA integrity of the 4 clones was analyzed by agarose gel electrophoreses. In Figure 3.6 we can see that all clones have a band close to the 5000 bp that corresponds to the expected size of the pIT2 plasmid containing the DNA fragments encoding the scFv Ab (Kenneth Murphy, 2011). This data suggests that the selected clones A3, B3, C3, and C6 have the full scFv sequence.

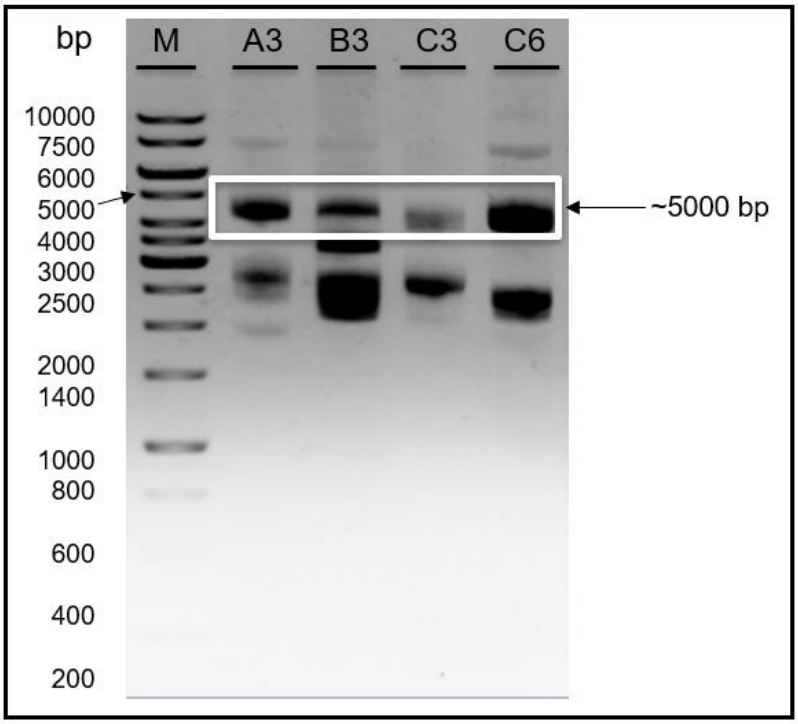

Figure 3.6. Agarose gel electrophoresis of plasmid DNA isolated from anti-JAG1 selected clones (lanes: A3, B3, C3, C6 clones). The 4 tested clones present a band near the 5000 bp that correspond to the size of the plasmid pIT2 with the scFv insert. The remaining bands present in the gel with lower molecular weight represent supercoiled versions of the respective DNA clone. Lane: M, Gene Ruler.

3.1.5.2 PCR of the selected clones

Next a PCR reaction was performed to evaluate the scFvs chain size by using the library recommended LMB3, pHEN and Link sequence primers. The LMB3 and the pHEN sequence primer pair amplify the entire scFv sequence, containing the variable heavy and light chains, permitting to verify if the sequence size matches the expected. Amplification with the LMB3 and Link sequence primers allow the amplification of the variable HC, and this way we were able to confirm the size of the LC as well. LMB3 primer amplifies the DNA sequence in the forward direction, instead of the pHEN and Link sequence primers that do it in the reverse direction.

In Figure 3.7, lanes 5 and E represent our negative controls prepared with no DNA but with all the remaining reagents of the experiment. In these lanes no band is observed, meaning that no DNA amplification occurred, as expected, validating the experiment.

In the PCR performed with the LMB3 and pHEN primers, in lanes 1, 2, 3, and 4 in Figure 3.7, we can observe a band with a size close to 935 bp, which corresponds to the correct size of the full scFv as indicated in the library datasheet. However, in lane 3 the band amplified from the clone C3 shows a lower intensity. Moreover, in this lane there is also a PCR product of near 600 bp not amplified in the other clones, which suggests a problem with the DNA sequence of the C3 clone, that it might comprises several scFv DNAs.

Analysis of the PCR products obtained with the LMB3 and the Link sequence primers

show a band with a size around 527 bp in the lanes correspondent to the clones A3, B3 and C6, with similar intensity (lanes A, B, and D in Figure 3.7). This band corresponds to the variable heavy chain sequence, according to the library datasheet information. In lane C that contains the DNA amplification product from the C3 clone, we can see a very faint band with the same size as in the other lanes (A, B and D). The presence of DNA bands with molecular weight higher 2000 bp are likely due to some unspecific binding of the primers. Together, these results suggest that the selected clones A3, B3 and C6 contains the full size scFv fragment, while the clone C3 scFv corresponds to a mix of clones.

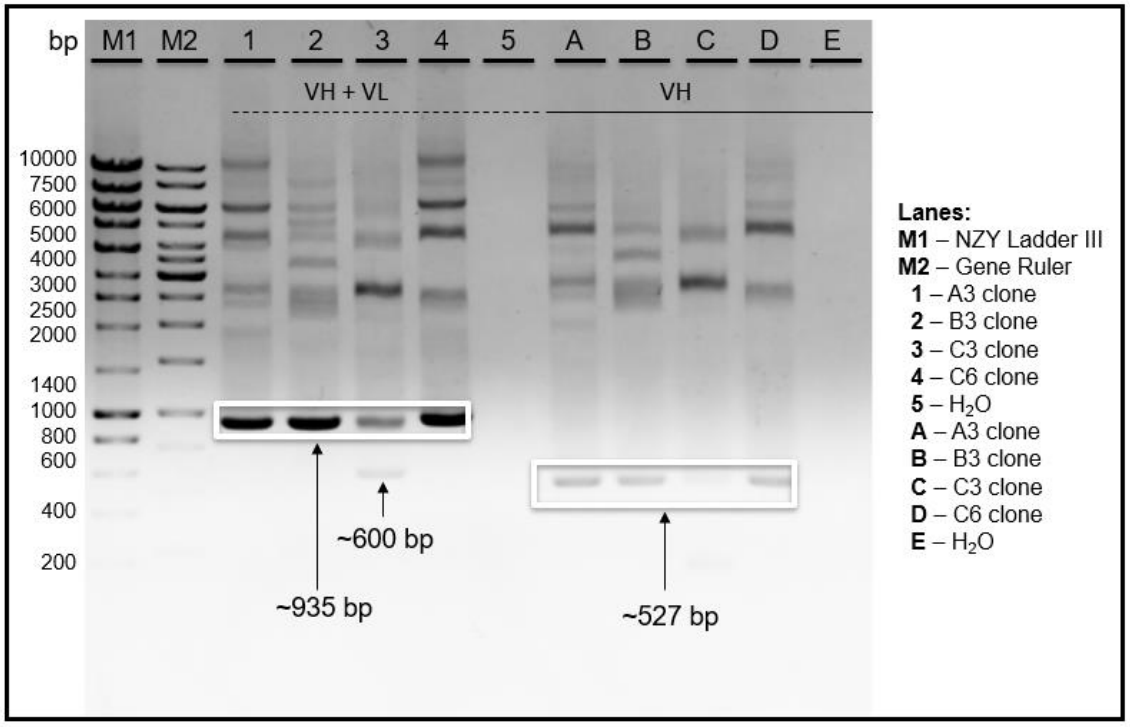

Figure 3.7. Agarose gel electrophoresis analysis of PCR amplification products of plasmid DNA extracted from the selected anti-JAG1 A3, B3, C3 and C6 scFv clones. VH+VL, PCR amplification of DNA fragments with VH and VL regions; VH, PCR amplification of VH regions. The PCR conditions were: Denaturing stage - 98°C; Annealing stage - 58°C; Extending stage - 72°C. M1, NZY Ladder III; M2, Gene Ruler.

3.1.5.3 DNA Sequencing of the selected clones

The DNA sequencing reaction was performed at the GATC company. For each clone, three reactions were performed using three different primers to ensure that the entire scFv nucleotide sequence was identified in both orientations. The LMB3 primer allows amplification of the scFv sequence from the 5´end beginning in the forward direction. The pHEN sequence primer amplifies the scFv sequence from the 3´ end in the reverse direction. The Link sequence primer amplifies the scFv sequence from the middle of the sequence in a reverse direction.

After the DNA sequences were determined, the sequences were analyzed using the Clone Manager and Chromas software. Analysis of the DNA sequences of clones A3, B3 and C6 confirmed they contained the full-length scFv sequence and revealed their DNA sequences were identical. DNA sequencing analysis of the C3 clone showed the presence of overlapping

nucleotides in the CDR regions indicating a mix of clones, as suggested from the PCR results. This observation might explain the low binding ability of this clone in comparison to the A3, B3 and C6 clones as observed in the ELISA assays (Figures 3.2 and 3.3).

The different clones within the C3 clone were segregated by plating various dilutions of this clone in 2YT-agar plates and analyzing the binding ability of the phages from the various resulting colonies to the JAG1-EGF3-Fc protein by ELISA as above. The results from these assays showed that none of the C3-segregated clones bound to the JAG1-EGF3-Fc protein (data not shown), suggesting the loss of the JAG1-EGF3-Fc-binding scFv clone within the C3. Another explanation is that the C3 was a false positive, a hypothesis supported by its low binding ability towards the JAG1-EGF3-Fc protein observed in the ELISA assays.

Altogether, these results showed we had one unique scFv sequence capable of recognizing the JAG1 protein.

Analysis of the amino acid sequences encoded by the scFv DNA fragment of the clones A3, B3, and C6, revealed the presence of an asparagine residue in the CDR2 of the HC (HCDR2), which can be glycosylated in the IgG format. Since glycosylation of CDR regions compromises the binding of the IgGs to the respective antigens, as it alters de Ab kinetics, stability and function (Mo et al., 2018), the identified scFv was reformatted into two IgGs: IgG48 where the HCDR2 asparagine residue was replaced by a glutamine, and IgG49 with the asparagine residue within the HCDR2. Bayer kindly supported the reformatting procedure of the scFv into the IgG format that were produced in mammalian cells and purified by chromatography.

3.1.6 Characterization of the generated anti-JAG1 IgG48 and IgG49 from the selected anti-JAG1 scFv

3.1.6.1 Characterization of anti-JAG1 IgG48 and IgG49 by ELISA

After reformatting the unique selected scFv resulting from the 1st panning into an IgG, ELISA assays were done to evaluate the binding properties towards the JAG1-EGF3-Fc recombinant protein. As mentioned above two IgGs were produced from the scFv sequence: the IgG49 containing the asparagine residue in the CDR2 of the HC; the IgG48 with the replacement of the asparagine in the CDR2 of the HC to a glutamine, to understand if the glycosylation of the IgG could affect its binding ability.

A dose response assay, using 2-fold-serial dilutions of each IgG with initial concentration of 100µg/mL, was performed to titrate the antibody towards the JAG1-EGF3-Fc protein, to allow understanding the optimal concentration at which the IgG would recognize the recombinant JAG1-EGF3-Fc protein. As in previous ELISA assays the Fc recombinant protein was used as a negative control. Non-coated wells were also used as negative controls to assess unspecific binding to the plastic. In these assays, the secondary antibody/detection Ab was used at 0.25µg/mL and 2.5µg/mL to evaluate which dosage produced better results with less background interference. An ELISA assay performed with a protein P and its specific detection antibody was also performed as a positive control for the ELISA assays.

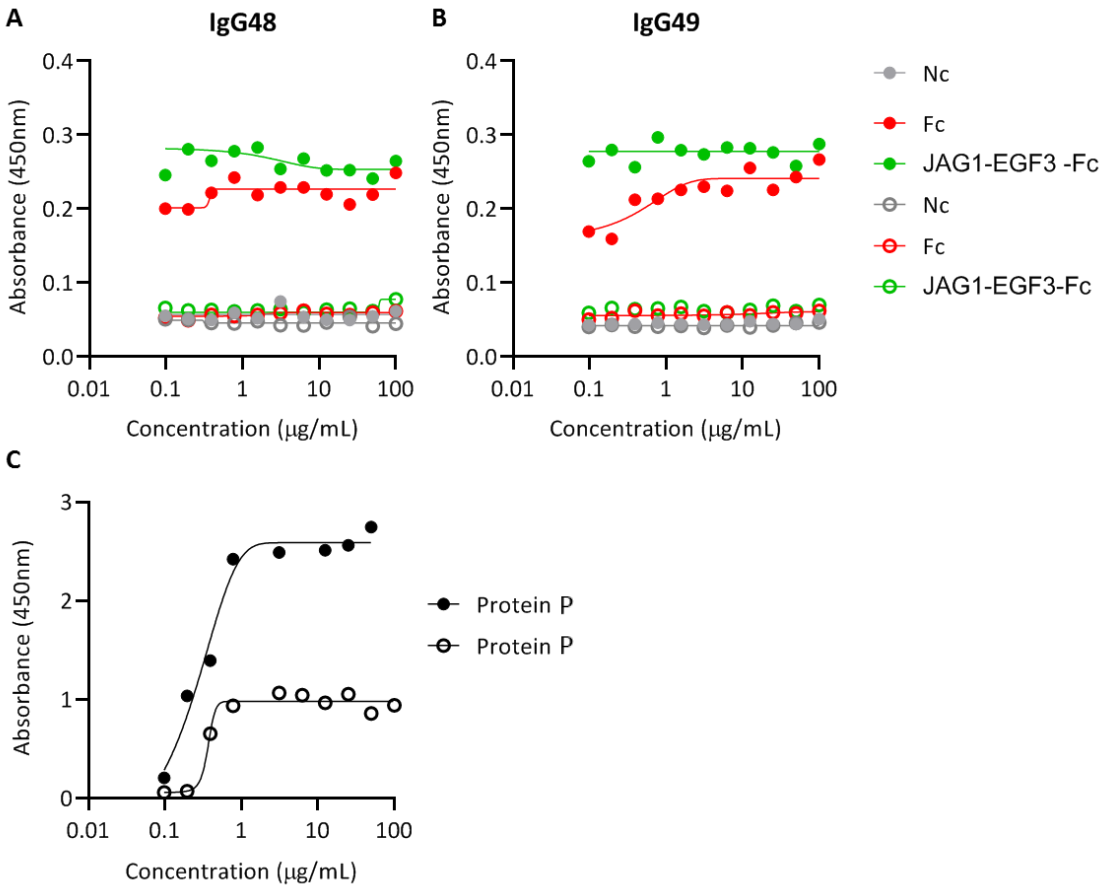

Figure 3.8. ELISA of IgG48, IgG49 and Protein P. (A-B), ELISA measurement binding assay of anti-JAG1 IgG48 and IgG49 to JAG1-EGF3-Fc protein. Non-coated (Nc) and coated wells with 5µg/mL of JAG1-EGF3-Fc or Fc control proteins were incubated with different concentrations of anti-JAG1 IgG58 (A) or IgG59 (B). **(C)**, wells were coated with 5µg/mL of protein A and were incubated with various amounts of anti-protein P antibody. IgG binding in A, B, an C was detected using 2.5µg/mL (filled symbols) or 0.25µg/mL (open symbols) of the secondary antibody.

Data presented in Figure 3.8 (panels A and B) on the binding of IgG48 and IgG49, respectively, show that these IgGs do not recognize the JAG1-EGF3-Fc protein at any tested concentration and condition.

Analysis of the binding ability of the anti-Protein P to its target protein (Figure 3.8, panel C) showed a dose-response curve with both concentrations of the secondary Ab (0.25µg/mL and 2.5µg/mL), indicating the anti-Protein P recognized its target antigen, validating the ELISA assay. However, when using a concentration of 2.5µg/mL of the secondary Ab we saw very high absorbance values. This indicates that the concentration of the secondary Ab should be lower than 2.5µg/mL.

Evaluation of the JAG1-EGF3-Fc protein quality in cellular assays showed it induced the expression of Notch-target genes (data not shown) confirming the good protein quality, indicating that the absence of binding of the IgG48 and IgG49 is not due to improper quality of the antigen. Indeed, a loss of binding capacity can occur after reformatting a scFv into an IgG due to some structural orientations that can make inaccessible the local of binding from the IgG. Another explanation is the presence of glycan groups in the IgG's that could block the access to

the recombinant JAG1 protein (Lee et al., 2017).

3.1.6.2 SDS-PAGE analysis of anti-JAG1 IgG48 and IgG49

Given the above results, next the anti-JAG1 IgG48 and IgG49 were analyzed by SDS-PAGE in reducing and non-reducing conditions to confirm their integrity, quality, and the potential presence of post-translational modifications. In reducing conditions, 2 bands should be detected: one band with a molecular weight of 50 kDa, corresponding to the heavy chains, and another band with 25 kDa, corresponding to the light chains, due to the break of the disulfide bonds that connect all the chains. In the non-reducing conditions, a single band of 150 kDa, corresponding to the entire Ab should be detected.

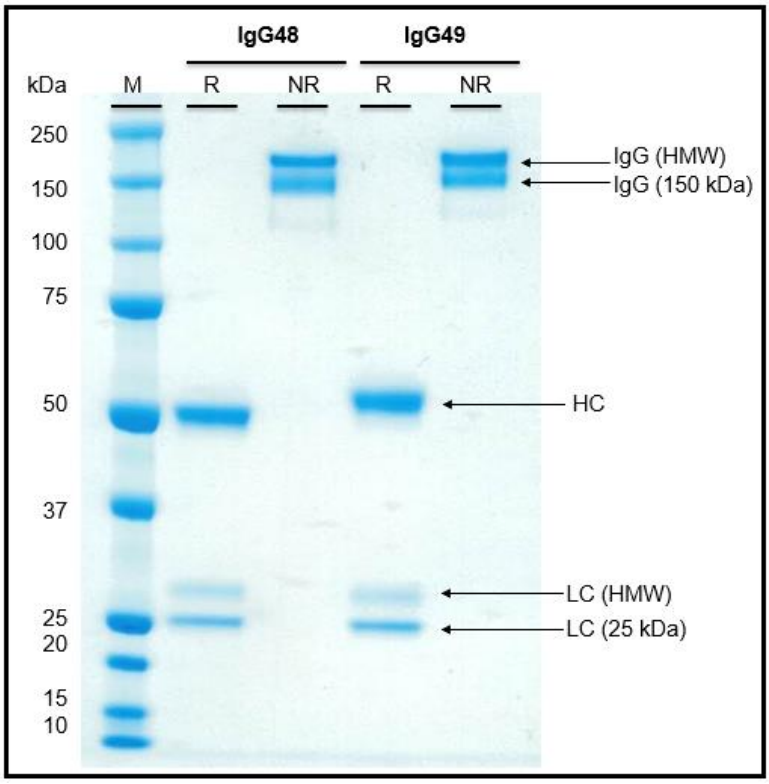

Figure 3.9. SDS-PAGE analysis of the reduced and non-reduce forms of the anti-JAG1 IgG48 and IgG49. Two bands in both IgGs in the non-reducing conditions suggest the existence of a high molecular weight (HMW) version of the IgGs. The presence of two bands near the 25 kDa in reducing conditions, corresponding to the LC, also suggests the existence of a HMW version of the LC. M-Precision Plus Protein Standard marker All blue. R, Reduced samples; NR, Non-reduced samples.

As shown in Figure 3.9 in reducing conditions both IgGs show the presence of three bands: a band of 25 kDa that corresponds to the LC; a band slightly above the 25 kDa that should also correspond to a LC variant; and a higher molecular weight band corresponding to the HC, with the expected 50 kDa in the IgG48 and a slightly higher molecular weight in the IgG49. The presence of a higher molecular weight HC in IgG49 was expected since it contains

a glycosylation site in the HCDR2. In non-reducing conditions, two bands are detected in both IgG samples instead of one. A band near the 150 kDa corresponding to the entire IgG and a second band with a significantly higher molecular weight that should also correspond to the IgG.

These observations together suggest that both IgGs are glycosylated, since glycosylation confers higher molecular weights to IgGs (Zheng et al., 2011). The presence of two bands in both IgGs in the non-reducing conditions indicates that not all Ab molecules from the same IgG are glycosylated, this could mean that the higher molecular band corresponds to the glycosylated Ab fraction and the 150 kDa band to the non-glycosylated forms. In the reduced IgGs, the presence of a fainter band above the 25 kDa suggests that both antibodies also contain glycosylated light chains. The higher molecular weight of the heavy chain of IgG49 in reducing conditions, in comparison to that of IgG48, indicates that IgG49 is more glycosylated than IgG48. This result was expected based on the amino acid sequence of the scFv and may indicate that the removal of the glycosylation site in the IgG48 heavy chain was successful.

3.1.6.3 Glycosylation analysis of the anti-JAG1 IgG48 and IgG49 with PNGase F

To evaluate if the existence of three bands in reducing conditions and two bands in non-reducing conditions in the SDS gel above (Figure 3.9) was due to a glycosylation modification of the IgGs, a deglycosylation reaction assay, was conducted using PNGase F enzyme. In this assay, the IgGs were incubated with the PNGase F enzyme, responsible for removing the glycan groups by cutting between an *N*-Acetylglucosamine and an asparagine residue of high mannose, hybrid, and complex oligosaccharides from N-linked glycoproteins.

This experiment was done using denaturated and non-denatured IgGs, as recommended by the enzyme supplier. As a negative control, samples of the IgG were incubated with the reagents without the PNGase F enzyme. As a positive control for the reaction conditions and functioning of the enzyme, the assay was also performed with a glycoprotein recommended by the enzyme suppliers. When the reactions were complete, the digestion products were analyzed by SDS-PAGE in reducing conditions. IgG samples in reduced and non-reduced forms were compared with the denaturated samples that resulted from this experiment (with and without PNGase F enzyme).

As shown in Figure 3.10, a similar pattern is observed between the reducing sample and the IgG denaturated and reduced sample without the enzyme as expected, due to the permanence of the glycan groups in the IgGs. We can observe two bands in the non-reduced sample that corresponds to the full glycosylated IgG and lacking any glycan groups. From the three bands observed in the reduced wells one correspond to the HC (near 50 kDa) and the other two bands to the LC, in which the band with higher molecular weight corresponds to the glycosylated LC. Comparison of the bands correspondent to the 50 kDa in the reducing wells from IgG48 and IgG49 shows that the band from the IgG49 is slightly higher than the IgG48 one.

When the PNGase F enzyme is added to the solution, it removes the glycan groups from the IgGs, and this is demonstrated by the absence of two bands near the 25 kDa MW but

rather only one is detected, and the 50 kDa band suffers a small decrease in molecular weight also consistent with the removal of the glycan groups.

In the control glycoprotein gel we can see a single band with a lower molecular weight (around 18 kDa) in the sample incubated without the PNGase F enzyme, and when we compare it to the sample treated with this enzyme we observe a decrease in the molecular weight, indicating reaction efficiency. Moreover, since we only see one band, we can say that the deglycosylation was complete and the reaction conditions were optimal, at least for this protein. The appearance of a new band in the samples containing the enzyme is due to the presence of PNGase F that has a molecular weight near the 35 kDa. In denaturing conditions, the deglycosylation was complete.

These results, showing only two bands near 50 and 25 kDa upon treatment with PNGase F enzyme demonstrate that the bands with atypical sizes in the SDS-PAGE in non-reducing and reducing conditions corresponded to glycosylated variants of both IgGs.

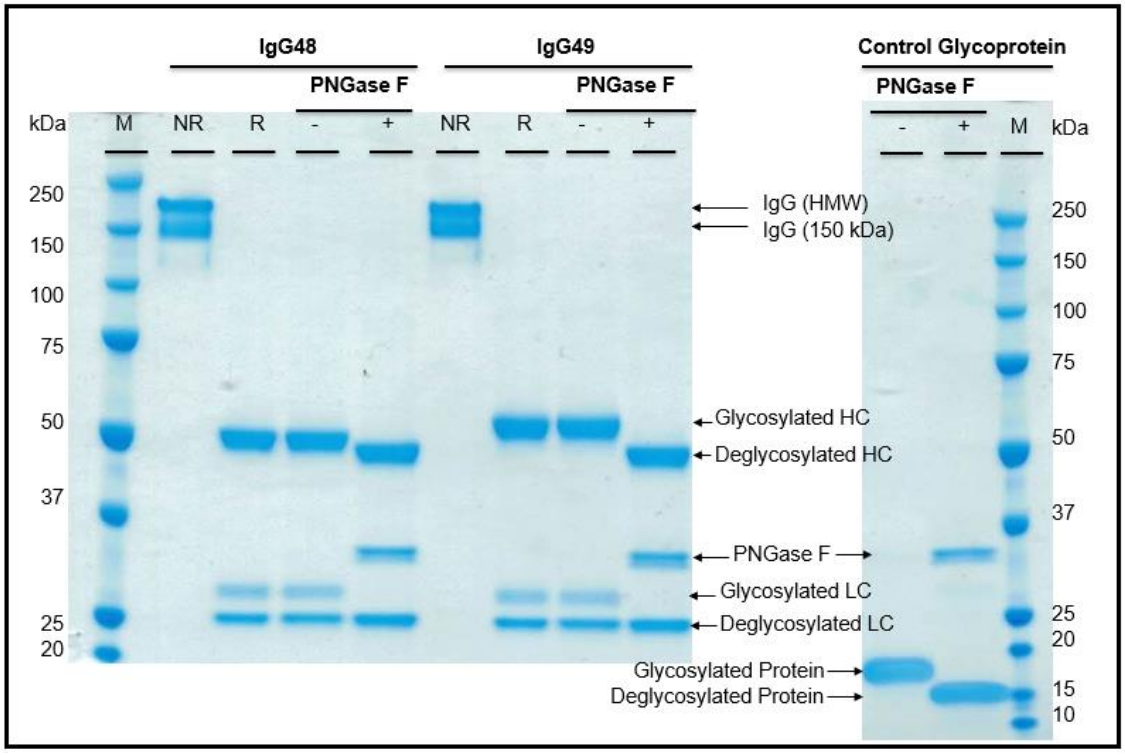

Figure 3.10. SDS-PAGE of denaturated IgG48 and IgG49 untreated and treated with PNGase F under reducing conditions. IgG samples present two bands in the gel approximately at 150 and 200 kDa in the non-reducing conditions, correspondent to the full IgG with high molecular weight (HMW) and with 150 kDa. In the samples incubated under reducing conditions three bands in the gel are detected, one correspondent to the HC and two to the LC with different molecular weights. The same band pattern is observed in denaturated samples not-incubated with the PNGase F enzyme. In the denaturated samples treated with PNGase F three bands are detected in the gel with a different pattern. Samples treated with the enzyme, when compared to the untreated sample, show a decrease in the molecular weight of the band correspondent to the HC. Also, the band correspondent to the LC (HMW) disappears, and the LC band in the 25 kDa seems to become bigger. The control glycoprotein presents a decrease in the molecular weight in the sample treated with the PNGase F enzyme, validating the assay. The bands observed in the gel near the 35 kDa correspond to the PNGase F enzyme in the solution. M, Precision Plus Protein Standard marker All Blue; R, Reduced.NR, Non-reduced; -, without PNGase F enzyme; +, with PNGase F enzyme.

However, in Figure 3.11, corresponding to samples treated with PNGase F enzyme in non-denaturing conditions, we see different results. The deglycosylation of the HC was complete in the IgG48, as shown by the decreased sizes of the band at 50 kDa, but not in the IgG49 observable by the difference in the molecular weight of both samples treated with PNGase F. The molecular weight difference between both IgGs could indicate that the IgG49 has more glycan groups then the IgG48 because in both samples, treated and non-treated with PNGase-F, the bands of the IgG49 presented a higher molecular weight. The LC remained glycosylated in both IgGs, proven by the presence of two bands near the 25 kDa, where the band with the highest molecular weight corresponds to the glycosylated version of the LC. This could be related with to the PNGase F reaction time that might not have been enough for the complete removal of the glycans to occur under non-denaturing conditions, or more probably, because the glycosylation site was not accessible to the PNGase F enzyme thus impairing the efficient removal the glycan group (Rudd et al., 1997).

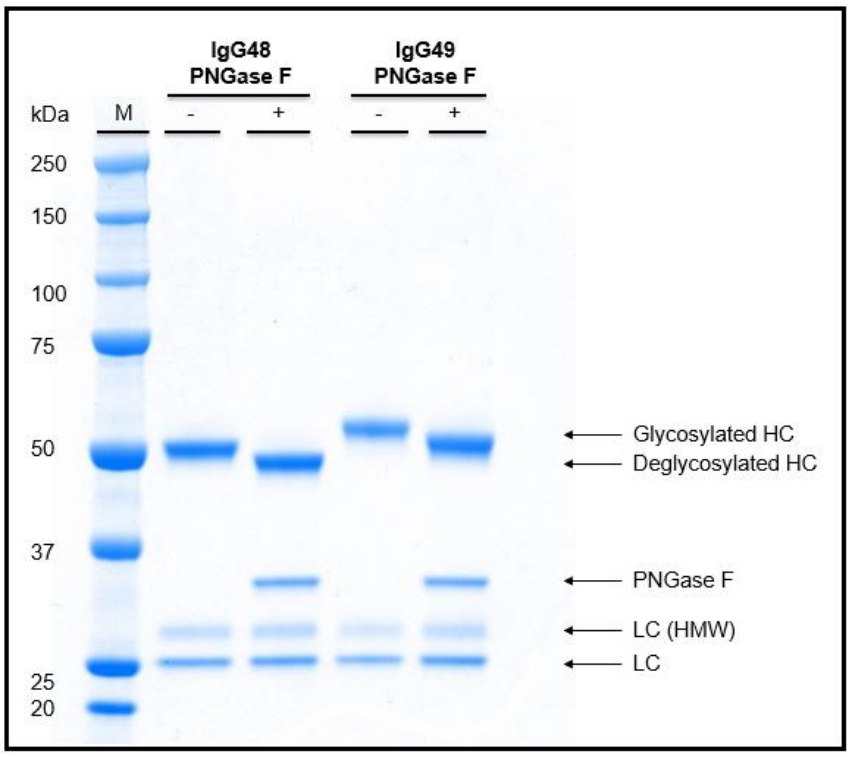

Figure 3.11. SDS-PAGE of native IgG48, and IgG49 untreated and treated with PNGase F under reducing conditions. Relative to control untreated proteins in reducing conditions, reduced IgGs treated with the PNGase F enzyme under native conditions show a decrease in the molecular weight of the HC band but not in the LC bands. The band near the 35 kDa correspondent to the PNGase F enzyme.. M, Precision Plus Protein Standard marker All Blue; -, without PNGase F; +, with PNGase F.

3.2 Selection of JAG1 scFv antibodies by Phage Display

3.2.1 2nd Library Panning

Considering the poor results obtained in the 1st panning, we pursued a series of tests to try to discover its origin and we concluded that it was due to library aliquots used. The inputs

and outputs of library pools used for the panning were analyzed. The pools used for the 1st panning selection had been previously submitted to several amplifications, and also to repeated freezing and thaw cycles, and this can lead to significant drops in the library titers. Because of that, new aliquots of the Tomlinson library with higher quality and titers, and only one amplification process, were obtained from collaborators from Maastricht University to perform another panning.

With the new aliquot we perform another panning using the same strategy as above, with three rounds of selection using the recombinant JAG1-EGF3-Fc protein immobilized via its Fc region, preceded by three depletion steps with non-coated immunotubes, as well as immunotubes coated with the off-targets - anti-human IgG-Fc specific Ab plus Fc control protein - to allow removal of unspecific binders. The selected phages were amplified between each round (Figure 3.1).

During the panning, we used 25µg/mL of recombinant protein JAG1-EGF3-Fc in the first and second rounds and 12.5µg/mL in the third round, to enforce specific selection. The proteins used in the depletion step were used at the same concentrations as the JAG1-EGF3-Fc protein. The concentration of phage in the output after each round was evaluated after titration.

Table 3.2. Phage concentration, recovery and enrichment after each round of selection from the 2nd panning.

Panning Round	Phage Input (cfu's/mL)	Phage Output (cfu's/mL)	% of input phage recovery	Enrichment
1st Round	2.5×10^{12}	1.3×10^{7}	5.2×10^{-4}	---
2nd Round	1.1×10^{13}	3.5×10^{7}	3.2×10^{-4}	0.6
3rd Round	5×10^{12}	2.9×10^{7}	5.8×10^{-4}	1,8

As we can see in table 3.2, our results show that the outputs obtained were in the expected range with values varying from 1.3 to 3.5 X 10^7 cfu's/mL throughout the rounds of selection. We can clearly see an improvement, especially after the first round of selection, in which before in the 1st panning we obtained an extremely high titer of 10^{10} cfu's/mL. These results indicate that the new aliquots of the Tomlinson library were in better conditions.

Moreover, in this strategy, the output concentration of the phages remained similar throughout rounds, suggesting that the enrichment of the JAG1-EGF3-Fc binding phages might not have happen as expected. However, to better assess this fact scFv-on-phage ELISAs were performed.

3.2.2 Analysis of scFv expression and specific binding towards JAG1-EGF3-Fc by scFv-on-phage ELISA

After the panning, *E.coli* bacteria were infected with the outputs from the second and third rounds. 88 clones from round 2 and 352 clones from round 3 were tested by ELISA assay,

in order to select specific scFv clones against the antigen JAG1-EGF3-Fc. To validate the experiment the scFv expression/display was confirmed by using an anti-c-Myc Ab.

Five 96 well plates were picked for scFv-on-Phage ELISAs assessment - 1 plate from round 2 and 4 plates from round 3. The ELISA results allowed to identify 80 scFvs positive clones capable of binding specifically to the JAG1-EGF3-Fc protein. This much higher number of positive scFv clones clearly demonstrates that in the 1st panning, where only 4 positive scFv clones were identified, the poor results were due to the low quality and reduced titers of the phage library aliquots used. Another result supporting this conclusion is the increase observed in the expression of the scFvs, which rose from 12.5% from the 1st panning to near 70% for the 2nd.

ELISA data from the second round of the panning, represented in Figure 3.12, panel A, shows that only 2 out of the 88 clones tested recognized the JAG1-EGF3-Fc protein. This value is quite low and indicates that two rounds of selection are not enough to have a phage pool enriched for JAG1, and thus more rounds of selection are needed to accomplish that. The phage expression obtained was in the 64% level.

In the first ELISA made with the clones from the third round of selection, 21 scFv were able to recognize the JAG1-EGF3-Fc recombinant protein, as we can see in Figure 3.12, panel B. This plate presented a 65% rate in phage expression. In the second ELISA made with phage pools selected from the third round (Figure 3.12, panel C) 9 scFv seem to recognize the target protein. In this assay the signals correspondent to the JAG1-EGF3-Fc protein were very low and the Fc signals seem very similar to these ones, suggesting the identified clones might be false positives. Despite that, we decided further test them. In this assay the incubator turned off during part of the period affecting the bacteria growth and the phage production, a fact that might explain the poor results herein obtained.

In the third and fourth ELISAs made with clones from the third round of selection (Figure 3.12, panels D and E) we had expression levels of 74 and 58% respectively, and were able to identify more 48 scFv able to recognize the JAG1-EGF3-Fc protein. Altogether, this assessment allowed identifying a total of 80 scFv capable of binding to the JAG1-EGF3-Fc protein and these were selected for further testes.

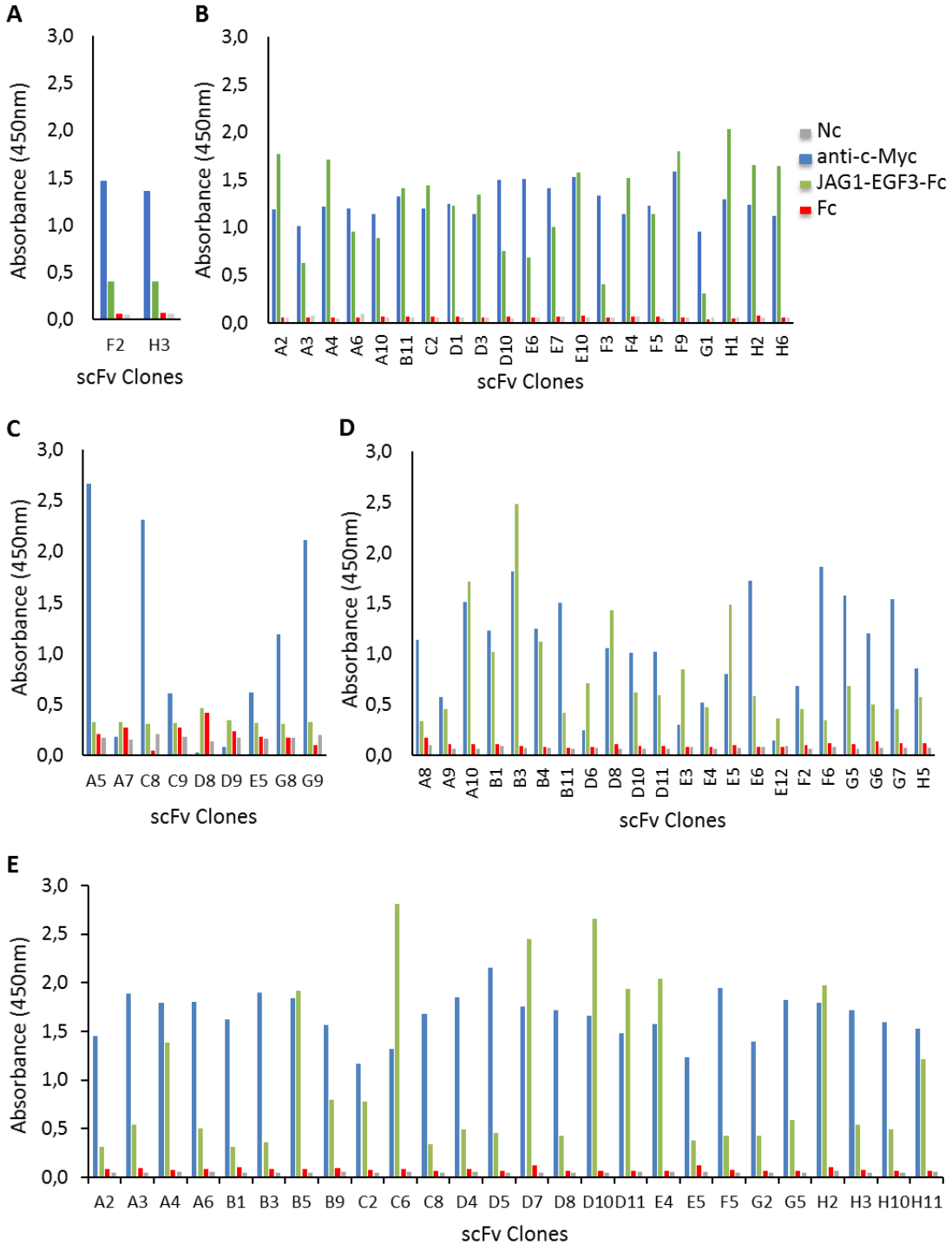

Figure 3.12. scFv-on-phage ELISA of clones from the 2nd panning that bound to JAG1-EGF3-Fc protein. The graphics show the binding of the anti-JAG1-EGF3-Fc scFv binders obtained from the second **(A)** and the third **(B-E)** rounds of selection to non-coated (Nc) wells and wells coated with anti-c-Myc Ab, and JAG1-EGF3-Fc and Fc proteins.

3.2.3 Binding ability of selected scFv from 2nd panning towards recombinant JAG1 and DLL1 proteins by scFv-on-phage ELISA

The next step was the confirmation of the previous ELISA results. For that a scFv-on-

phage ELISA assay with all the 80 selected scFv from the previous scFv-on-phage ELISA was done. To do that, anti-JAG1-EGF3 scFv clones resulting from the second and third pannings were picked from the glycerol stock plates and inoculated into a new plate (re-array plate) to be amplified and expressed as indicated in the material and methods section. Then, their binding to JAG1-EGF3-Fc recombinant protein was evaluated. As positive control for the anti-JAG1 scFv, we used the A3 positive scFv clone selected in the 1st panning. Two assays were conducted. One to evaluate the binding of the selected clones to both recombinant JAG1-EGF3-Fc and JAG1-ECD-Fc proteins. Another to evaluate the specificity of the anti-JAG1 scFv towards JAG1 protein in which the DLL1-EGF3-Fc protein was also used to test for eventual cross-reactivity to another Notch ligand. As in the previous ELISA assays, uncoated wells were used to set the minimal absorbance background, and wells coated with Fc proteins were used as negative control. As before, a coating with an anti-c-Myc Ab was also done to control for the scFv expression and validate the results.

Results from the first assay showed that, from the 80 anti-JAG1-EGF3 scFv 22 no longer bound to the JAG1 recombinant proteins, even though they were being expressed according to the absorbance values obtained with the anti-c-Myc antibody (Figure 3.13). These results leaded to the hypothesis that these 22 scFvs were most likely false positive that gave wrong signals in the first assay, and as such they were discarded. Moreover, results from these assay show that the scFv recognizing the JAG1-EGF3-Fc protein also recognize the recombinant JAG1 protein containing the full ECD (i.e. JAG1-ECD-Fc).

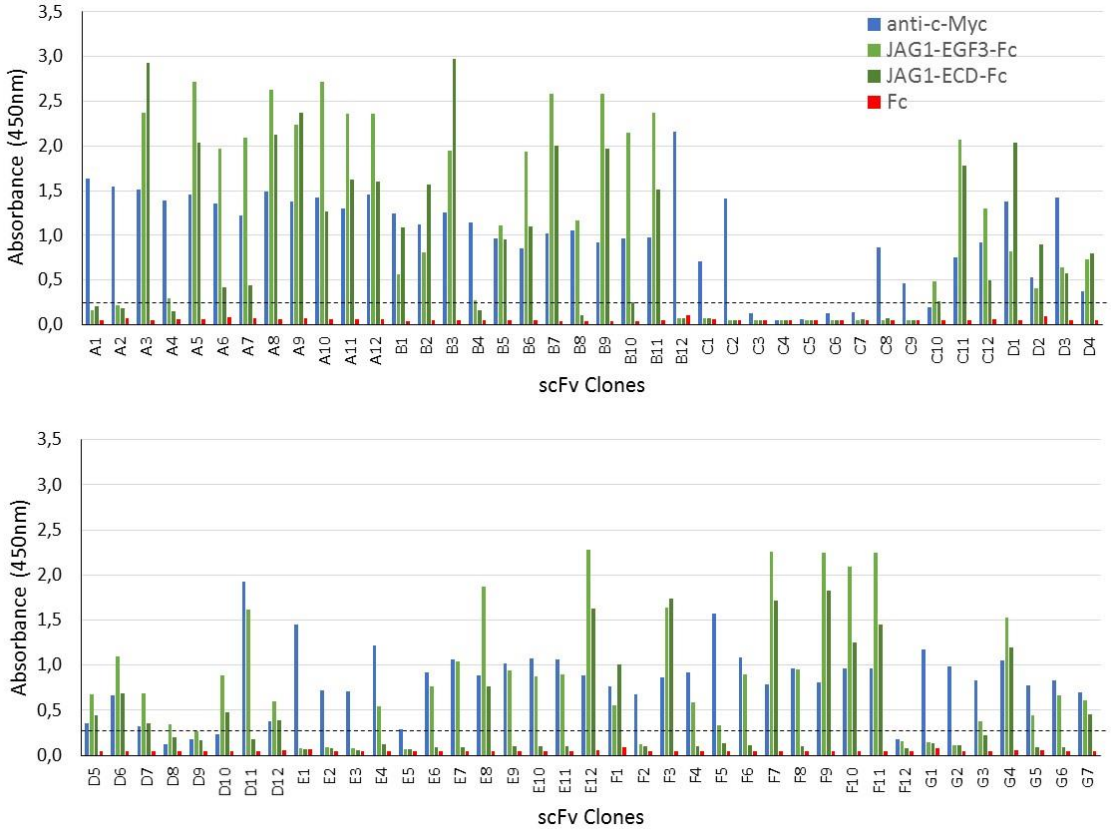

Figure 3.13. scFv-on-phage ELISA assay using JAG1-EGF3-Fc, JAG1-ECD-Fc, and Fc proteins and anti-c-Myc Ab. The graphics show the binding of the anti-JAG1-EGF3-Fc scFv obtained from the 2nd

panning.

Results from ELISA assay performed with the recombinant DLL1-EGF3-Fc protein showed that 3 other scFv clones were recognizing the DLL1-EGF3-Fc or the Fc proteins (clones E2, E4 and F6 in Figure 3.14), making them unspecific for the JAG1 ligand and due to that fact they were discarded.

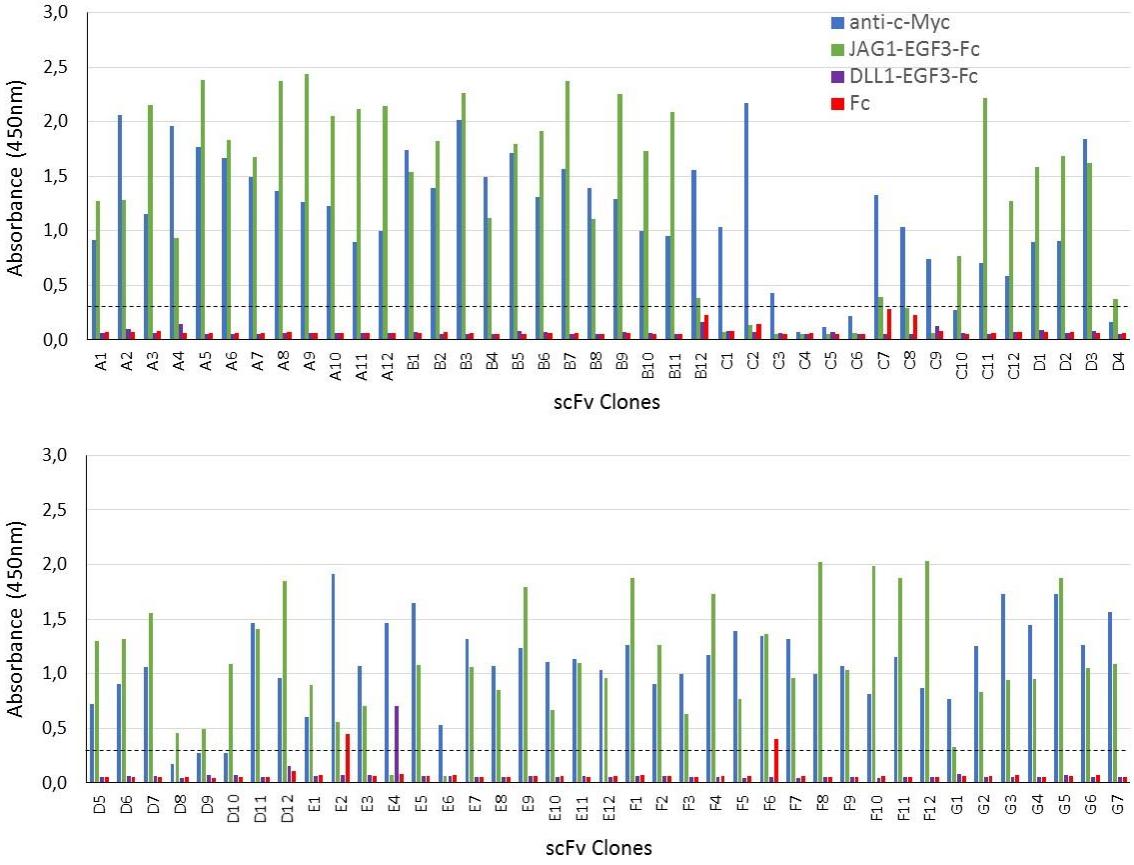

Figure 3.14. scFv-on-phage ELISA specificity assay using JAG1-EGF3-Fc, DLL1-EGF3-Fc and Fc proteins and anti-c-Myc Ab. The graphics show the binding of the anti-JAG1-EGF3-Fc scFv obtained from the 2nd panning.

In conclusion, analysis of the results from the ELISA assays performed with clones selected from the 2nd panning allowed the identification of 55 clones able to specifically recognize the JAG1 recombinant proteins (Figure 3.15).

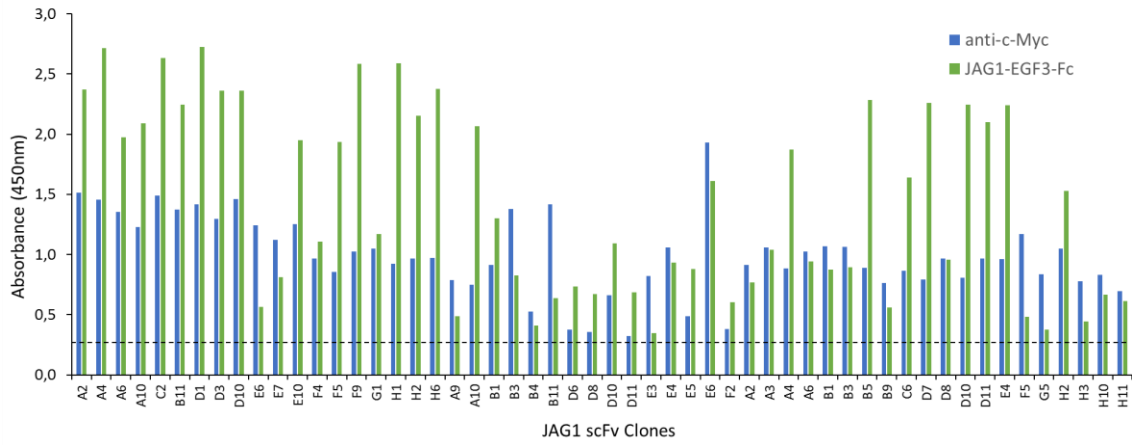

Figure 3.15. scFv-on-phage ELISA confirmation of clones from the 2nd panning that bound to JAG1EGF3-Fc protein. The discontinuous line in black represents the minimum absorbance value for which a result was considered positive.

3.2.4 DNA Sequencing

In order to determine the unique clones and evaluate their integrity, the scFv DNA sequence of the 55 selected clones against the JAG1 proteins, identified above, was determined using the LMB3, pHEN and Link sequence primers. Sequencing was performed by an outsourced company.

Analysis of the resulting DNA sequences from the 55 scFv clones, considering the differences in the variable region of both heavy and light chains, permitted the identification of 19 unique scFv sequences, all of them containing the complete scFv nucleotide sequence. Out of these 19 unique sequences, 7 scFv clones presented no glycosylation sites in the variable regions and were selected for subsequent reformatting into IgGs. The remaining 12 unique clones contain glycosylation sites in their CDR regions: 7 clones with 1 glycosite; 5 clones with 2 glycosites. These clones were discarded since the presence of glycosites in the CDR regions of the antibodies can lead to an impairment of the binding of these molecules to their target, even if certain residues are deleted or replaced by amino acids found in the germline CDRs (Lee et al., 2017). Of note, this was the case of the unique clone identified during the 1st panning, that bound to the JAG1 recombinant proteins in the scFv format but not in the IgG format (Figures 3.2, 3.3 and 3.8).

3.2.5 Flow Cytometry

3.2.5.1 Binding of scFv to endogenous cellular JAG1 protein

An evaluation of the binding properties of the scFv towards JAG1 protein in cells was also tested, as a first attempt, to see if they were able to recognize the native cellular protein. The capacity of the scFv to recognize endogenous JAG1 protein was tested using two cell lines: MDA-MB-231 triple negative breast cancer cells that express high JAG1, and the MCF-7 luminal A BC cells expressing very low JAG1 levels (Figure 3.14).

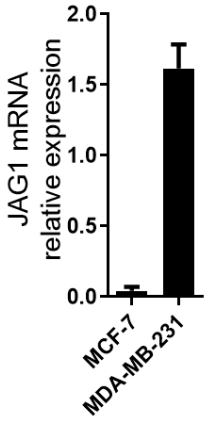

Figure 3.16. JAG1 mRNA expression levels in MCF-7 and MDA-MB-231 cell lines. Expression of JAG1 mRNA levels in luminal A MCF-7 and triple-negative MDA-MB-231 breast cancer cells were quantitated by qRT-PCR. The JAG1 mRNA values were normalized against the housekeeping gene HPRT1 mRNA levels in the same samples.

Results from this experiment, presented in Figure 3.15, showed that some of the scFv bound to the MDA-MB-231 cells and not to the MCF-7 ones, as reflected by an increase in the fluorescence signal in the MDA-MB-231 cells in comparison to MCF-7 cells and control cells treated with secondary Ab alone. The exceptions were the clones A09 and F12 that increased the fluorescence signal in MCF-7 cells.

Given the much higher JAG1 expression in the MDA-MB-231 cells relative to MCF-7 cells this data might suggest that the significant increase in the fluorescence value obtained in MDA-MB-231 cells incubated with anti-JAG1 scFv clones is due to their specific binding to the JAG1 cellular protein.

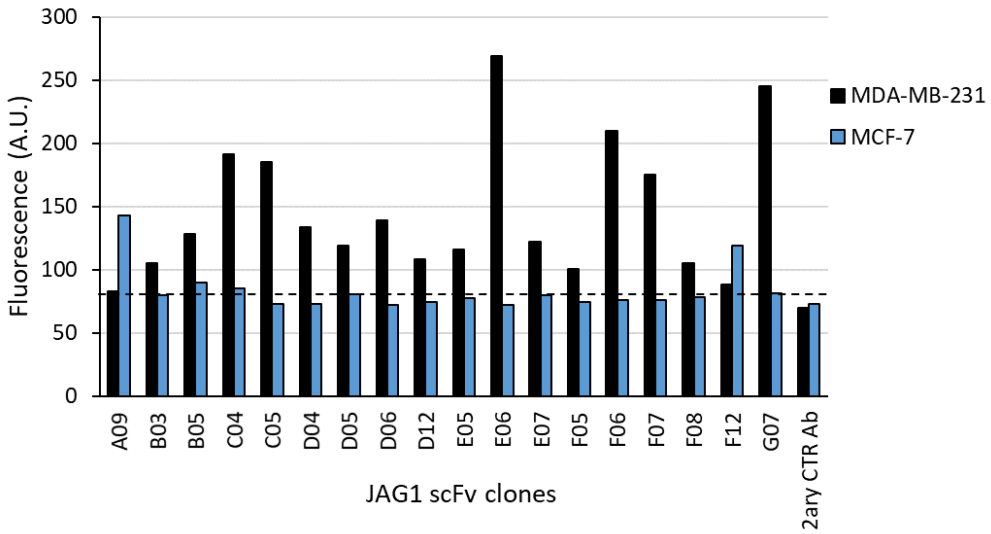

Figure 3.17. Fluorescence levels of MDA-MB-231 (JAG1 high expression) and MCF-7 (JAG1 very low expression) cell lines incubated with the indicated anti-JAG1 scFv clones. The MDA-MB-231 cells incubated with the indicated clones present higher fluorescence levels when compared with the MCF-7 and control cells treated with secondary Ab (2^{ary} CTR Ab) with the exception for the A09 and F12 scFv clones. The discontinuous line in black represents the minimum fluorescence value for which a result was considered positive.

To validate these results, a scFv-on-phage ELISA was performed using the anti-c-Myc Ab as a control for the expression of the scFvs. Figure 3.16 shows that the majority of the scFvs

were being expressed, validating the results in terms of their binding to MDA-MB-231 cells. The exceptions were the C4 and C5 clones that did not express the c-Myc protein but bound to MDA-MB-231 cells possibly due to unspecific binding of some bacterial remains to the plastic or a problem with their expression.

In order to validate these results, and clearly assess the specific binding of the anti-JAG1 scFv clones to cellular JAG1 a stable CHO-K1 cell line overexpressing human JAG1 (CHO-k1/JAG1^{+}) and a negative control cell line without human JAG1 (CHO-k1/control vector) was recently generated in the laboratory.

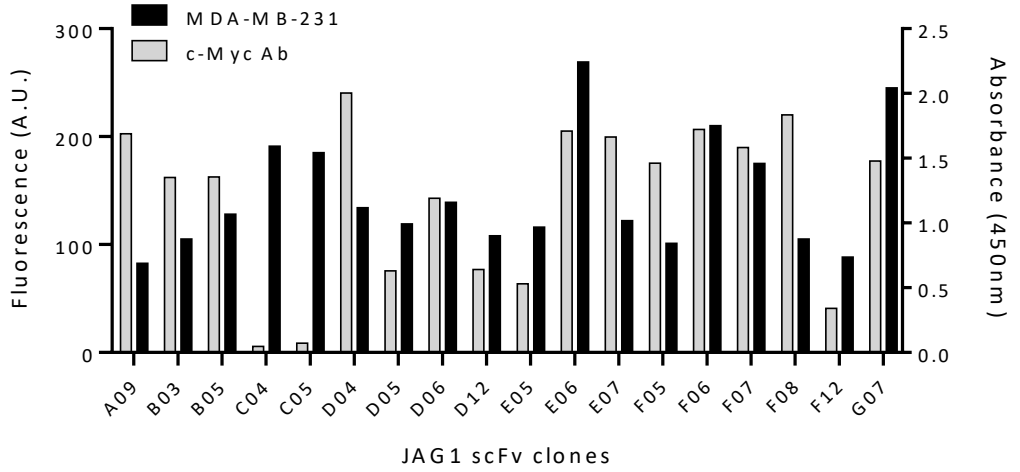

Figure 3.18. Fluorescence levels in the MDA-MB-231 cells incubated with the indicated anti-JAG1 scFv clones vs. their expression levels determined by scFv-on-phage ELISA. The majority of anti-JAG1 scFv clones that bind to MDA-MB-231 cells display their scFv as detected by ELISA. The exceptions are the C04 and C05 clones.

4. Conclusions and Future Perspectives

In summary, the work performed during this thesis allowed the selection by phage display of 84 scFv antibody fragments capable of recognizing the JAG1 protein. Evaluation of their binding properties towards JAG1 recombinant proteins by ELISA confirmed the selection of 55 anti-JAG1 scFvs. Sequencing analysis of these clones led to the identification of 19 unique anti-JAG1 scFvs. Out of these 19 unique sequences, 7 scFv clones present no glycosylation sites in the variable regions. Therefore, the two first goals of this thesis were achieved. ELISA assays performed with different peptides of conserved JAG1 regions, however, did not allow identifying the epitope regions of the selected anti-JAG1 scFvs.

One of the identified anti-JAG1 scFv, containing a glycosylation site in the HCDR2 region, was reformatted into 2 IgGs - one with a glycosite in HCDR2 and the other without. Characterization of these IgGs by ELISA showed that none of them recognized the JAG1 protein. SDS-PAGE and glycosylation assays indicate that both IgGs contain glycosylated variants.

In the future, the 7 unique anti-JAG1 scFvs without glycosites in their HCDR2 regions will be reformatted into IgGs, produced in mammalian cells, and purified using chromatography techniques. The generated IgGs will be then characterized in terms of their binding ability and affinity towards recombinant JAG1 proteins by ELISA and by flow cytometry to cellular JAG1 using a CHO-K1 stable cell line overexpressing human JAG1. Thereafter, the cellular effects of the specific anti-JAG1 IgGs will be assessed in cellular models of TNBC cells.

5. References

Acar, A.; Simões, B.; Clarke, R.; Brennan, K., 2016: A Role for Notch Signalling in Breast Cancer and Endocrine Resistance. *Stem Cells International*., **2016**.

Ahmad, Z.; Yeap, S.; Ali, A.; Ho, W.; Alitheen, N.; Hamid, M., 2012: ScFv antibody: Principles and clinical application. *Clinical and Developmental Immunology*., **2012**.

Alan F. Williams and A. Neil Barclay, 1988: The Immunoglobulin Superfamily—Domains for Cell Surface Recognition. *Annual Review of Immunology*., **6**, 381–405.

Andersson, E.; Sandberg, R.; Lendahl, U., 2011: Notch signaling: simplicity in design, versatility in function. *Development*., **138**, 3593–3612.

Andrieu, G.; Tran, A.; Strissel, K.; Denis, G., 2016: BRD4 regulates breast cancer dissemination through Jagged1/Notch1 signaling. *Cancer Research*., **76**, 6555–6567.

Anne Diévart, N., 1999: Involvement of Notch1 in the development of mouse mammary tumors. *Oncogene*., **18**, 5973–5981.

Aster, J.; Pear, W.; Blacklow, S., 2017: The Varied Roles of Notch in Cancer. *Annual Review of Pathology: Mechanisms of Disease*., **12**, 245–275.

Balint, K.; Xiao, M.; Pinnix, C.; Soma, A.; Veres, I.; Juhasz, I.; Brown, E.; Capobianco, A.; Herlyn, M.; Liu, Z., 2005: Activation of Notch1 signaling is required for β-catenin-mediated human primary melanoma progression. *Journal of Clinical Investigation*.

Bazan, J.; Całkosiński, I.; Gamian, A., 2012: Phage display—A powerful technique for immunotherapy. *Human Vaccines & Immunotherapeutics*., **8**, 1817–1828.

Benedito, R.; Roca, C.; Sörensen, I.; Adams, S.; Gossler, A.; Fruttiger, M.; Adams, R. H., 2009: The Notch Ligands Dll4 and Jagged1 Have Opposing Effects on Angiogenesis. *Cell*., **137**, 1124–1135.

Bolós, V.; Mira, E.; Martínez-Poveda, B.; Luxán, G.; Cañamero, M.; Martínez-A, C.; Mañes, S.; de la Pompa, J. L., 2013: Notch activation stimulates migration of breast cancer cells and promotes tumor growth. *Breast cancer research : BCR*., **15**, R54.

Bray, S. J., 2016: Notch signalling in context. *Nature Reviews Molecular Cell Biology*., **17**, 722–735.

Breitling, F.; Diibel, S.; Seehaus, T.; Klewinghaus, I.; Little, M., 1991: A surface expression vector for antibody screening (Phage gene III; fusion protein; phagemid; library; recombinant DNA). *Gene*., **104**, 147–353.

Brinkmann, U.; Kontermann, R., 2017: The making of bispecific antibodies. *mAbs*., **9**, 182–212.

Brou, C.; Logeat, F.; Gupta, N.; Bessia, C.; LeBail, O.; Doedens, J. R.; Cumano, A.; Roux, P.; Black, R.; Israël, A., 2000: A novel proteolytic cleavage involved in Notch

signaling: The role of the disintegrin-metalloprotease TACE. *Molecular Cell*., **5**, 207–216.
Brzozowa-Zasada, M.; Piecuch, A.; Michalski, M.; Segiet, O.; Kurek, J.; Harabin-Słowińska, M.; Wojnicz, R., 2017: Notch and its oncogenic activity in human malignancies. *European Surgery - Acta Chirurgica Austriaca*., **49**, 199–209.
Cabral, M., 2014: Phage Display as a tool for development of novel therapeutics for breast cancer.
Charng, W.; Yamamoto, S.; Jaiswal, M.; Bayat, V.; Xiong, B.; Zhang, K.; Sandoval, H.; David, G.; Gibbs, S.; Lu, H.; Chen, K.; Giagtzoglou, N.; Bellen, H., 2014: Drosophila Tempura, a Novel Protein Prenyltransferase α Subunit, Regulates Notch Signaling Via Rab1 and Rab11. *PLoS Biology*., **12**.
Chillakuri, C.; Sheppard, D.; Lea, S.; Handford, P., 2012: Notch receptor-ligand binding and activation: Insights from molecular studies. *Seminars in Cell and Developmental Biology*., **23**, 421–428.
Chillakuri, C.; Sheppard, D.; Ilagan, M.; Holt, L.; Abbott, F.; Liang, S.; Kopan, R.; Handford, P.; Lea, S., 2013: Structural Analysis Uncovers Lipid-Binding Properties of Notch Ligands. *Cell Reports*., **5**, 861–867.
Choi, J.; Park, J.; Davidson, B.; Morin, P.; Shih, I.; Wang, T., 2008: Jagged-1 and Notch3 juxtacrine loop regulates ovarian tumor growth and adhesion. *Cancer Research*., **68**, 5716–5723.
Christopher M. Grochowski, Kathleen M. Loomes, and Nancy B. Spinner, 2016: Jagged1 (JAG1): Structure, Expression, and Disease Associations. *Gene*., **576**, 381–384.
Clements, W.; Kim, A.; Ong, K.; Moore, J.; Lawson, N.; Traver, D., 2011: A somitic Wnt16/Notch pathway specifies haematopoietic stem cells. *Nature*., **474**, 220–225.
Cordle, J.; Redfield, C.; Stacey, M.; Van Der Merwe, P.; Willis, A.; Champion, B.; Hambleton, S.; Handford, P., 2008a: Localization of the delta-like-1-binding site in human Notch-1 and its modulation by calcium affinity. *Journal of Biological Chemistry*., **283**, 11785–11793.
Cordle, J.; Johnson, S.; Zi Yan Tay, J.; Roversi, P.; Wilkin, M. B.; De Madrid, B.; Shimizu, H.; Jensen, S.; Whiteman, P.; Jin, B.; Redfield, C.; Baron, M.; Lea, S.; Handford, P., 2008b: A conserved face of the Jagged/Serrate DSL domain is involved in Notch trans-activation and cis-inhibition. *Nature Structural and Molecular Biology*., **15**, 849–857.
Cox, Michael M.; Nelson, D., 2010: *Lehninger Principles of Biochemistry: W. H. Freeman*.
Coyle, K.; Boudreau, J.; Marcato, P., 2017: Genetic mutations and epigenetic

modifications: Driving cancer and informing precision medicine. *BioMed Research International*., **2017**.
Creighton, C.; Li, X.; Landis, M.; Dixon, J.; Neumeister, V.; Sjolund, A.; Rimm, D.; Wong, H.; Rodriguez, A.; Herschkowitz, J.; Fan, C.; Zhang, X.; He, X.; Pavlick, A.; Gutierrez, M.; Renshaw, L.; Larionov, A.; Faratian, D.; Hilsenbeck, S. et al., 2009: Residual breast cancers after conventional therapy display mesenchymal as well as tumor-initiating features. *Proceedings of the National Academy of Sciences*., **106**, 13820–13825.
Curtis R. Pickering, Jane H. Zhou, J. Jack Lee, Jennifer A. Drummond, S. Andrew Peng, Rami E. Saade, Kenneth Y. Tsai, Jonathan L. Curry, Michael T. Tetzlaff, Stephen Y Lai, Jun Yu, Donna M. Muzny, Harshavardhan Doddapaneni, Eve Shinbrot, 2015: Mutational landscape of aggressive cutaneous squamous cell carcinoma. *Clin Cancer Res*., **20**, 6582–6592.
Dai, X.; , Ting Li, Zhonghu Bai , Yankun Yang , Xiuxia Liu , Jinling Zhan, B., 2015: Breast cancer intrinsic subtype classification, clinical use and future trends. *American Journal of Cancer Research*., **5**, 2929–2943.
Dai, X.; Cheng, H.; Bai, Z.; Li, J., 2017: Breast cancer cell line classification and Its relevance with breast tumor subtyping. *Journal of Cancer*., **8**, 3131–3141.
Dang, T.; Sepetavec, T.; Hande, K.; Carbone, D.; Gazdar, A.; Virmani, A.; Minna, J.; Roberts, J., 2000: Chromosome 19 translocation, overexpression of Notch3, and human lung cancer. *Journal of the National Cancer Institute*., **92**, 1355–1357.
Dantas-Barbosa, C.; Brigido, M.; Maranhao, A., 2012: Antibody phage display libraries: Contributions to oncology. *International Journal of Molecular Sciences*., **13**, 5420–5440.
Davis, S. L.; Lorusso, P.; Xu, L.; Hill, D.; Kapoun, A. M.; Dupont, J.; Munster, P.; Eckhardt, S. G.; Patnaik, A., 2013: A first-in-human phase I study of the novel cancer stem cell (CSC) targeting antibody OMP-52M51 (anti-Notch1) administered intravenously to patients with certain advanced solid tumors Notch1 IHC Pre-Clinical Data OMP-52M51 Related AEs (All Grades).
Dufraine, J.; Funahashi, Y.; Kitajewski, J., 2008: Notch signaling regulates tumor angiogenesis by diverse mechanisms. *Oncogene*., **27**, 5132–5137.
Jones, Clement-Jones, D., 2000: JAGGED1 expression in human embryos: correlation with the Alagille syndrome phenotype. *Journal of Medical Genetics*., **37**, 658–662.
Ecker, D.; Jones, S.; Levine, H., 2015: The therapeutic monoclonal antibody market. *mAbs*., **7**, 9–14.
Efstratiadis, A.; Szabolcs, M.; Klinakis, A., 2007: Notch, Myc and breast cancer. *Cell Cycle*., **6**, 418–429.

Ellisen, L.; Bird, J.; West, D.; Soreng, A.; Reynolds, T.; Smith, S.; Sklar, J., 1991: TAN-1, the human homolog of the Drosophila Notch gene, is broken by chromosomal translocations in T lymphoblastic neoplasms. *Cell*., **66**, 649–661.
Espinoza, I.; Miele, L., 2013: Notch inhibitors for cancer treatment. *Pharmacology and Therapeutics*., **139**, 95–110.
Ferreira, 2015: Phage Display as a Tool for Generation of Bio- therapeutic Agents for Breast Cancer.
Fiona K. Rae, Sally-Anne Stephenson, 2000: Novel Association of a Diverse Range of Genes With Renal Cell. *International Journal of Cancer*., **732**, 726–732.
Fre, S.; Huyghe, M.; Mourikis, P.; Robine, S.; Louvard, D.; Artavanis-Tsakonas, S., 2005: Notch signals control the fate of immature progenitor cells in the intestine. *Nature*., **435**, 964–968.
Frenzel, A.; Hust, M.; Schirrmann, T., 2013: Expression of recombinant antibodies. *Frontiers in Immunology*., **4**, 1–20.
Frenzel, A.; Kügler, J.; Helmsing, S.; Meier, D.; Schirrmann, T.; Hust, M.; Dübel, S., 2017: Designing Human Antibodies by Phage Display. *Transfusion Medicine and Hemotherapy*., **44**, 312–318.
Friec, G. Le; Sheppard, D.; Whiteman, P.; Karsten, C..; Shamoun, T.; Laing, A.; Bugeon, L.; Dallman, M., 2012: The CD46 and Jagged1 interaction is critical for human T helper 1 immunity. *Nature Immunology*., **13**, 1213–1221.
Fu, Y.; Kaushiva, A.; Arhancet, J. P.; Kohaar, I.; Porter-Gill, P.; Shah, A.; Prokunina-Olsson, L.; Edvardsen, H.; Landmark-Høyvik, H.; Børresen-Dale, A.; Kristensen, V.; Fosså, S.; Howe, T.; Ambs, S.; Naume, B., 2010: NOTCH2 in breast cancer: Association of SNP rs11249433 with gene expression in ER-positive breast tumors without TP53 mutations. *Molecular Cancer*., **9**, 1–11.
Gallahan, D.; Callahan, R., 1987: Mammary tumorigenesis in feral mice: identification of a new int locus in mouse mammary tumor virus (Czech II)-induced mammary tumors. *Journal of virology*., **61**, 66–74.
Gasperowicz, M.; Otto, F., 2008: The Notch Signalling Pathway in the Development of the Mouse Placenta. *Placenta*., **29**, 651–659.
Gianni, L.; Pienkowski, T.; Y.; Roman, L.; Tseng, L.; Liu, M.; Lluch, A.; Staroslawska, E.; de la Haba-Rodriguez, J.; Im, S.; Pedrini, J.; Poirier, B.; Morandi, P.; Semiglazov, V.; Srimuninnimit, V.; Bianchi, G.; Szado, T.; Ratnayake, J.; Ross, G. et al., 2012: Efficacy and safety of neoadjuvant pertuzumab and trastuzumab in women with locally advanced, inflammatory, or early HER2-positive breast cancer (NeoSphere): A randomised multicentre, open-label, phase 2 trial. *The Lancet Oncology*., **13**, 25–32.
Gilbert, C.; Daou, M.; Moser, R.; Ross, A., 2010: Γ-Secretase Inhibitors Enhance

Temozolomide Treatment of Human Gliomas By Inhibiting Neurosphere Repopulation and Xenograft Recurrence. *Cancer Research*.
Glittenberg, M.; Pitsouli, C.; Garvey, C.; Delidakis, C.; Bray, S., 2006: Role of conserved intracellular motifs in Serrate signalling, cis-inhibition and endocytosis. *EMBO Journal*., **25**, 4697–4706.
Goldsby, R.; Kindt, T.; Osborne, B.; Kuby, J., 2003: *Immunology*. *W.H. Freeman and Company, New York*.
Gordon, W.; Vardar-Ulu, D.; L'Heureux, S.; Ashworth, T.; Malecki, M.; Sanchez-Irizarry, C.; McArthur, D.; Histen, G.; Mitchell, J.; Aster, J.; Blacklow, S., 2009: Effects of S1 cleavage on the structure, surface export, and signaling activity of human Notch1 and Notch2. *PLoS ONE*., **4**.
Gray, G.; Mann, R.; Mitsiadis, E.; Henrique, D.; Carcangiu, M.; Banks, A.; Leiman, J.; Ward, D.; Ish-Horowitz, D.; Artavanis-Tsakonas, S., 1999: Human ligands of the Notch receptor. *American Journal of Pathology*., **154**, 785–794.
Greg Winter & César Milstein, 1991: Man-made antibodies. *Nature*., **353**, 412–414.
Groff, K.; Brown, J.; Clippinger, A., 2015: Modern affinity reagents: Recombinant antibodies and aptamers. *Biotechnology Advances*., **33**, 1787–1798.
Guarnaccia, C.; Pintar, A.; Pongor, S., 2004: Exon 6 of human Jagged-1 encodes an autonomously folding unit. *FEBS Letters*., **574**, 156–160.
H. Hirose, H. Ishii, K. Mimori, D. Ohta, M. Ohkuma, H. Tsujii, T. Saito, M. Sekimoto, Y. Doki and M. Mori, 1994: Notch pathway as candidate therapeutic target in Her2/Neu/ErbB2 receptor-negative breast tumors. *Oncology Reports*., **1**, 993–996.
Hammers, C.; Stanley, J., 2014: Antibody phage display: Technique and applications. *Journal of Investigative Dermatology*., **134**, 1–5.
Hanqiu Zheng, Yangjin Bae, Sabine Kasimir-bauer, Rebecca Tang, Jin Chen, Guangwen Ren, Min Yuan, Mark Esposito, Wenyang Li, Yong Wei, Minhong Shen, Lanjing Zhang, Nikolai Tupitsyn, Klaus Pantel, Chadwick King, Jan Sun, Jodi Morigu, 2017: Therapeutic Antibody Targeting Tumor- and Osteoblastic Niche-Derived Jagged1 Sensitizes Bone Metastasis to Chemotherapy. *Cancer Cell*., **32**, 31–747.
Harrison, H.; Farnie, G.; Howell, S.; Rock, R.; Stylianou, S.; Brennan, K.; Bundred, N.; Clarke, R., 2010: Regulation of breast cancer stem cell activity by signaling through the Notch4 receptor. *Cancer Research*., **70**, 709–718.
Hassanpour, S.; Dehghani, M., 2017: Review of cancer from perspective of molecular. *Journal of Cancer Research and Practice*., **4**, 127–129.
Henderson, S.; Gao, D.; Lambie, E.; Kimble, J., 1994: lag-2 may encode a signaling ligand for the GLP-1 and LIN-12 receptors of C. elegans. *Development (Cambridge, England)*., **120**, 2913–2924.

Henderson, S.; Gao, D.; Christensen, S.; Kimble, J., 1997: Functional domains of LAG-2, a putative signaling ligand for LIN-12 and GLP-1 receptors in Caenorhabditis elegans. *Molecular Biology of the Cell*., **8**, 1751–1762.
Hoet, R.; Cohen, E.; Kent, R.; Rookey, K.; Schoonbroodt, S.; Hogan, S.; Rem, L.; Frans, N.; Daukandt, M.; Pieters, H.; Van Hegelsom, R.; Coolen-Van Neer, N.; Nastri, H.; Rondon, I.; Leeds, J.; Hufton, S.; Huang, L.; Kashin, I.; Devlin, M. et al., 2005: Generation of high-affinity human antibodies by combining donor-derived and synthetic complementarity-determining-region diversity. *Nature Biotechnology*., **23**, 344–348.
Hoogenboom, H.; de Bruïne, A.; Hufton, S.; Hoet, R.; Arends, J.; Roovers, R.; de Bruïne, A.; Hufton, S.; Hoet, R.; Arends, J.; Roovers, R., 1998: Antibody phage display technology and its applications. *Immunotechnology : an international journal of immunological engineering*., **4**, 1–20.
International Agency for Research on Cancer - World Health Organization, 2018: Globocan 2018. Population Fact Sheets: Portugal, **270**, 2018–2019.
Iso, T.; Kedes, L.; Hamamori, Y., 2003: HES and HERP families: Multiple effectors of the Notch signaling pathway. *Journal of Cellular Physiology*., **194**, 237–255.
Jacobson, A., 1972: Role of F pili in the penetration of bacteriophage fl. *Journal of virology*., **10**, 835–843.
Jinpeng Wanga, Yanli Liua, Tambet Teesaluc, Kazuki N. Sugaharac, Venkata Ramana Kotamrajuac, Jonathan D. Adamsd, Brian S. Fergusona, Qiang Gonge, Seung Soo Ohb, Andrew T. Csordase, Minseon Choa, Erkki Ruoslahtic, Yi Xiaoa, and H. Tom, 2011: Selection of phage-displayed peptides on live adherent cells in microfluidic channels. *PNAS*., **108**, 6909–6914.
Julie George, Jing Shan Lim, Se Jin Jang, Yupeng Cun, Luka Ozretić, Gu Kong, Frauke Leenders, Xin Lu, Lynnette Fernández-Cuesta, Graziella Bosco, Christian Müller, Ilona Dahmen, Nadine S. Jahchan, Kwon-Sik Park, Dian Yang, Anthony N. et al. P. 29 Nature. A. manuscript; available in P. 2016 M. 09. A. M. M. M. M.; Nürnberg, Christian Reinhardt, Sven Perner, Lukas Heukamp, Reinhard Büttner, Stefan A. Haas, Elisabeth Brambilla, Martin Peifer, Julien Sage, and R., 2016: Comprehensive genomic profiles of small cell lung cancer. *Nature*., **524**, 47–53.
Ke, X.; Shen, L., 2017: Molecular targeted therapy of cancer: The progress and future prospect. *Frontiers in Laboratory Medicine*., **1**, 69–75.
Kenneth Murphy, C., 2011: *Human Single Fold scFv Libraries I+J (Tomlinson I+J)*. *Taylor & Francis Grou*.
Kevin Fitzgerald, Anne Harrington and Philip Leder, 2000: Ras pathway signals are required for notch-mediated oncogenesis. *Oncogene*., **19**, 4191–4198.
Koch, U.; Radtke, F., 2007: Notch and cancer: A double-edged sword. *Cellular and*

Molecular Life Sciences., **64**, 2746–2762.
Koch, U.; Radtke, F., 2018: *Targeting Notch in Cancer*. *Nature*.
Kontomanolis, E.; Panteliadou, M.; Giatromanolaki, A.; Pouliliou, S.; Efremidou, E.; Limberis, V.; Galazios, G.; Sivridis, E.; Koukourakis, M., 2014: Delta-like ligand 4 (DLL4) in the plasma and neoplastic tissues from breast cancer patients: Correlation with metastasis. *Medical Oncology*., **31**.
Kopan, Raphael; Ilagan, M., 2009: The Canonical Notch Signaling Pathway: Unfolding the Activation Mechanism. *Cell*., **137**, 216–233.
Kopan, R.; Ilagan, M., 2009: The Canonical Notch Signaling Pathway: Unfolding the Activation Mechanism. *Cell*., **137**, 216–233.
Kopan, R., 2012a: Notch signaling. *Cold Spring Harbor Laboratory Press*., **4**, 1–4.
Kopan, R., 2012b: Notch signaling. *Otology Japan*., **13**, 516.
Lafkas, D.; Shelton, A.; Chiu, C.; De Leon Boenig, G.; Chen, Y.; Stawicki, S.; Siltanen, C.; Reichelt, M.; Zhou, M.; Wu, X.; Eastham-Anderson, J.; Moore, H.; Roose-Girma, M.; Chinn, Y.; Hang, J.; Warming, S.; Egen, J.; Lee, W.; Austin, C. et al., 2015: Therapeutic antibodies reveal Notch control of transdifferentiation in the adult lung. *Nature*., **528**, 127–131.
Lai, J., 2016: Protein and Antibody Engineering by Phage Display. *Methods Enzymol*., **580**, 45–87.
Lamy, M.; Ferreira, A.; Dias, J.; Braga, S.; Silva, G.; Barbas, A., 2017: Notch-out for breast cancer therapies. *New Biotechnology*., **39**, 215–221.
Lee, H.; Im, W., 2017: Effects of N-Glycan Composition on Structure and Dynamics of IgG1 Fc and Their Implications for Antibody Engineering. *Scientific Reports*., **7**, 1–10.
Leong, K.; Niessen, K.; Kulic, I.; Raouf, A.; Eaves, C.; Pollet, I.; Karsan, A., 2007: Jagged1-mediated Notch activation induces epithelial-to-mesenchymal transition through Slug-induced repression of E-cadherin. *The Journal of Experimental Medicine*., **204**, 2935–2948.
Li, D., 2014: The Notch ligand Jagged1 as a target for anti-tumor therapy. *Frontiers in Oncology*., **4**, 1–13.
Li, L.; Krantz, I.; Deng, Y.; Genin, A.; Banta, A.; Collins, C.; Qi, M.; Trask, B.; Kuo, W.; Cochran, J.; Costa, T.; Pierpont, M. E.; Rand, E.; Piccoli, D.; Hood, L.; Spinner, N., 1997: Alagille syndrome is caused by mutations in human Jagged1, which encodes a ligand for notch1. *Nature Genetics*., **16**, 243–251.
Lin Xin, Jiaqing Cao, Hua Cheng, Fei Zeng, Xiaoyun Hu, J., 2013: Human monoclonal antibodies in cancer therapy: a review of recent developments. *Front Biosci (Landmark Ed)*., Vol. 1pp. 765–772.
Lindsell, C.; Shawber, C.; Boulter, J.; Weinmaster, G., 1995: Jagged: A Mammalian

Ligand That Activates Notch1. *Cell Press*., **80**, 909–917.
Liu, H.; Bulseco, G.; Sun, J., 2006a: Effect of posttranslational modifications on the thermal stability of a recombinant monoclonal antibody. *Immunology Letters*., **106**, 144–153.
Liu, J.; Sato, C.; Cerletti, M.; Wagers, A., 2010: *Notch signaling in the regulation of stem cell self-renewal and differentiation*. *Current Topics in Developmental Biology*. Elsevier Inc., Vol. 92.
Liu, Z.; Xiao, M.; Balint, K.; Smalley, K.; Brafford, P.; Qiu, R.; Pinnix, C.; Li, X.; Herlyn, M., 2006b: Notch1 signaling promotes primary melanoma progression by activating mitogen-activated protein kinase/phosphatidylinositol 3-kinase-Akt pathways and up-regulating N-cadherin expression. *Cancer Research*., **66**, 4182–4190.
Logeat, F.; Bessia, C.; Brou, C.; LeBail, O.; Jarriault, S.; Seidah, N.; Israel, A., 1998: The Notch1 receptor is cleaved constitutively by a furin-like convertase. *Proceedings of the National Academy of Sciences*., **95**, 8108–8112.
Lòpez-Ribot, J.; Díez-Orejas, R.; Gil, C., 2007: Antibodies. *Immunology of Fungal Infections*., 235–256.
Lu, J.; Ye, X.; Fan, F.; Xia, L.; Bhattacharya, R.; Bellister, S.; Tozzi, F.; Sceusi, E.; Zhou, Y.; Tachibana, I.; Maru, D.; Hawke, D.; Rak, J.; Mani, S.; Zweidler-McKay, P.; Ellis, L., 2013: Endothelial Cells Promote the Colorectal Cancer Stem Cell Phenotype through a Soluble Form of Jagged-1. *Cancer Cell*., **23**, 171–185.
Malhotra, G.; Zhao, X.; Band, H.; Band, V., 2010: Histological, molecular and functional subtypes of breast cancers. *Cancer Biology and Therapy*., **10**, 955–960.
McCafferty, J.; Griffiths, A.; Winter, G.; Chiswell, D., 1990: Phage antibodies: filamentous phage displaying antibody variable domains. *Nature*.
Meurette, O.; Mehlen, P., 2018: Notch Signaling in the Tumor Microenvironment. *Cancer Cell*., **34**, 536–548.
Mittal, S.; Subramanyam, D.; Dey, D.; Kumar, R.; Rangarajan, A., 2009: Cooperation of Notch and Ras/MAPK signaling pathways in human breast carcinogenesis. *Molecular Cancer*., **8**, 1–12.
Mo, J.; Jin, R.; Yan, Q.; Sokolowska, I.; Lewis, M.; Hu, P., 2018: Quantitative analysis of glycation and its impact on antigen binding. *mAbs*., **10**, 406–415.
Mumm, J.; Schroeter, E.; Saxena, M.; Griesemer, A.; Tian, X.; Pan, D.; Ray, W.; Kopan, R., 2000: A ligand-induced extracellular cleavage regulates γ-secretase-like proteolytic activation of Notch1. *Molecular Cell*., **5**, 197–206.
Muyldermans, S., 2013: Nanobodies: Natural Single-Domain Antibodies. *Annual Review of Biochemistry*., **82**, 775–797.
Nowell, C.; Radtke, F., 2017: Notch as a tumour suppressor. *Nature Reviews Cancer*.,

17, 145–159.
Ozlem Yersal, S.; Ozlem, 2014: Biological subtypes of breast cancer: Prognostic and therapeutic implications. *World Journal of Clinical Oncology*., **5**, 412–424.
Parmley, S.; Smith, G., 1988: Antibody-selectable filamentous fd phage vectors: affinity purification of target genes. *Gene*., **73**, 305–318.
Politi, K.; Feirt, N.; Kitajewski, J., 2004: Notch in mammary gland development and breast cancer. *Seminars in Cancer Biology*., **14**, 341–347.
R. L. Siegel, L. A.Torre, A. Jemal, F. Bray, J. Ferlay, 2018: Global Cancer Statistics 2018: GLOBOCAN Estimates of Incidence and Mortality Worldwide for 36 Cancers in 185 Countries. *Cancer Journal for Clinicians*., **0**, 3–31.
Rami, A.; Behdani, M.; Yardehnavi, N.; Habibi-Anbouhi, M.; Kazemi-Lomedasht, F., 2017: An overview on application of phage display technique in immunological studies. *Asian Pacific Journal of Tropical Biomedicine*., **7**, 599–602.
Rana, N.; Haltiwanger, R., 2012: Fringe-mediated extension of O-linked fucose in the ligand-binding region of Notch1 increases binding to mammalian Notch ligands. *Proc Natl Acad Sci U S A*., **21**, 583–589.
Rebecca L. Siegel, Kimberly D. Miller, A., 2019: Cancer Statistics, 2019. *CA: A Cancer Journal for Clinicians*., **69**, 7–34.
Reedijk, M.; Odorcic, S.; Chang, L.; Zhang, H.; Miller, N.; McCready, D. R.; Lockwood, G.; Sean, E., 2005: High-level coexpression of JAG1 and NOTCH1 is observed in human breast cancer and is associated with poor overall survival. *Cancer Research*., **65**, 8530–8537.
Regan, J.; Long, F., 2013: Notch signaling and bone remodeling. *Current Osteoporosis Reports*., **11**, 126–129.
Riaz, M.; van Jaarsveld, M.; Hollestelle, A.; Prager-van der Smissen, W.; Heine, A.; Boersma, A.; Liu, J.; Helmijr, J.; Ozturk, B.; Smid, M.; Wiemer, E.; Foekens, J.; Martens, J., 2013: MiRNA expression profiling of 51 human breast cancer cell lines reveals subtype and driver mutation-specific miRNAs. *Breast Cancer Research*., **15**.
Rizzo, P.; Miao, H.; D'Souza, G.; Osipo, C.; Yun, J.; Zhao, H.; Mascarenhas, J.; Wyatt, D.; Antico, G.; Hao, L.; Yao, K.; Rajan, P.; Hicks, C.; Siziopikou, K.; Selvaggi, S.; Bashir, A.; Bhandari, D.; Marchese, A.; Lendahl, U. et al., 2008: Cross-talk between notch and the estrogen receptor in breast cancer suggests novel therapeutic approaches. *Cancer Research*., **68**, 5226–5235.
Rodilla, V.; Villanueva, A.; Obrador-Hevia, A.; Robert-Moreno, A.; Fernandez-Majada, V.; Grilli, A.; Lopez-Bigas, N.; Bellora, N.; Alba, M.; Torres, F.; Dunach, M.; Sanjuan, X.; Gonzalez, S.; Gridley, T.; Capella, G.; Bigas, A.; Espinosa, L., 2009: Jagged1 is the pathological link between Wnt and Notch pathways in colorectal cancer. *Proceedings*

of the National Academy of Sciences., **106**, 6315–6320.
Rudd, P.; Dwek, R., 1997: Glycosylation: Heterogeneity and the 3D structure of proteins. *Critical Reviews in Biochemistry and Molecular Biology*., **32**, 1–100.
Sales-Dias, J.; Silva, G.; Lamy, M.; Ferreira, A.; Barbas, A., 2019: The Notch ligand DLL1 exerts carcinogenic features in human breast cancer cells. *PLoS ONE*., **14**, 1–22.
Sansone, P.; Storci, G.; Tavolari, S.; Guarnieri, T.; Giovannini, C.; Taffurelli, M.; Ceccarelli, C.; Santini, D.; Paterini, P.; Marcu, K.; Chieco, P.; Bonafè, M., 2007: IL-6 triggers malignant features in mammospheres from human ductal breast carcinoma and normal mammary gland. *The Journal of Clinical Investigation*., **117**, 3968–4002.
Schirrmann, T.; Meyer, T.; Schütte, M.; Frenzel, A.; Hust, M., 2011: Phage display for the generation of antibodies for proteome research, diagnostics and therapy. *Molecules*., **16**, 412–426.
Schroeder, Harry W; Cavacini, L. (University of A. at B., 2013: Structure and Functions of Immunoglobulins, **125**.
Schroeter, E.; Kisslinger, J.; Kopan, R., 1998: Notch-1 signalling requires ligand-induced proteolytic release of intracellular domain. *Nature*., **393**, 382–386.
Scott, A. M.; Wolchok, J.; Old, L., 2012: Antibody therapy of cancer. *Nature Reviews Cancer*., **12**, 278–287.
Sethi, N.; Kang, Y., 2011a: Notch signalling in cancer progression and bone metastasis. *British Journal of Cancer*., **105**, 1805–1810.
Sethi, N.; Dai, X.; Winter, C.; Kang, Y., 2011b: Tumor-Derived Jagged1 Promotes Osteolytic Bone Metastasis of Breast Cancer by Engaging Notch Signaling in Bone Cells. *Cancer Cell*., **19**, 192–205.
Shang, Y.; Smith, S.; Hu, X., 2016: Role of Notch signaling in regulating innate immunity and inflammation in health and disease. *Protein and Cell*., **7**, 159–174.
Shao, S.; Zhao, X.; Zhang, X.; Luo, M.; Zuo, X.; Huang, S.; Wang, Y.; Gu, S.; Zhao, X., 2015: Notch1 signaling regulates the epithelial-mesenchymal transition and invasion of breast cancer in a Slug-dependent manner. *Molecular Cancer*., **14**, 1–17.
Sharma, A.; Paranjape, A.; Rangarajan, A.; Dighe, R., 2012: A Monoclonal Antibody against Human Notch1 Ligand-Binding Domain Depletes Subpopulation of Putative Breast Cancer Stem-like Cells. *Molecular Cancer Therapeutics*., **11**, 77–86.
Sharma, A.; Rangarajan, A.; Dighe, R., 2013: Antibodies against the extracellular domain of human Notch1 receptor reveal the critical role of epidermal-growth-factor-like repeats 25–26in ligand binding and receptor activation. *Biochemical Journal*., **449**, 519–530.
Shimizu, M.; Cohen, B.; Goldvasser, P.; Berman, H.; Virtanen, C.; Reedijk, M., 2011: Plasminogen activator uPA is a direct transcriptional target of the JAG1-notch receptor

signaling pathway in breast cancer. *Cancer Research*., **71**, 277–286.
Shinya Yamamoto , Karen L. Schulze, 2014: Introduction to Notch Signaling. *Notch Signaling: Methods and Protocols, Methods in Molecular Biology*., **1187**.
Sibéril, S.; De Romeuf, C.; Bihoreau, N.; Fernandez, N.; Meterreau, J.; Regenman, A.; Nony, E.; Gaucher, C.; Glacet, A.; Jorieux, S.; Klein, P.; Hogarth, M.; Fridman, W.; Bourel, D.; Béliard, R.; Teillaud, J., 2006: Selection of a human anti-RhD monoclonal antibody for therapeutic use: Impact of IgG glycosylation on activating and inhibitory FcγR functions. *Clinical Immunology*., **118**, 170–179.
Silverman;, 2001: *Phage Display: A Laboratory Manual*. *Cold Spring Harbor Laboratory Press*.
Singh, A.; Settleman, J., 2010: EMT, cancer stem cells and drug resistance: An emerging axis of evil in the war on cancer. *Oncogene*., **29**, 4741–4751.
Six, E.; Ndiaye, D.; Laabi, Y.; Brou, C.; Gupta-Rossi, N.; Israël, a; Logeat, F., 2003: The Notch ligand Delta1 is sequentially cleaved by an ADAM protease and gamma-secretase. *Proceedings of the National Academy of Sciences of the United States of America*., **100**, 7638–7643.
Smith, G.; Petrenko, V., 1997: Phage display. *Chemical Reviews*., **97**, 391–410.
South, A.; Purdie, K.; Watt, S.; Haldenby, S.; Den Breems, N.; Dimon, M.; Arron, S.; Kluk, M.; Aster, J.; McHugh, A.; Xue, D.; Dayal, J.; Robinson, K.; Rizvi, S.; Proby, C.; Harwood, C.; Leigh, I., 2014: NOTCH1 mutations occur early during cutaneous squamous cell carcinogenesis. *Journal of Investigative Dermatology*., **134**, 2630–2638.
Takaya Oda, Abdel G. Elkahloun, Brian L. Pike, Kazuki Okajima, Ian D. Krantz, Anna Genin, David A. Piccoli, Paul S. Meltzer, Nancy B. Spinner F., 1997: Mutations in the human Jagged1 gene are responsible for Alagille syndrome. *Nature Genetics*., **16**, 235–242.
Tax, F.; Yeargers, J.; Thomas, J., 1994: Sequence of C. elegans lag-2 reveals a cell-signalling domain shared with Delta and Serrate of Drosophila. *Nature*., **368**, 150–154.
Timmerman, L.; Raya, A.; Bertra, E.; Aranda, S.; Palomo, S.; Mccormick, F.; Izpisu, J. C., 2008: Notch promotes epithelial-mesenchymal transition during cardiac development and oncogenic transformation. *Genes & Development*., **5**, 99–115.
Tolcher, A.; Messersmith, W.; Mikulski, S.; Papadopoulos, K.; Kwak, E.; Gibbon, D.; Patnaik, A.; Falchook, G.; Dasari, A.; Shapiro, G.; Boylan, J.; Xu, Z.; Wang, K.; Koehler, A.; Song, J.; Middleton, S.; Deutsch, J.; DeMario, M.; Kurzrock, R. et al., 2012: Phase I study of RO4929097, a gamma secretase inhibitor of notch signaling, in patients with refractory metastatic or locally advanced solid tumors. *Journal of Clinical Oncology*., **30**, 2348–2353.
Wang, Q.; Shi, Y.; Butler, H.; Xue, J.; Wang, G.; Duan, P.; Zheng, H., 2017: Role of

delta-like ligand-4 in chemoresistance against docetaxel in MCF-7 cells. *Human and Experimental Toxicology*., **36**, 328–338.
Watkins, N. A.; Ouwehand, W. H., 2000: Introduction to antibody engineering and phage display. *Vox Sanguinis*., **78**, 72–79.
William E Paul, 2013: *Fundamental Immunology* 7th ed. Li. Williams and Wilkins, Philadelphia.
Wilson, A.; Radtke, F., 2006: Multiple functions of Notch signaling in self-renewing organs and cancer. *FEBS Letters*., **580**, 2860–2868.
Wu, L.; Aster, J.; Blacklow, S.; Lake, R.; Artavanis-Tsakonas, S.; Griffin, J., 2000: MAML1, a human homologue of Drosophila mastermind, is a transcriptional co-activator for NOTCH receptors. *Nature Genetics*., **26**, 484–489.
Wu, Y.; Cain-Hom, C.; Choy, L.; Hagenbeek, T.; De Leon, G.; Chen, Y.; Finkle, D.; Venook, R.; Wu, X.; Ridgway, J.; Schahin-Reed, D.; Dow, G.; Shelton, A.; Stawicki, S.; Watts, R.; Zhang, J.; Choy, R.; Howard, P.; Kadyk, L. et al., 2010: Therapeutic antibody targeting of individual Notch receptors. *Nature*., **464**, 1052–1057.
Xia, J.; Zhang, Y.; Qian, J.; Zhu, X.; Zhang, Y.; Zhang, J.; Zhao, G., 2013: Isolation, identification and expression of specific human CD133 antibodies. *Scientific Reports*., **3**, 1–9.
Xiaokun Li, 2018: Bioengineering of FGFs and New Drug Developments. *Fibroblast Growth Factors*., pp. 477–558.
Xing, F.; Okuda, H.; Watabe, M.; Kobayashi, A.; Pai, S.; Liu, W.; Pandey, P.; Fukuda, K.; Hirota, S.; Sugai, T.; Wakabayshi, G.; Koeda, K.; Kashiwaba, M.; Suzuki, K.; Chiba, T.; Endo, M.; Mo, Y.; Watabe, K., 2011: Hypoxia-induced Jagged2 promotes breast cancer metastasis and self-renewal of cancer stem-like cells. *Oncogene*., **30**, 4075–4086.
Xing, F.; Liu, Y.; Watabe, M.; Liu, W.; Kobayashi, A.; Watabe, K.; Iiizumi, M.; Fukuda, K.; Moore, B.; Hirota, S.; Sharma, S.; Wilber, A.; Peralta, E.; Pandey, P.; Pai, S.; Mo, Y.; Okuda, H.; Wu, K., 2013: Reactive astrocytes promote the metastatic growth of breast cancer stem-like cells by activating Notch signalling in brain. *EMBO Molecular Medicine*.
Xu Chen, Alexander Stoeck, Soo Jung Lee, Ie-Ming Shih, Michael M. Wang, , 2010: Jagged1 expression regulated by Notch3 and Wnt/Beta-catenin signaling pathways in ovarian cancer. *Oncotarget*.
Yamamoto, S.; Charng, W.; Bellen, H., 2010: Endocytosis and intracellular trafficking of notch and its ligands. *Current Topics in Developmental Biology*., **92**, 165–200.
Yashiro-Ohtani, Y.; Ohtani, T.; Pear, W., 2010: Notch regulation of early thymocyte development. *Seminars in Immunology*., **22**, 261–269.

Yavropoulou, M.; Maladaki, A.; Yovos, J., 2015: The role of Notch and Hedgehog signaling pathways in pituitary development and pathogenesis of pituitary adenomas. *Hormones*., **14**, 5–18.
Yen, W. C.; Fischer, M. M.; Axelrod, F.; Bond, C.; Cain, J.; Cancilla, B.; Henner, W. R.; Meisner, R.; Sato, A.; Shah, J.; Tang, T.; Wallace, B.; Wang, M.; Zhang, C.; Kapoun, A. M.; Lewicki, J.; Gurney, A.; Hoey, T., 2015: Targeting notch signaling with a Notch2/Notch3 antagonist (Tarextumab) inhibits tumor growth and decreases tumor-initiating cell frequency. *Clinical Cancer Research*., **21**, 2084–2095.
Zavadil, J.; Cermak, L.; Soto-Nieves, N.; Böttinger, E. P., 2004: Integration of TGF-β/Smad and Jagged1/Notch signalling in epithelial-to-mesenchymal transition. *EMBO Journal*., **23**, 1155–1165.
Zheng, K.; Bantog, C.; Bayer, R., 2011: The impact of glycosylation on monoclonal antibody conformation and stability. *mAbs*., **3**, 568–576.

LOMBADA